



**University  
of Antwerp**



Faculty of Applied Engineering

Programa de Pós-graduação em Engenharia Civil

# **Alkali-activated binders with reclaimed asphalt aggregates as a potential base layer of pavements**

A thesis submitted in fulfilment of the requirements for the joint degree of doctor in Applied Engineering at the University of Antwerp and doctor in Civil Engineering at CEFET-MG

**Juliana Oliveira COSTA**

Supervisors:

Prof. dr, Wim Van den bergh

Prof. dr. Johan Blom

Prof. dr. Augusto Cesar da Silva Bezerra

Prof. dr. Flávio Antônio dos Santos

Antwerp, 2022

C838a Costa, Juliana Oliveira  
Alkali-activated binders with reclaimed asphalt aggregates as a potential base layer of pavements / Juliana Oliveira Costa. – 2022.  
178 f. : il., gráfs, tabs., fotos.

Tese apresentada em cumprimento aos requisitos para a titulação conjunta de doutor em Engenharia Aplicada pela University of Antwerp e doutor em Engenharia Civil pelo CEFET-MG

Orientadores: Wim Van den bergh, Johan Blom, Augusto Cesar da Silva Bezerra e Flávio Antônio dos Santos.

Inclui bibliografias.

Tese (doutorado) – Centro Federal de Educação Tecnológica de Minas Gerais, Departamento de Engenharia Civil.

1. Pavimentos de asfalto – Reaproveitamento – Teses. 2. Materiais de construção – Teses. 3. Polímeros – Teses. I. Van den bergh, Wim. II. Blom, Johan. III. Bezerra, Augusto Cesar da Silva. IV. Santos, Flávio Antônio. V. Centro Federal de Educação Tecnológica de Minas Gerais. Departamento de Engenharia Civil. VI. University of Antwerp VII. Título.

CDD 625.85

# JURY

---

Prof. dr. Pieter Billen University of Antwerp, Faculty of Applied Engineering,	<b>Chair</b>
Prof. dr. Bart Craeye University of Antwerp, Faculty of Applied Engineering, EMIB research group	<b>Secretary</b>
Prof. dr. Wim Van den bergh University of Antwerp, Faculty of Applied Engineering, EMIB research group	<b>Supervisor</b>
Prof. dr. Johan Blom University of Antwerp, Faculty of Applied Engineering, EMIB research group	<b>Supervisor</b>
Prof. dr. Flávio Antônio dos Santos Federal Center for Technological Education of Minas Gerais (CEFET-MG), Department of Civil Engineering	<b>Supervisor</b>
Prof. dr. Augusto Cesar da Silva Bezerra Federal Center for Technological Education of Minas Gerais (CEFET-MG), Department of Civil Engineering	<b>Supervisor</b>
Prof. dr. João Paulo de Castro Gomes University of Beira Interior Department of Civil Engineering and Architecture	<b>Member</b>
Prof. dr. Hubert Rahier Vrije Universiteit Brussels Department of Materials and Chemistry	<b>Member</b>

## Contact:

Juliana Oliveira Costa  
Email: [Juliana.OliveiraCosta@uantwerpen.be](mailto:Juliana.OliveiraCosta@uantwerpen.be)

# TABLE OF CONTENTS

---

## ABSTRACT

## ACKNOWLEDGMENT

## LIST OF ABBREVIATIONS

1. INTRODUCTION	1
1.1. BACKGROUND & MOTIVATION	1
1.2. OBJECTIVES & JUSTIFICATION	4
1.3. THESIS CONTENT	6
1.4. RESEARCH DISSEMINATION	10
BIBLIOGRAPHY	12
<b>2. CEMENTITIOUS BINDERS AND RAP AGGREGATES FOR PAVEMENT LAYER</b>	<b>15</b>
2.1. INTRODUCTION	16
2.2. STATE OF THE ART	18
2.2.1. <i>RECLAIMED ASPHALT PAVEMENT (RAP)</i>	18
2.2.2. <i>THE USE OF RAP AGGREGATES IN PAVEMENT BASE LAYERS</i>	21
2.2.3. <i>RAP AGGREGATES IN PC MATRICES</i>	23
2.2.4. <i>ALKALI-ACTIVATED MATERIALS AS BINDERS</i>	29
2.2.5. <i>RAP AND ALKALI-ACTIVATED MATERIALS</i>	35
2.3. REFLECTIONS FROM LITERATURE	39
2.3.1. <i>POTENTIAL, CHALLENGES AND RESEARCH GAPS ON RAP-AAM</i>	40
2.3.1.1. <i>COST AND AVAILABILITY OF LOCAL MATERIALS</i>	40
2.3.1.2. <i>PERFORMANCE AND DURABILITY OF RAP-AAM</i>	41
2.3.1.3. <i>LIFE CYCLE ASSESSMENT (LCA) OF RAP-AAM</i>	42
2.4. CONCLUSIONS	42
BIBLIOGRAPHY	45
<b>3. MATERIALS CHARACTERISATION &amp; EXPERIMENTAL TECHNIQUES</b>	<b>59</b>
3.1. INTRODUCTION	59
3.2. MATERIALS	60
3.2.1. <i>BINDERS &amp; PRECURSORS</i>	60
3.2.1.1. <i>GROUND GRANULATED BLAST FURNACE SLAG</i>	60
3.2.1.2. <i>METAKAOLIN</i>	62
3.2.1.3. <i>CEMENT</i>	63
3.2.2. <i>ACTIVATORS</i>	64



3.2.3. <i>AGGREGATES</i>	65
3.2.3.1. <i>FINE NATURAL AGGREGATE (NA)</i>	66
3.2.3.2. <i>FINE RAP AGGREGATE</i>	66
3.2.3.3. <i>COARSE RAP AGGREGATE</i>	67
3.3. MIXTURE PROPORTIONS & PROCEDURES	69
3.3.1. <i>PASTES</i>	69
3.3.2. <i>MORTARS</i>	70
3.3.3. <i>CONCRETE</i>	73
3.4. EXPERIMENTAL METHODOLOGIES	75
3.4.1. <i>CHARACTERISATION OF PASTES</i>	75
3.4.2. <i>CHARACTERISATION OF MORTARS</i>	76
3.4.2.1. <i>CALORIMETRY</i>	76
3.4.2.2. <i>SHRINKAGE ASSESSMENT</i>	77
3.4.2.3. <i>FLEXURAL STRENGTH AND COMPRESSIVE STRENGTH</i>	78
3.4.2.4. <i>MERCURY INTRUSION POROSIMETRY (MIP)</i>	79
3.4.2.5. <i>APPARENT POROSITY</i>	80
3.4.2.6. <i>MICROSTRUCTURE ANALYSIS</i>	80
3.4.3. <i>CHARACTERISATION OF CONCRETES</i>	82
3.4.3.1. <i>COMPRESSIVE AND SPLITTING TENSILE STRENGTH</i>	82
3.4.3.2. <i>MODULUS OF ELASTICITY AND ULTRASONIC PULSE                     VELOCITY (UPV)</i>	82
3.4.3.3. <i>FREEZE AND THAW (F&amp;T)</i>	83
BIBLIOGRAPHY	85
<b>4. THE EFFECT OF RAP AGGREGATED ON ALKALI-ACTIVATED MORTARS</b>	<b>87</b>
4.1. INTRODUCTION	88
4.2. EXPERIMENTAL SUMMARY	88
4.3. RESULTS & DISCUSSION	89
4.3.1. <i>ISOTHERMAL CALORIMETRY</i>	89
4.3.2. <i>COMPRESSIVE AND FLEXURAL STRENGTH</i>	94
4.3.3. <i>MERCURY INTRUSION POROSIMETRY</i>	99
4.3.4. <i>MICROSTRUCTURE OBSERVATION OF THE MORTARS</i>	101
4.4. CONCLUSIONS	107
BIBLIOGRAPHY	110
<b>5. BLENDED RAP-AAM: MECHANICAL &amp; MICROSTRUCTURAL PROPERTIES</b>	<b>113</b>
5.1. INTRODUCTION	114

5.2. EXPERIMENTAL SUMMARY	115
5.3. RESULTS & DISCUSSION	116
5.3.1. <i>PRELIMINARY STUDY ON 4%Na<sub>2</sub>O ACTIVATED SAMPLES</i>	116
5.3.2. <i>STUDY ON 8%Na<sub>2</sub>O ACTIVATED SAMPLES</i>	120
5.3.2.1. CALORIMETRY	120
5.3.2.2. SHRINKAGE	123
5.3.3. <i>FTIR</i>	126
5.3.4. <i>SEM AND CONFOCAL MICROSCOPY</i>	128
5.3.5. <i>COMPRESSIVE AND FLEXURAL STRENGTH AND APPARENT POROSITY</i>	131
5.3.6. <i>DISCUSSION OVERVIEW</i>	133
5.4. CONCLUSION	136
BIBLIOGRAPHY	138
<b>6. RAP-AAM LEAN CONCRETE FOR PAVEMENT BASE LAYER</b>	<b>143</b>
6.1. INTRODUCTION	144
6.2. EXPERIMENTAL SUMMARY	145
6.3. RESULTS & DISCUSSION	146
6.3.1. <i>PROCTOR COMPACTION ON RAP AGGREGATES AND AAM LEAN CONCRETE</i>	146
6.3.2. <i>COMPRESSIVE STRENGTH AND SPLITTING TENSILE STRENGTH</i>	148
6.3.3. <i>MODULUS OF ELASTICITY (ME)</i>	150
6.3.4. <i>DYNAMIC MODULUS OF ELASTICITY (DME)</i>	157
6.3.5. <i>FREEZE AND THAW (F&amp;T)</i>	158
6.4. CONCLUSIONS	162
BIBLIOGRAPHY	165
<b>7. CONCLUSIONS &amp; RECOMMENDATIONS</b>	<b>171</b>
7.1. RESEARCH SUMMARY	171
7.2. CONCLUSIONS	173
7.3. RECOMMENDATIONS FOR FUTURE RESEARCH	176

# ABSTRACT

---

The pavement infrastructure comprises 16.3 million kilometres worldwide, and the pavement-related industrial sectors are said to be responsible for 21% of the global Greenhouse Gas (GHG) emissions worldwide (Plati, 2019). Sustainable actions on materials for those pavement layers mostly consider replacing (i) natural aggregates (NA) with recycled ones and (ii) Portland cement (PC) used as binder/stabiliser with binders with a lower ecological footprint. This research investigates the possibility of incorporating recycled asphalt pavement (RAP) as an aggregate replacement and alkali-activated material (AAM) as Portland cement (PC) replacement in/for base layer materials.

So far, most studies focused on the use of RAP and PC or supplementary cementitious materials. The combination of RAP with alkali-activated matrices may be an even more sustainable solution, given that not only the aggregate is recycled, but also PC is absent from the matrix. Properly designed AAMs are stronger and more durable than PC-based materials. It is, therefore, very likely that the employment of RAP in AAM will result in materials that achieve the minimum requirements for road applications.

This research produced an alkali-activated material containing fine and/or coarse RAP aggregates (RAP-AAM) as a replacement for natural aggregates to be used as base layers of pavements. The main objective of this thesis is to determine whether **AAM can incorporate high amounts of RAP and be used as pavement base layers without compromising mechanical and durability performance.**

During this research, two innovative characterization methods were used as an alternative to those often employed for Portland concrete. Firstly, the observation of the interfacial transition zone (ITZ) was improved by combining a laser scanning confocal microscope (LSCM) and a scanning electron microscope (SEM). The combination of both techniques permitted a better observation of the heterogeneous asphalt coating of the RAP particles, the presence of clusters, and cracks at the border and within the activated matrix. Secondly, the thesis proposes an alternative methodology to observe and quantify the shrinkage of RAP-AAM or any

other cementitious materials by employing simplified optical imaging. Although this method only allows for the observation of total shrinkage, it is an almost inexpensive method that could give a clear indication of volume changes over time.

The experimental data demonstrated that an ideal alkali-activated binder composition to produce RAP-AAM lean concrete would have 10% MK replacement (BFS vol%) and the activator would have 8% Na<sub>2</sub>O and Ms= 0 (i.e., activated with NaOH and no sodium silicate). This selection was based on the minimum activator amount required to reach the target compressive strength for a weak to medium lean concrete (5 to 10 MPa), while also minimizing the shrinkage effect. The durability assessment to freeze and thaw indicated similar performance for RAP-AAM and reference (RAP-PC). The findings of this research showed that RAP-AAM is a promising material for pavement base layers and more investigation is needed on long-term strength and durability.

Keywords: RAP, recycling, pavement, road base material, geopolymer, alkali-activation

# DUTCH ABSTRACT

---

De weginfrastructuur beslaat 16.3 miljoen kilometers wereldwijd. De wegenbouw is verantwoordelijk voor 21% van de broeikasgassen. Een meer duurzame (sustainable) aanpak in de wegenbouw is noodzakelijk. Dit kan door natuurlijke granulaten te vervangen door gerecycleerde materialen en Portland cement (PC) te vervangen door evenwaardige bindmiddelen met een lagere ecologische impact.

Dit vernieuwend onderzoek gaat de mogelijkheid na of asfaltgranulaten (RAP) en alkali geactiveerde materialen (AAM) kunnen gebruikt worden in onderlagen. Tot dusver waren de meeste studies gericht op het gebruik van RAP en Portland cement (PC) of aanvullende cementgebonden materialen. De combinatie van RAP met alkali-geactiveerde matrices kan een duurzamere oplossing zijn, aangezien in deze niet alleen het aggregaat wordt gerecycleerd, maar ook cement (PC) wordt vervangen. Optimaal ontworpen AAM zijn sterker en duurzamer dan materialen op basis van PC waardoor het gebruik van RAP in AAM kan leiden tot materialen die voldoen aan de minimumeisen voor wegen.

Dit onderzoek resulteerde in een alkalisch geactiveerd materiaal, dat fijne en/of grove RAP-aggregaten bevat (RAP-AAM) ter vervanging van natuurlijke aggregaten. Het hoofddoel van deze dissertatie was te bepalen of **AAM grote hoeveelheden RAP kan bevatten en gebruikt kan worden als funderingslaag voor verhardingen zonder afbreuk te doen aan de mechanische en duurzaamheidsprestaties.**

Bovendien zijn twee innovatieve karakteriseringsmethoden ontwikkeld en gebruikt als alternatief voor de methoden om portlandbeton te onderzoeken. Ten eerste werd de observatie van de grensvlakovergangszone (ITZ) verbeterd door een laserscanning confocal microscope (LSCM) en een scanning electron microscope (SEM) te combineren. Deze combinatie verbeterde de observatie van de heterogene asfaltcoating van de RAP-deeltjes, de aanwezigheid van clusters en scheuren aan de grens en binnen de geactiveerde matrix. Een tweede techniek is een alternatieve methode om de krimp van RAP-AAM of andere cementgebonden materialen te observeren en te

kwantificeren door gebruik te maken van vereenvoudigde optische beeldvorming. Hoewel met deze methode alleen de totale krimp kan worden waargenomen, is het een goedkopere methode die een duidelijke indicatie kan geven van volumeveranderingen in de tijd.

De experimentele gegevens toonden aan dat een ideale alkali-geactiveerde bindmiddelsamenstelling om RAP-AAM mager beton te produceren, 10% MK-vervanging zou hebben (BFS vol%) en de activator 8%  $\text{Na}_2\text{O}$  en  $M_s = 0$ , hetgeen geactiveerd is met  $\text{NaOH}$  en geen natriumsilicaat bevat. Deze keuze was gebaseerd op de minimale hoeveelheid activator die nodig is om de beoogde druksterkte te bereiken voor een zwak tot middelmatig mager beton (5 tot 10 MPa), terwijl ook het krimpeffect wordt geminimaliseerd. De beoordeling van de duurzaamheid bij vorst en dooi en uitloging wees op vergelijkbare prestaties voor RAP-AAM en de referentie (RAP-PC).

De bevindingen van dit onderzoek toonden aan dat RAP-AAM een veelbelovend materiaal is voor funderingslagen en hierdoor vervolgonderzoek naar de sterkte en duurzaamheid op lange termijn aangewezen.

# PORTUGUESE ABSTRACT

---

A infraestrutura rodoviária global tem 16,3 milhões de quilômetros e, em conjunto com os setores industriais relacionados, são responsáveis por 21% das emissões globais de gases de efeito estufa (Plati, 2019). As principais considerações visando um aumento da sustentabilidade dessas camadas de pavimento são a substituição (i) de agregados naturais (NA) por reciclados e (ii) de cimento Portland (PC) usado como ligante/estabilizador por ligantes alternativos de menor impacto ambiental. Esta pesquisa investiga a possibilidade de incorporar o pavimento asfáltico fresado (RAP) como um substituto de NA e materiais álcali-ativados (AAM) como substitutos do cimento Portland (PC) em/ para materiais de base.

Até agora, a maioria dos estudos concentrou-se no uso de RAP e PC ou materiais cimentícios suplementares. A combinação de RAP com AAM pode ser uma solução ainda mais sustentável, visto que não apenas o agregado é reciclado, mas também o PC está ausente da matriz. Os AAM quando adequadamente projetados são mais resistentes e apresentam maior durabilidade do que os materiais baseados em PC. É, portanto, muito provável que o emprego de RAP no AAM resulte em materiais que atinjam os requisitos mínimos para aplicações rodoviárias.

Esta pesquisa produziu um material alcalino ativado contendo agregados de RAP (RAP-AAM) como um substituto para os agregados naturais a serem usados como camadas de base de pavimentos. O principal objetivo desta tese é determinar se o **AAM pode incorporar grandes quantidades de RAP e ser usado como camadas de base de pavimento sem comprometer o desempenho mecânico e a durabilidade.**

Durante esta pesquisa, dois métodos inovadores de caracterização foram utilizados. Primeiramente, a observação da zona de transição interfacial (ITZ) foi melhorada pelo uso combinado de um microscópio confocal de varredura a laser (LSCM) e um microscópio eletrônico de varredura (SEM). A combinação de ambas as técnicas permitiu uma melhor observação da composição heterogênea das partículas RAP, e

fissuras na borda e dentro da matriz ativada. Em segundo lugar, a tese propõe uma metodologia alternativa para observar e quantificar a retração do RAP-AAM ou qualquer outro material cimentício, empregando análise de imagens. Embora este método só permita a observação da retração total, é um método de baixo custo que pode dar uma indicação clara das mudanças de volume ao longo do tempo.

Os dados experimentais demonstraram que a composição ideal de ligante ativado para produzir concreto magro RAP-AAM possui 10% em volume de metacaulim em substituição a escória de alto-forno como ligante e o ativador possui 8% de  $\text{Na}_2\text{O}$  na forma de NaOH (sem silicato de sódio). Esta seleção foi baseada na quantidade mínima de ativador necessária para atingir uma resistência a compressão entre 5 e 10 MPa, e minimizando o efeito de retração. A avaliação de durabilidade a gelo/desgelo indicou um desempenho semelhante para RAP-AAM ao da amostra de referência (RAP-PC). Os resultados desta pesquisa mostraram que o RAP-AAM é um material promissor para as camadas de base do pavimento e mais investigações são necessárias para melhor entendimento de suas propriedades a longo prazo.



# ACKNOWLEDGEMENTS

---

The academic environment is one of my favorite places and I was very excited when selected as a Ph.D. candidate at CEFET-MG. This research started in Brazil when Prof. Flavio dos Santos accepted being my supervisor. As the subject of the research evolved and changed, Prof. Augusto Bezerra also joined us. I'll be forever in debt to Prof. Flavio and Prof. Augusto for believing that I could return to science.

However, it was only when the joint agreement between CEFET-MG and the University of Antwerp was drafted that this research found its identity. I will never be able to express in words my gratitude to Prof. Wim Van den bergh and Prof. Johan Blom, for the warm welcome and extraordinary mentorship during this research. Thank you for your guidance during the experimental and writing process, but also for your understanding and support during my time of doubts and the difficulties brought by the pandemic.

The drafting of the joint agreement was a long process that only succeeded because of the help of many people from both institutions. I would like to express my gratitude to the International Affairs Office from CEFET-MG (especially to Ms. Liliane Neves) and to Ms. Simone Kramer (from UAntwerp) for the hard work in getting all the paperwork ready.

I would like to thank the jury members: Prof. Pieter Billen, Prof. Bart Craye (UAntwerp), Prof. João Paulo Castro Gomes (Universidade Beira Interior) and Prof. Hubert Rahier (Vrije Universiteit Brussels) for their contribution during the review and examination process which significantly improved this thesis.

I was very lucky to have met wonderful colleagues during this research. I will always cherish the time in the office with the girls in Brazil – Veronica, Taciana and Renata – and (lucky me) there was a girl's office in Antwerp too – with Ablenya, Ecem and Karolien. I would like to deeply thank my colleagues in Antwerp (Navid, Ian, David, Kostas, Ben, Reza, Alex, Patricia, Koen, Taher, Geert and George) and in Brazil (Elaine,

Camila, and Vitor). I was also very fortunate to meet Jaffer and Tamara and for their friendship.

Furthermore, thanks to Jan, Ali and Lacy for making the hard and heavy lab work always fun and pleasant. To Ivan, Adalberto (from CEFET-MG), Guido and Sofie (from UAntwerp) for the help with technical and administrative issues.

Last, I would like to acknowledge the amazing and unconditional support of my family, without whom none of it would be possible. Thanks to my parents for being my whole models and highlighting the value of education; to my brother and sister and their constant presence in my life. But the hard work of supporting my struggles during this time laid on the shoulders of my husband and daughter. Thank you, Paulo and Lis, for embarking with me in on this cross-continental journey and only keeping your eyes on the road ahead.

# LIST OF ABBREVIATIONS

---

3PB	Three-point bending
AAB	Alkali-activated binder(s)
AAM	Alkali-activated material(s)
AB&AT	Abrasion and attrition
AL	Asphalt layer
BFS	Ground granulated blast furnace slag
B&S	Base and subbase
C-A-S-H	Calcium (alumino)silicate hydrate
CH	Calcium hydroxide
CLSM	Confocal Laser Scanning Microscopy
CS	Concrete surface layer
C-S-H	Calcium
CT	Cement treated
Ed	Dynamic modulus of elasticity
Es	Secant modulus of elasticity
ELAS	Elastic modulus
F&T	Freeze and thaw
FDR	Full-depth reclamation
FTIR	Fourier Transform Infrared Microscopy
GB	Granular base
GS	Granular sub base
ITZ	Interfacial transition zone(s)
LC	Lean concrete
LCA	Life cycle assessment
LCL	Lower concrete layer
LON	Longitudinal dynamic modulus
MDD	Maximum dry density
ME	Modulus of elasticity
MIP	Mercury intrusion porosimetry
MK	Metakaolin
Ms	Silica Modulus
NA	Natural aggregates
N-A-S-H	Sodium aluminosilicate
OMC	Optimum moisture content
PC	Portland cement
PCC	Portland cement concrete

PFA	Pulverised fly ash
PSD	Particle size distribution
RAP	Reclaimed asphalt pavement
RC	Roller compacted
SEM	Scanning electron microscopy
TRAN	Transverse dynamic modulus
UCS	Unconfined compressive strength
UPV	Ultrasonic pulse velocity
UV	Ultraviolet light
XRD	X-ray diffraction
XRF	X-ray fluorescence

# INTRODUCTION

---

## 1.1 Background & Motivation

The United Nations set up 17 interlinked global goals, known as Sustainable Development Goals; they work as a guideline to help achieve a more sustainable future for everyone (Figure 1.1). Every economic sector can - or needs to - relate and contribute to one or more of the goals. The development of sustainable construction materials using recycling materials fits goals number 9, 11, and 12.



Figure 1.1. Sustainable Development Goals (United Nations, n.d.)

We consume vast quantities of construction materials and, at the same time, produce large amounts of construction and demolition waste. In most countries, construction and demolition waste surpass the quantities of municipal solid waste (Kaza et al., 2018). Reclaimed asphalt pavement, also known as RAP, is one of the waste materials generated by construction activities that could return as an alternative source of aggregates.

RAP is a milled granular waste, a product from removing distressed asphalt pavement sections for renovation, and can be used as a replacement for natural aggregates (NA). However, it is considered an inferior material compared to NA due to (i) the presence of agglomerated particles and bitumen coating and (ii) the impact that the milling procedure may have on its gradation and incorporation of dust (Arulrajah et al., 2014; Debbarma et al., 2019; Saride et al., 2016).

Recently, a considerable effort to promote a higher use of this material in new pavement layers (e.g. base course and top layers) has been observed. Recycling RAP reduces the need for disposal and demand for virgin materials, and the overall cost of pavement sections could reduce by 40-46% (Debbarma et al., 2019; Singh et al., 2018c). However, recyclable materials in pavement sections should not compromise their service life, durability or increase the need for maintenance.

It is already standard practice to use RAP in new asphalt mixes in many countries. The recycled material can be added cold or preheated; however, when cold recycling is used, most standards set a maximum of 20% of bitumen replacement (Anthonissen et al., 2016). But not all RAP products get recycled in asphalt, and more recycling alternatives are necessary to maximise the use of this material.

Another recycling possibility for RAP is as unbound and stabilised base/subbase material. Several road agencies make provisions to use unbound layers with RAP aggregates, but values vary between them, ranging from 10% to 100% by weight (Hoppe et al., 2015). The biggest challenge when using RAP as stabilised base material is ascribed to the thin, aged bitumen coating on the surface of the aggregate, which leads to inferior properties (Arulrajah et al., 2014; Saride et al., 2016). Hence,

RAP's performance needs to be improved by blending it with natural aggregates (NA). Still, some transportation/road agencies recommend a maximum RAP content of about 30% by weight of VA. However, the material usually does not reach the minimum strength requirement when stabilised with low-calcium sources (such as fly ash, bottom ash, and blast furnace slag) and alkaline activation could be used to increase the reactivity of the binder and its strength (Avirneni et al., 2016). Mohammadinia et al. (2016) observed higher compressive strength of alkali-activated samples stabilised with slag than fly ash.

Many authors investigated the use of RAP in Portland Cement (PC)-based concrete mixes for road application (Boussetta et al., 2018; Pasetto and Baldo, 2017; Van den bergh et al., 2017). Most studies indicated a negative effect on the fresh and mechanical properties of the concrete due to the bitumen coating layer on the surface of the aggregate (Debbarma et al., 2019; Singh et al., 2018a). An even more pronounced reduction was observed when only RAP aggregates' fine fraction was used (Abraham and Ransinchung, 2018; Singh et al., 2018b, 2018a). Hence, the coarser fraction has a higher potential for replacing VA than the finer fraction.

Nevertheless, the poor performance of RAP-PC concrete should not discourage the use of RAP in pavements: one viable alternative could be the employment of RAP as aggregates for alkali-activated matrices. Studies about the use of RAP in alkali-activated concretes are still scarce.

Alkali-activated materials or binders (AAM or AAB), when properly designed are sustainable binding systems resulting from the reaction of an aluminosilicate and an alkaline activator (Provis, 2018). AAM may also be referred to as geopolymers when it is the product of the activation of low-calcium aluminosilicate precursors (Provis, 2014). A binder has a high calcium content if the  $\text{Ca}/(\text{Si} + \text{Al})$  ratio is approximately 1 (Provis and Bernal, 2014). The aluminosilicate is usually an industrial by-product or wastes supplied in powder form, such as: fly ash (low and high calcium), coal bottom ash, rice husk ash, palm oils fuel ash, blast furnace slag, phosphorus slag, steel slag, silico-manganese slag, metakaolin, natural minerals (albite, volcanic ashes /natural pozzolans, kaolinite), volcanic glass, zeolite, silica fume, non-ferrous slag, mineral processing tailings (such as coal gangue, red mud and mine tailings), catalyst

residues (from crude oil processing in petroleum refineries), waste glass, waste ceramics, incinerated sludges such as paper sludge, water treatment sludge (Provis et al., 2015; Shi et al., 2011).

In the production of AAM, the aluminosilicates need an alkaline source to reduce their usually very long setting time and increase their early strength. The alkaline source may come from adding a strong alkaline solution as a solid or even from the dissolved PC clinker (Provis et al., 2015). The most used alkali hydroxide is sodium hydroxide, followed by potassium hydroxide and calcium hydroxide. It is also possible to activate with alkali silicates - such as sodium silicate or potassium silicate - alkali carbonate and alkali sulphate.

The hardened activated product may have high mechanical strength, chemical resistance (acidic and sulphate environments), and comparable chloride ingress to PC-based materials (Provis, 2018).

## 1.2 Objectives & Justification

The use of RAP as an aggregate replacement in pavement layers is a great recycling opportunity but it may require the use of cement-based materials to compensate for strength loss. The combination of RAP with alkali-activated matrices may be an even more environmentally-friendly solution, in addition to the recycled aggregate, since PC is absent from the matrix. Properly designed AAMs are stronger and more durable than PC-based materials (Provis, 2014; Singh and Middendorf, 2020; Van Deventer et al., 2012). Hence, one can expect that the employment of RAP in AAM achieves the typical minimum requirements for hydraulically bound lean concrete mixes for road applications, as described in Table 1.1.

In addition to being a recycling alternative, the study of RAP-AAM may maximise the use of RAP granulates by either using higher replacement levels or using it in a thicker pavement layer (such as base layers). Maximising the use of recycling aggregates is of great importance to the Belgium pavement sector due to the high cost of NA and sustainability efforts. Still, the global transportation infrastructure is largely based on



flexural pavements, which will inevitably become RAP, and therefore, the research of RAP recycling alternatives is of global interest.

*Table 1.1. Typical minimal properties for PC-based lean concrete (Nick Thom, 2015)*

<b>Mixture type</b>	<b>Compressive 28 days, MPa</b>	<b>Cement Content kg/m<sup>3</sup></b>	<b>Water Content l/m<sup>3</sup></b>
Medium lean concrete	10	220	150
Weak lean concrete	5	150	150

The amount of research on RAP-AAM is limited; most studies used only pulverised fly ash (PFA) as a precursor, and still little is known about mechanical and durability properties. Studies on RAP-AAM based on the alkaline activation of ground granulated blast furnace slag (BFS) are scarce. Nevertheless, BFS is one of the main precursors for AAM and a byproduct of the steel industry that represents interest for Belgium and Brazil, the countries involved in this joint doctoral research. In addition, it is also considered a precursor that required low activation level and can react without the need of thermal treatment.

This research will study AAM containing fine or coarse RAP aggregates as a replacement for NA, hereafter referred to as RAP-AAM, used as hydraulically bound base layers of pavements. The investigation will target the maximisation of RAP granules without compromising the performance of the material. The main objective of this thesis is to understand the mechanisms behind RAP-AAM to guide the future design of adequately strong, durable, and sustainable pavement base layers. The main research question is:

**Could AAM incorporate high amounts of RAP, and be used as pavement base layers without compromising mechanical and durability performance?**

The specific objectives of the study are:

- (i) To make a thorough review of the state-of-the-art and highlight the potential, challenges, and knowledge gaps of using RAP-AAM as solutions for pavement base layer.
- (ii) Assess the effect of replacing NA with RAP aggregates in AAM mortars on the properties of RAP-AAM, to determine the optimum activator composition and content for an alkali-activated BFS matrix.
- (iii) Determine whether the choice of high-calcium systems (activated BFS) or a blended system (with metakaolin) plays an essential role in the ultimate mechanical and durability properties of RAP-AAM.
- (iv) To assess the influence of different RAP aggregates (different bitumen content) on the physical and mechanical characteristics of - RAP-AAM concretes.
- (v) To assess the durability of RAP-AAM concretes to freeze-thaw.

The experiments are designed to follow routes depending on the specific object targeted. Objectives (ii) and (iii) were tackled by using pastes and mortars, while concretes were employed for objectives (iv) and (v). The choice of systems is based on resource availability, equipment specifications, and materials consumption.

### 1.3 Thesis Content

This thesis is divided into seven chapters. Chapter 1 is a brief introduction to the subject. Chapter 2 will present a state-of-the-art literature review and will be followed by a material and methods section (Chapter 3). Chapters 4 and 5 are studies on mortars. Concrete specimens are evaluated in Chapter 6, leading to the main thesis conclusion in Chapter 7. A more extensive description of each chapter is offered below:

- **Chapter 1** provides background information and an introduction to the research subject – RAP aggregates and AAM. It presents the motivation of the study and contextualizes it with Belgium and the global sector. This section includes the research question, specific objectives, and the thesis outline.

- **Chapter 2** offers an extensive state-of-the-art review on the use of RAP in cementitious systems and how it could be applied in pavement layers. Due to the lack of studies on the use of RAP in AAM, the review also focused on PC systems and contemplates similarities between them. The conclusion of this chapter offers a reflection on the potential, challenges, and research needs of RAP-AAM.
- **Chapter 3** is the materials and methods section. It characterises the raw materials used (aggregates, binders, and chemicals), a detailed description of the manufacture of the samples (concrete, mortar, and pastes), and the general test methods. Some special methods are described in their corresponding chapter.
- The objective of **Chapter 4** is to investigate the impact of replacing NA with RAP in BFS-based alkali-activated mortar. The effect of different activator dosages is assessed, i.e., either 4% or 6% Na<sub>2</sub>O (wt. slag) combined with a modulus of silica (Ms) equal to 0, 0.5, and 1.0. The results are compared to control samples produced with NA. The investigation was performed by looking into hydration kinetics (Isothermal Calorimetry), pore size distribution (Mercury Intrusion Porosimetry), mechanical performance (Compressive and Flexural strength), and microstructure analysis.
- The aluminosilicate aluminosil is a crucial consideration for AAM, and blended systems with metakaolin (MK) may have an improved microstructure (fewer pores) and better mechanical performance. **Chapter 5** studies the partial replacement of BFS by MK (10 and 20 vol.%) in the properties of mortars activated with solutions prepared with Ms 0 and 1.0. The total shrinkage of the samples was observed using digital image correlation and the reaction products using FTIR (Fourier Transform Infrared Microscopy). A combination of Scanning Electron Microscopy and Confocal Laser Scanning Microscopy offered a better way to observe the interface between aggregates, bitumen, and alkali-activated matrices.
- The impact of different bitumen content on RAP granules is investigated in **Chapter 6**. RAP with lower bitumen content could bind better to the matrix and therefore have better mechanical

performance. Concrete samples were studied using two lab-produced RAP (with low and high bitumen content) and a commercially sourced RAP. The mechanical properties of RAP-AAM concrete were compared to RAP-PC to assess any possible improvement of the alternative material. AAM often has better chemical stability and thus durability than PC. The second part of this chapter investigates durability using an accelerated freeze and thaw test.

Finally, **Chapter 7** summarises the findings, conclusions, and recommendations for future research.

A graphical description of the thesis and its chapters is presented in Figure 1.2.

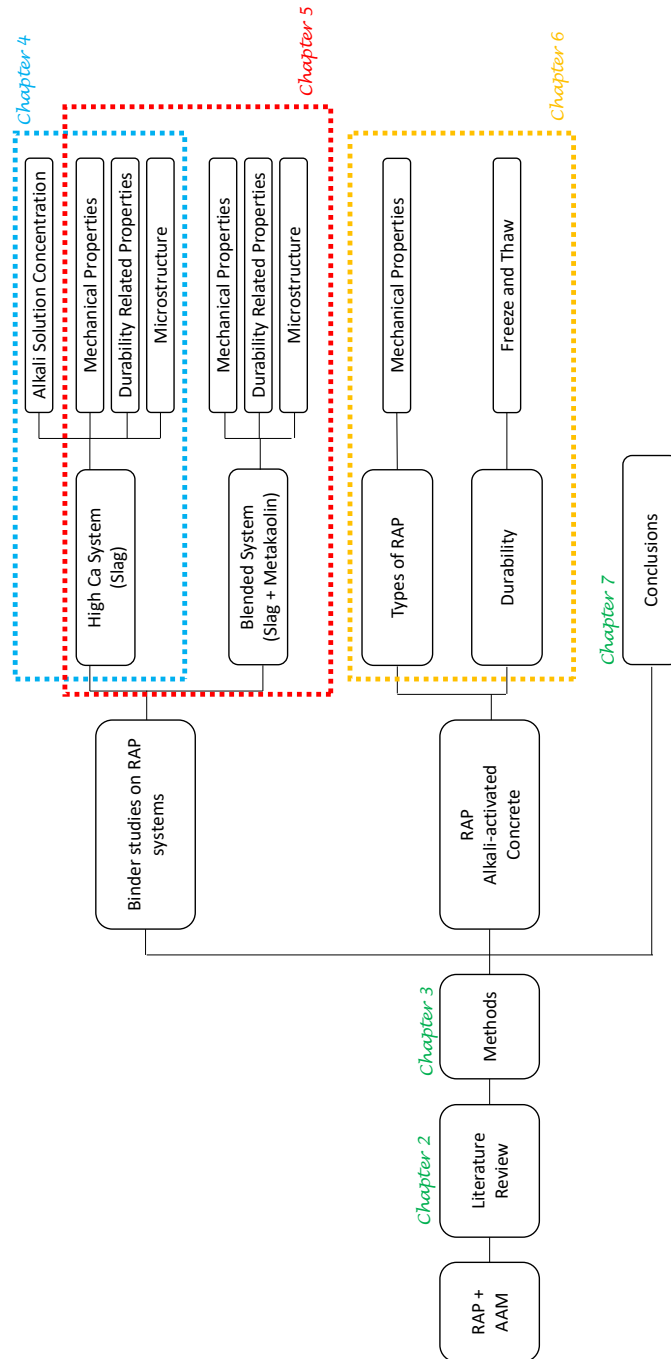


Figure 1.2. Research plan

## 1.4 Research Dissemination

Published papers at journals and conferences:

- Costa, J.O., Blom, J., Van den bergh, W., dos Santos, F.A., Bezerra, A.C.S.,Borges, P.H.R., 2022. Reclaimed asphalt and alkali-activated slag systems: the effect of metakaolin. Eng. Proc. 2022, 17, 28. <https://doi.org/10.3390/engproc2022017028>
- Costa, J.O., Borges, P.H.R., dos Santos, F.A., Bezerra, A.C.S., Blom, J., Van den bergh, W., 2021. The Effect of Reclaimed Asphalt Pavement (RAP) Aggregates on the Reaction, Mechanical Properties, and Microstructure of Alkali-Activated Slag. CivilEng 2, 794–810. <https://doi.org/10.3390/civileng2030043>
- Costa, J.O., Borges, P.H.R., dos Santos, F.A., Bezerra, A.C.S., Van den bergh, W., Blom, J., 2020. Cementitious binders and reclaimed asphalt aggregates for sustainable pavement base layers: Potential, challenges, and research needs. Constr. Build. Mater. 265, 120325. <https://doi.org/10.1016/j.conbuildmat.2020.120325> \*
- Batista, R.P., Costa, J.O., Borges, P.H.R., Dos Santos, F.A., Lameiras, F.S., 2019. High-performance alkali-activated composites containing an iron-ore mine tailing as aggregate. MATEC Web Conf. 274, 02004. <https://doi.org/10.1051/mateconf/201927402004>

Participations as a presenter:

- Costa, J.O., 2019. Alkali activated concrete with RA as a base material for pavement sections. Asphalt Innovation Symposium. <https://www.uantwerpen.be/en/researchgroups/emib/rers/activiteits/ais/ais2019/>

Submitted documents at journals:

- Barisoglu, E.N., Costa, J.O., Theys, F., Blom, J., Vuye, C., Van den bergh, W. The Effect of Active Filler Type, Compaction Method and Slag-based Geopolymer on Volumetrical and Mechanical Properties of Cold Foamed Bitumen Mixes with 100% RAP, Submitted to Road Materials and Pavement Design
- Borineli, J.B., Portilho-Estrada, M., Costa, J.O., Blom, J., Hernando, D., Van den bergh, W., Vuye,C. Reduction of volatile organic compound emission from crumb rubber modified bitumen using additives. Submitted to the Journal of Cleaner Production.

Upcomming documents:

- Costa, J.O., Borges, P.H.R., dos Santos, F.A., Bezerra, A.C.S., Van den bergh, W., Blom, J., Blended Alkali-activated systems as binders for RAP aggregates: mechanical and microstructural properties.
- Costa, J.O., Borges, Craeye, B.,Stoop, J., dos Santos, F.A., Bezerra, A.C.S., Van den bergh, W., Blom, J., RAP, and Alkali-activated as lean concrete for base layers .

# BIBLIOGRAPHY

---

Abraham, S.M., Ransinchung, G.D.R.N., 2018. Strength and permeation characteristics of cement mortar with Reclaimed Asphalt Pavement Aggregates. *Constr. Build. Mater.* 167, 700–706. <https://doi.org/10.1016/j.conbuildmat.2018.02.075>

Anthonissen, J., Van den bergh, W., Braet, J., 2016. Review and environmental impact assessment of green technologies for base courses in bituminous pavements. *Environ. Impact Assess. Rev.* 60, 139–147. <https://doi.org/10.1016/j.eiar.2016.04.005>

Arulrajah, A., Piratheepan, J., Disfani, M.M., 2014. Reclaimed asphalt pavement and recycled concrete aggregate blends in pavement subbases: Laboratory and field evaluation. *J. Mater. Civ. Eng.* [https://doi.org/10.1061/\(ASCE\)MT.1943-5533.0000850](https://doi.org/10.1061/(ASCE)MT.1943-5533.0000850)

Avirneni, D., Peddinti, P.R.T.T., Saride, S., 2016. Durability and long term performance of geopolymer stabilized reclaimed asphalt pavement base courses. *Constr. Build. Mater.* 121, 198–209. <https://doi.org/10.1016/j.conbuildmat.2016.05.162>

Boussetta, I., El Euch Khay, S., Neji, J., 2018. Experimental testing and modelling of roller compacted concrete incorporating RAP waste as aggregates. *Eur. J. Environ. Civ. Eng.* 8189, 1–15. <https://doi.org/10.1080/19648189.2018.1482792>

Debbarma, S., Ransinchung, G.D., Singh, S., 2019. Feasibility of roller compacted concrete pavement containing different fractions of reclaimed asphalt pavement. *Constr. Build. Mater.* 199, 508–525. <https://doi.org/10.1016/j.conbuildmat.2018.12.047>

Hoppe, J.E., Lane, D.S., Fitch, G.M., Shetty, S., 2015. Feasibility of Reclaimed Asphalt Pavement ( RAP ) Use As Road Base and Subbase Material, A Report: Virginia Center for Transportation Innovation and Research University of Virginia, Charlottesville, Virginia VCTIR 15-R6. Charlottesville.

Kaza, S., Yao, L., Bhada-Tata, P., Van Woerden, F., 2018. What a Waste



2.0: A Global Snapshot of Solid Waste Management to 2050, What a Waste 2.0: A Global Snapshot of Solid Waste Management to 2050. The World Bank, Washington, DC. <https://doi.org/10.1596/978-1-4648-1329-0>

Mohammadinia, A., Arulrajah, A., Sanjayan, J.G., Disfani, M.M., Bo, M.W., Darmawan, S., 2016. Strength Development and Microfabric Structure of Construction and Demolition Aggregates Stabilized with Fly Ash–Based Geopolymers. *J. Mater. Civ. Eng.* 28, 04016141. [https://doi.org/10.1061/\(ASCE\)MT.1943-5533.0001652](https://doi.org/10.1061/(ASCE)MT.1943-5533.0001652)

Nick Thom, 2015. Hydraulically-bound material, in: *Principles of Pavement Engineering*. Thomas Telford Publishing Ltd, pp. 110–135. <https://doi.org/10.1680/pope.34808.0008>

Pasetto, M., Baldo, N., 2017. Unified approach to fatigue study of high performance recycled asphalt concretes. *Mater. Struct. Constr.* 50, 1–15. <https://doi.org/10.1617/s11527-016-0981-7>

Provis, J.L., 2018. Alkali-activated materials. *Cem. Concr. Res.* 114, 40–48. <https://doi.org/10.1016/j.cemconres.2017.02.009>

Provis, J.L., 2014. Geopolymers and other alkali activated materials: why, how, and what? *Mater. Struct.* 47, 11–25. <https://doi.org/10.1617/s11527-013-0211-5>

Provis, J.L., Bernal, S.A., 2014. Geopolymers and related alkali-activated materials. *Annu. Rev. Mater. Res.* 44, 299–330. <https://doi.org/10.1146/annurev-matsci-070813-113515>

Provis, J.L., Palomo, A., Shi, C., 2015. Advances in understanding alkali-activated materials. *Cem. Concr. Res.* 78, 110–125. <https://doi.org/10.1016/j.cemconres.2015.04.013>

Saride, S., Avirneni, D., Challapalli, S., 2016. Micro-mechanical interaction of activated fly ash mortar and reclaimed asphalt pavement materials. *Constr. Build. Mater.* 123, 424–435. <https://doi.org/10.1016/j.conbuildmat.2016.07.016>

Shi, C., Ana, F.-J., Palomo, A., 2011. New cements for the 21st century:

The pursuit of an alternative to Portland cement. *Cem. Concr. Res.* 41, 750–763. <https://doi.org/10.1016/j.cemconres.2011.03.016>

Singh, N.B., Middendorf, B., 2020. Geopolymers as an alternative to Portland cement: An overview. *Constr. Build. Mater.* 237, 117455. <https://doi.org/10.1016/j.conbuildmat.2019.117455>

Singh, S., Ransinchung, G.D., Debbarma, S., Kumar, P., 2018a. Utilization of reclaimed asphalt pavement aggregates containing waste from Sugarcane Mill for production of concrete mixes. *J. Clean. Prod.* 174, 42–52. <https://doi.org/10.1016/j.jclepro.2017.10.179>

Singh, S., Ransinchung, G.D.R.N., Monu, K., Kumar, P., 2018b. Laboratory investigation of RAP aggregates for dry lean concrete mixes. *Constr. Build. Mater.* 166, 808–816. <https://doi.org/10.1016/j.conbuildmat.2018.01.131>

Singh, S., Shintre, D., Ransinchung, G.D., Kumar, P., 2018c. Performance of fine RAP concrete containing flyash, silica fume, and bagasse ash. *J. Mater. Civ. Eng.* 30, 1–11. [https://doi.org/10.1061/\(ASCE\)MT.1943-5533.0002408](https://doi.org/10.1061/(ASCE)MT.1943-5533.0002408)

United Nations, n.d. Sustainable Development Goals [WWW Document]. URL <https://www.un.org/sustainabledevelopment/sustainable-development-goals/> (accessed 3.4.22).

Van den bergh, W., Kara, P., Anthonissen, J., Margaritis, A., Jacobs, G., Couscheir, K., 2017. Recommendations and strategies for using reclaimed asphalt pavement in the Flemish Region based on a first life cycle assessment research. *IOP Conf. Ser. Mater. Sci. Eng.* 236. <https://doi.org/10.1088/1757-899X/236/1/012088>

Van Deventer, J.S.J., Provis, J.L., Duxson, P., 2012. Technical and commercial progress in the adoption of geopolymer cement. *Miner. Eng.* 29, 89–104. <https://doi.org/10.1016/j.mineng.2011.09.009>

## CEMENTITIOUS BINDERS AND RAP AGGREGATES FOR PAVEMENT LAYERS

---

Reclaimed asphalt pavement (RAP) has been increasingly used to replace natural aggregates in different pavement layers in the past few decades. However, regardless of layer choice or use of binders, the replacement level employed is usually low, and large quantities of RAP are still left unused or used inadequately. Often neglected, foundation layers have higher prospects to consume recycled materials due to their increased thickness. This chapter is a **state-of-the-art review** of the use of RAP aggregates with cementitious materials for pavement foundation layers (base and sub-base). Special attention is given to the use of alkali-activated materials (AAM) as a binder in substitution for Portland cement (PC). This chapter discusses the mechanical and durability properties of RAP-cementitious matrices and studies the changes in the microstructure. The biggest challenge with using RAP on both systems, RAP-PC and RAP-AAM, is the bond issues caused by the presence of asphalt mortar/bitumen on the surface of the aggregates. Some researchers addressed how physical or chemical pre-treatments to the RAP could improve adherence to the paste, but few studies focused on optimising the binder. A literature survey indicated that an optimised mix design, durability studies, and life cycle assessment (LCA) are essential research needs for developing RAP-AAM. RAP-AAM is a promising solution for foundation pavement layers despite lacking research evidence.

## 2.1 Introduction

The road infrastructure comprises 21 million kilometres worldwide (World Bank Group, 2018). Huang et al. (2013) reported CO<sub>2</sub> emissions per kilometre of construction from 897 to 3228 t/km, with materials accounting for up to 92%. Natural aggregates are a non-renewable source and a major component of pavements. Any small recyclability actions may significantly reduce the environmental impact of the infrastructure sector. Currently, pavement sustainability actions comprise the employment of several types of recycled aggregates. The most used recycled aggregates are recycled concrete (Kisku et al., 2017), steel slag (Huang et al., 2007), waste foundry sand (Yazoghli-Marzouk et al., 2014), waste glass (Jamshidi et al., 2016), crushed brick (Mohammadinia et al., 2017) and reclaimed asphalt pavement (RAP) (Antunes et al., 2019).

RAP is a waste produced during asphalt road rehabilitation; Europe and the United States of America combined produced well over 100 million tons of RAP in 2017 (EAPA, 2017). In Europe, 68% of the reclaimed asphalt is reused in asphalt mixes, 19% is used as granular materials in unbound layers, 1.25% finds application in other civil engineering projects, and 11% ends in landfills (EAPA, 2017). Most studies recommend using between 20-50% of RAP as an aggregate replacement; in the US, many State Department of Transportation agencies limit the RAP content to 15% to avoid variabilities in the hot mix asphalt (Ullah and Tanyu, 2019). Zhang et al. (2019) presented a detailed review of the production process and performance of RAP-containing asphalt hot mixes. In Belgium, RAP also finds applications in cement-stabilized and loose bases / sub-bases (Van den bergh et al., 2017).

Worldwide a relatively high amount of RAP is yet not recycled and disposed of in stockpiles. Other recycling actions are in place, such as using RAP as a replacement for natural aggregates in Portland cement (PC)-based materials (mainly concrete). However, the poor adhesion of RAP granules to the cement paste compromises the concrete's mechanical and durability properties (El Euch Ben Said et al., 2017).

Alkali-activated materials (AAM) emerged as sustainable building materials to replace PC for some applications in the last two decades

(Provis, 2018). However, the environmental gain depends on the choice of raw materials, transportation, and the need for thermal curing (Adesanya et al., 2021; Habert et al., 2011; Turner and Collins, 2013). Duxson et al. (2007) reported an 80% reduction in CO<sub>2</sub> emissions compared to PC. These new binders rely on the alkaline activation of natural materials (mainly clay and metakaolin) and industrial residues or wastes (such as pulverised fly ash, ground granulated blast furnace slag, and mining residues, among others). AAM has been studied as stabilisers in base-subbase layers and is more recently employed with RAP aggregates (Kang et al., 2015b, 2015a). Although the results appear to be promising, the literature on this subject is still scarce.

Most research on sustainable materials for pavement sections focuses on the hot or warm asphalt mixtures and few emphasised the foundation layers' recycling potential. The foundation layers are thicker than asphalt layers, can consume higher volumes of recycled materials, and have lower strength requirements. The use of larger quantities of recycled aggregates represents, in general, a loss of mechanical properties (due to its different physical, chemical and mechanical properties) that need to be compensated with the use of cementitious binders or stabilisers. The most used stabiliser for base layers is PC, a material with a high carbon footprint and, therefore not sustainable. One of the possible more sustainable substitutes for PC is AAM. An adequately designed alkali-activated binder could reduce carbon footprint, high early strength, low water permeability, and higher resistance to chemical attacks (Gao et al., 2015; Mo et al., 2016). However, designing the alkaline-activated binder is not easy, especially when aspiring for sustainability: the type and amount of raw materials must be carefully selected. Miranda et al. (2020) performed a test track using AAM for the soil stabilisation of base layers and observed an equivalent mechanical performance to traditional binders (PC and lime). The authors suggested that the mix design for this kind of application must be further optimised and recommended using solid activators.

Recently there has been a significant rise in publications investigating construction materials with high RAP content and alternative binders (AAM) (Hossiney et al., 2020; Hoy et al., 2018; Jallu et al., 2020; Rahman and Khattak, 2021). The use of RAP-AAM could reduce the environmental impact of the construction industry and its costs. The main question is

whether RAP-AAM is a sustainable and suitable material for pavement layers, particularly base layers.

This review focuses on using RAP as an aggregate replacement in cement-bound pavement sections and the use of AAM as an alternative cementitious system. This chapter offers an overview of the literature published in the literature, the existing knowledge gaps, and available opportunities. Some of the topics discussed herein are:

- (i) How the research of RAP in cement-bound pavement layers has evolved.
- (ii) Which AAM is more suitable for application in pavement layers.
- (iii) Which methodologies are the most used to study RAP-AAM.
- (iv) How the performance of RAP-AAM compares with the currently used practice.
- (v) How RAP-AAM is related to sustainability.

Section 2.2 presents the state of the art of RAP-cementitious binders. It will start with the main properties of RAP, how it is being investigated as an aggregate replacement for pavement layers, and the properties of RAP in PC matrices (fresh, mechanical and durability). The use of alkali-activated binders as PC replacement will also be introduced in Section 2.2, followed by the main differences between systems with high calcium content and low calcium content, and the extent of the research so far in RAP-AAM. Section 2.3 debates the literature findings and proposes future research needs, and Section 2.4 presents the conclusion of the review.

## **2.2 State of the art**

### ***2.2.1 Reclaimed asphalt pavement (RAP)***

RAP is a material obtained during the removal of distressed pavement sections for renovation. The European standard NBN EN 13108-8:2016 defines reclaimed asphalt as ‘the processed site-won asphalt, suitable and ready to be used as a constituent material for asphalt, after being tested, assessed and classified according to this standard. The assessment includes particle size distribution, type of binder and content, presence of foreign matter (cement concrete, bricks, subbase material, synthetic

materials, metal, wood, or plastics), as well as the homogeneity and frequency of testing of the feedstock.

Milling machines may be costly and, in some developing countries, backhoes and bulldozers are often used to rip and break the pavement in an uncontrolled milling procedure. Ripping and breaking the pavement bring variations in the characteristics and quality of RAP aggregates (Kumari et al., 2018).

For many years, the production of new (hot and cold) bituminous mixes incorporates some amount of RAP. There is an indication that the replacement of natural aggregates (NA) and binder by RAP has a positive effect on rutting and stiffness and contradictory reports on the fatigue resistance of pavements (Anthonissen et al., 2016; Apeagyei et al., 2011; Colbert and You, 2012; Lopes et al., 2015; Margaritis et al., 2019; Zhao et al., 2013). Nevertheless, the employment of RAP on pavements has become common practice in many European countries such as Germany, Netherlands, Denmark and Belgium (EAPA, 2008). The employment of RAP in new asphalt mixes is beyond the scope of this review. Antunes et al. (2019) and Zhang et al. (2019) published a comprehensive study on this subject.

Despite the recent recycling activities, large quantities of unused RAP are disposed of in stockpiles or landfills worldwide (Bennert et al., 2000). Recently, it is observed an effort to promote a higher use of RAP in unbound layers and other pavement layers (base or subbase). RAP can be used as a substitute for NA, thus reducing its disposal and demand (Arshad and Ahmed, 2017). Some studies claim that the recycling of RAP could reduce the overall cost of material in a pavement layer by 40%-46% (Debbarma et al., 2019; Singh et al., 2018a).

The biggest challenge to the use of RAP on cementitious binders is due to the thin, aged bitumen coating on the surface of the aggregate, which leads to inferior properties (Arulrajah et al., 2014; Saride et al., 2016). RAP performance is often improved by blending with VA or stabilising with additives.

In general, RAP aggregates are inferior to NA regarding their gradation, strength and stiffness (Saride et al., 2016). This is mainly due to the presence of agglomerated particles and bitumen coating, and the impact that the milling procedure can have on its gradation and incorporation of dust (Arulrajah et al., 2014; Debbarma et al., 2019; Saride et al., 2016). The hydrophobic bitumen layer on the interface of the aggregate is responsible for the lower water absorption of the material and the weak bonding between the aggregate and the cementitious mortar (Brand and Roesler, 2017a; Saride et al., 2016; Singh et al., 2017; Su et al., 2014). According to Saride et al. (2016), the exposed area of aggregates ranges from 15% to 70% (averaging 34%), but the beneficiation process can help with the partial or complete removal of the asphalt mortar from the coarse aggregate. Some beneficiation methods use solvents to facilitate the cleansing of the aggregates, but those are considered expensive and unavailable at a large scale (Singh et al., 2017).

Singh et al. (2017) studied the impact of several RAP beneficiation methods on the mechanical properties of PC concrete. The authors only tested mechanical methods (i.e., did not use any solvent) such as sieving, washing and AB&AT (abrasion and attrition). In the latter, the beneficiation method involves a concrete tumble mixer fed with RAP along with several charging balls. The results found a small improvement in mechanical properties from sieving to washing and a more substantial improvement for samples produced with aggregates from the AB&AT method. PC concrete produced with treated RAP aggregates presented lower water absorption, coefficient of sorptivity, and permeable voids than the ones produced with NA. Brand et al. (2012) compared washed and "dirty" coarse RAP replacement (up to 50%) and concluded that washing did not improve the strength of the concrete.

Screening through the 4.75 mm sieve separates the coarse and fine fraction of RAP. Fine RAP is coarser than natural sand aggregates, likely due to the bitumen acting as an adhesive to fine RAP particles (Mohammadinia et al., 2016a; Singh et al., 2018a). Both fractions show lower specific gravity and bulk density than natural aggregates, possibly a consequence of the low density of the bitumen coating. The aggregates may present a higher water absorption due to the increased water demand



from the dust layer (Abraham and Ransinchung, 2018a; Debbarma et al., 2019; Singh et al., 2018a).

Age may also play a role in the properties of RAP aggregates. Singh et al. (2018c) observed that coarse RAP aggregates from new pavements yielded a concrete less workable and with worse hardened properties than an old RAP. The new RAP aggregate was from 2.5 years old pavement freshly milled, while the old aggregate was from 20 years old pavement after eight months of stockpiling. Older RAP aggregates originated from pavements that have been a long time in service or stockpiles have a more oxidised asphalt layer. Brand and Roesler (2017b) suggested that chemical oxidation could successfully modify the surface chemistry of the asphalt leading to better wettability and bonding with cement paste. The authors used an oxidation/ pre-treatment for asphalt: nitric acid ( $\text{HNO}_3$ ), sulfuric acid ( $\text{H}_2\text{SO}_4$ ), hydrochloric acid ( $\text{HCl}$ ), phosphoric acid ( $\text{H}_3\text{PO}_4$ ), potassium permanganate ( $\text{KMnO}_4$ ), maleic anhydride ( $\text{C}_2\text{H}_2(\text{CO})_2\text{O}$ ) and ultraviolet light (UV).

### ***2.2.2 The use of RAP aggregates in pavements base layers***

Pavement structure comprises several layers and all of which offer a different opportunity for the use of more sustainable materials. Despite the overall choice of the pavement structure (flexible, semi-rigid, or rigid), lower layers present higher prospects to incorporate high volumes of sustainable materials (especially cement-treated subbase/base layer) (Plati, 2019). The typical base layers can be unbound granular, asphalt treated, cement treated, permeable and recycled. Whereas subbase may be absent if there is an appropriately strong subgrade or low traffic (Su et al., 2017).

Figure 2.1 illustrates the typical/possible cross-sections of different types of pavements (Plati, 2019). Sustainable actions on materials for those pavement layers mostly consider replacing natural aggregates for recycled ones and also replacing PC used as binder/stabiliser with sustainable binders.

RAP and other recycled aggregates are a suitable alternative when opting for unbound layers (layers GB and GS in Figure 2.1). However, the most significant opportunity to use a combination of RAP with AAM for pavement layer is while considering cement-treated bases (such as layers CT and maybe GS) and concrete layers (RC, LC and LCL).

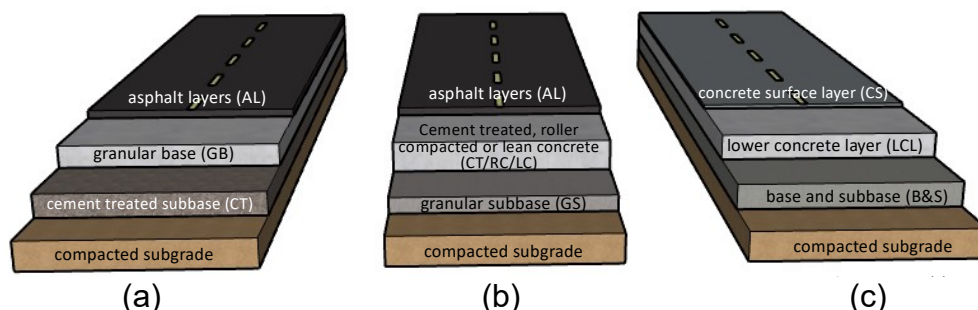


Figure 2.1. Typical cross-section of pavements (a) flexible, (b) semi-rigid and (c) rigid pavements. Modified from Plati (2019)

When used as unbound aggregate, studies show that 100% RAP reduces the strength and increases the permanent potential deformation of the unbound bases (Thakur et al., 2012). Seferoğlu et al. (2018) have found that the performance significantly increases with 3% PC treatment. According to the authors, RAP- 3% PC and 20% RAP – 80% NA have similar deformation performance, which was 50% less than that of a conventional base course made with 100% NA.

The strain capacity appears to be also a function of the binder content present on the RAP particles (Ullah and Tanyu, 2019). Arshad and Ahmed (2017) presented results from other authors who systematically agree that RAP addition to NA will (i) decrease the dry density, (ii) decrease the bearing capacity (measured by the California Bearing Ratio) and (iii) increase the resilient modulus<sup>1</sup>.

Roller compacted (RC), and lean concrete (LC) concrete with RAP aggregates are also an alternative for wearing courses in semi-rigid pavements (see Figure 2.1). A 50% RAP replacement in RC concrete (fine

---

<sup>1</sup> Defined as a ratio of deviator stress to the resilient strain experienced by the material under repeated loading simulating traffic load (Arshad and Ahmed, 2017).

and coarse aggregates) reduced the 28 days compressive strength and conversely increased the flexural strength (Settari et al., 2015). According to Debbarma et al. (2019), RAP aggregates also help reduce the permeable voids, and water absorption in RC concrete, as well as lowering the cost per cubic meter by 6%. However, the cost reductions by employing RAP aggregates may be overtaken by the need to increase the (more costly) binder content. Singh (Singh and Ransinchung, 2020) investigated dry lean concrete and observed that the mixes required at least 50% extra PC to compensate for the strength loss caused by 100% coarse RAP replacement.

The term full-depth reclamation (FDR) is found in the literature to designate stabilised bases composed of recycled RAP together with parts of underneath aggregates (Antunes et al., 2019; Ghanizadeh et al., 2018). The study by Castañeda López et al. (2018) shows that the addition of RAP in the cement-treated base as FDR may reduce the flexural strength but leads to more ductile behaviour. The fatigue life of cement-treated RAP depends much on the composition (PC and RAP content) and the thickness of the layer. Consequently, it is possible to use higher RAP content by playing with other variables (PC content and thickness).

### ***2.2.3 RAP aggregates in PC matrices***

Most studies on RAP as an aggregate replacement choose between replacing either the fine or the coarse fraction (see Table 2.1). The level of replacement also varies, and a combination of RAP aggregates and natural aggregates is often employed. Overall, the employment of RAP aggregates in PC-based matrices has a significant effect on both fresh and hardened state (Guo et al., 2018).

Table 2.1. RAP replacement in PC matrices and strength results - 28 days (ELAS: elastic modulus, LON: longitudinal dynamic modulus, TRAN: transverse dynamic modulus)

Author	Type of RAP	Replacement	w/c	Compressive (MPa)	Splitting tensile (MPa)	Modulus (GPa)
Su et al. (2014)	Coarse + Fine	0%	0.5	42.06	3.38	34.8 ELAS
		20%	0.5	31.21	2.90	26.8 ELAS
		40%	0.5	23.12	2.28	19.9 ELAS
		70%	0.5	17.33	1.90	14.5 ELAS
Brand and Roesler (2017b)	Fine	100%	0.5	11.93	1.51	10.5 ELAS
		100%	0.42	15.89	2.42	25.84 LONG 25.98 TRAN
Shi et al. (2017)	Coarse (different sources)	0%	0.40	33.61	4.39	32.95 ELAS
		20%	0.40	23.78-30.54	4.2-4.5	27.1-30.4 ELAS
		40%	0.40	17.77-26.97	3.1-3.9	24.1-26.1 ELAS
Thomas et al. (2018)	Coarse	0%	0.47	73.8	-	-
Abraham and Ransinchung (2018a)	Fine	25%-50%	0.47	47.4-30.1	-	-
		0%	0.44	~51	~4.9	-
		25%-100%	0.44	~46-34	~3.3-2.3	-
Singh et al. (2018c)	Ref	0%	-	17.8	-	-
	Coarse/ Old	25%-100%	-	~13-9.0	-	-
	Coarse/ New	25%-100%	-	~11-5.3	-	-
	Fine/ Old	25%-100%	-	~11-7	-	-
	Fine/ New	75%-100%	-	~5.5-4	-	-
Singh et al. (2018a)	Ref	0%	0.38	~43	~4.6	-
	Fine	50%	0.38	35.3	~2.6	-
		100%	0.38	27.2	~3.7	-

Author	Type of RAP	Replacement	w/c	Compressive (MPa)	Splitting tensile (MPa)	Modulus (GPa)
Hossiney et al. (2010)	Coarse + Fine	0% 10-40%	0.53 0.53	38.58 34.03-17.38	3.73 3.11-2.34	32.95 ELAS 27.6-16.2 ELAS
Shatarat et al. (2019)	Coarse	0% 20-100%	0.57 0.57	~46 ~45-30	- -	- -
Debbarna et al. (2019)	Reference	0%	0.37	~37	~4.2	-
	Coarse	50%	0.36	~28	~3.6	-
		100%	0.35	~25	~3.2	-
	Fine	50%	0.40	~39	~2.6	-
		100%	0.39	~32	~2.8	-
	Coarse + Fine	50%	0.40	~29	~2.8	-
		100%	0.41	~23	~2.2	-
Huang et al. (2005)	Reference	0%	0.5	37.7	3.21	-
	Coarse	100%	0.5	22.1	3.06	-
	Fine	100%	0.5	18.8	2.54	-
El Euch Ben Said et al. (2018)	Coarse + Fine	100%	0.5	10.4	1.59	-
		0%	0.6	30.1	3.1	31.1 ELAS
		20%	0.6	23.8	2.8	28.9 ELAS
	Coarse + Fine	40%	0.6	20.7	2.3	24.6 ELAS
		60%	0.6	16.7	2.2	22.3 ELAS
		75%	0.6	13.7	2.0	20.1 ELAS
Papakonstantinou (2018)	Reference	100%	0.6	11.4	1.7	14.5 ELAS
	Fine	0%	0.45	~34	-	28.52 ELAS
	Coarse + Fine	20-100% 5-15%	0.45 0.45	~33-24 ~30-28	- -	26.8-22.9 ELAS 26.9-30.0 ELAS
Brand et al. (2012)	Coarse	0%	0.37	46.0	6.3	44.4 ELAS
		20%	0.37	37.2	4.7	37.4 ELAS
		35%	0.37	32.7	3.4	31.9 ELAS
		50%	0.37	27.9	3.0	30.9 ELAS

Singh et al. (2018a) studied the incorporation of coarse and fine RAP into PC concrete and found a significant reduction in the workability of samples. The strength reduction was more substantial with the employment of the fine fraction. When compared with concretes containing NA, the replacement of 100% coarse RAP reduced the slump by 29%, while 100% fine RAP reduced the slump by 100%. The authors attributed this to the absorption of the mixing water by the dust that accumulated on RAP during stockpiling. A reduction in workability was also observed by other authors (Guo et al., 2018; Su et al., 2014), although opposite findings were also reported (Brand et al., 2012; Huang et al., 2005; Shi et al., 2017). In general, it is still not clear how the following different parameters affect the workability of the fresh product: (i) hydrophobic properties and the high viscosity of the bitumen layer on the aggregate surface; (ii) high water demand of the adhered dust layer and (iii) the particle shape of the aggregates

Through the production of RAP-PC, it is possible to observe the formation of three interfacial transition zones (ITZ) in the microstructure: between (i) the aggregates and bitumen layer, (ii) aggregates and cementitious matrix, and (iii) the bitumen layer and cementitious matrix (Figure 2.2). The weakest ITZ is the one formed between bitumen and cementitious matrix (El Euch Ben Said et al., 2018; Singh et al., 2018a). Brand and Roesler (2017a) observed that ITZ changed as the samples aged; over time the samples with RAP developed higher porosity, larger ITZ width, and fewer hydrates. The authors suggested that the high pH of the pore solution could leach organic compounds from the asphalt, which compromises the hydration process and formation of calcium hydroxide (CH) and calcium silicate hydrate (C-S-H). The consequence is the weakening of the ITZ over time. Fracture samples with RAP have shown that most of the cracks propagated within the bitumen and aggregate (Brand and Roesler, 2017b) instead of an adhesive failure of the bitumen-cement paste.

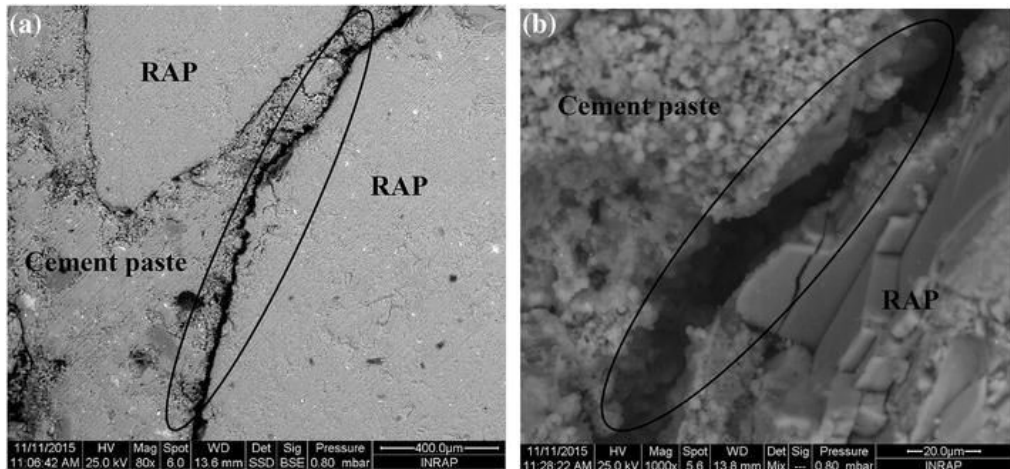


Figure 2.2. - ITZ SEM (Scanning Electron Microscopy) x80(a) and x1000(b) magnification (El Euch Ben Said et al., 2018)

Therefore, the use of fine and coarse RAP aggregates in the production of PC concrete can drastically reduce the mechanical properties, such as compressive strength, splitting tensile strength, and elastic modulus, as well as increase the toughness of the material (Abraham and Ransinchung, 2018a; Singh et al., 2018a, 2018c; Su et al., 2014). Concretes with 20-50% coarse aggregate replacement presented 30-60% compressive strength reduction (Thomas et al., 2018).

Some authors observed that the use of fine RAP to produce mortars could cause high shrinkage, a reduction of 41.7% on compressive strength, 39.3% on flexural strength, and 51.5% on splitting tensile strength (2018a; Shi et al., 2020). Nevertheless, RAP-mortars also showed better ductility, toughness and crack resistance when compared to NA-mortars (Shi et al., 2020).

In general, the coarse RAP fraction is less detrimental to the mechanical properties (Singh et al., 2018a). However, the study of Debbarma et al. (2019) on RC concrete, found that fine RAP mixes had a better compressive strength performance than the ones with coarse RAP. The improvement in strength was most likely due to the specific properties of the fine RAP used, such as low bitumen content and better gradation.

The inclusion of RAP on concretes and mortars reduces the splitting and flexural strength of the samples, which is more prominent when fine RAP

is used (Abraham and Ransinchung, 2018a; Debbarma et al., 2019; Su et al., 2014). However, the percentage reduction in flexural strength is lower than in compressive strength (Brand et al., 2012; Shi et al., 2017). It is believed that better flexural performance is due to the visco-elastic nature of the bitumen coating, which also is responsible for an increase in the toughness of the mixes (Huang et al., 2005).

Shatarat et al. (2019) tested concrete columns and observed a 31.06% reduction in the compressive load capacity in comparison with the control sample. The RAP samples also showed less cracking and lower spalling. The coefficient of thermal expansion and drying shrinkage does not seem to be impacted by the use of RAP aggregates (Hossiney et al., 2010).

- ***Durability***

The porosity of mortars increases in the presence of fine RAP aggregates due to the more porous and larger ITZ. Mercury intrusion porosimetry (MIP) analysis showed an increase in mesopores and macropores. According to Abraham and Ransinchung (2019), the threshold diameters<sup>2</sup> and large capillaries decreased up to 50% RAP replacement, followed by an increase of both after that, suggesting a higher risk for chemical ingress (Abraham and Ransinchung, 2019).

The presence of coarse RAP decreases the water absorption on concretes, the concentration of total permeable voids, and sorptivity (Debbarma et al., 2019; Singh et al., 2018a). However, Abraham and Ransinchung (2018a, 2018b) noted that this behaviour was in contradiction with the higher porosity of the RAP aggregates. The authors suggested that the decrease in sorptivity was due to the molten asphalt clogging the pores of the samples during oven drying. To avoid the melting of the asphalt present in RAP, the authors have adopted a different preparation procedure, and vacuum dried the samples at 35°C. Singh and Ransinchung (2018) suggested oven drying at 48°C for eight days.

---

<sup>2</sup> Threshold diameter is the pore size through which mercury penetrates the bulk of the sample, i.e., the equivalent pore size corresponding to the steepest slope of the curve (Cook and Hover, 1993; Winslow and Diamond, 1969).



The inclusion of fine RAP can significantly impact the abrasion resistance of concrete samples; there is a 75% reduction in abrasion resistance when 100% RAP replacement is employed (Singh et al., 2018b). Still, samples produced with either coarse or fine RAP mixes produced enough abrasion resistance to be used as pavement's wearing course (Debbarma et al., 2019).

The replacement of NA with fine RAP had an impact on the pH of the hardened concrete; the pH reduces as the replacement level increase. This reduction is reported to be subtle (up to 3.8%), and all RAP-PC still present pH values above 12 (Singh et al., 2018b). No carbonation was observed after 120 days of moist curing (Debbarma et al., 2019; Singh et al., 2018b).

Under sulphate attack, RAP-PC concrete samples also showed a higher mass and strength loss than the reference PC concrete, with rates increasing with RAP content (Abraham and Ransinchung, 2018b; Debbarma et al., 2019). Singh et al. (2018b) reported a weight loss of nearly 11.26% for concrete samples produced with 100% fine RAP replacement under  $H_2SO_4$  exposure.

The freeze and thaw resistance of PC concrete is associated with the concrete's ability to withstand the water expansion inside its pores and cracks during thermal cycling. It is also related to the material's pore structure. In that sense, the higher percentage of air voids in RAP-PC concrete is beneficial and can help accommodate the expanding freezing water without damage to the matrix. Guo et al. (2018) and Thomas et al. (2018) reported an increase in freeze-thaw resistance when NA is replaced by RAP aggregates, while Brand et al. (2012) observed a reduction.

#### ***2.2.4 Alkali-activated materials as binders***

The term alkali activation may be applied to the reaction between any precursor and an alkali activator to produce a new binder (Liew et al., 2016; Provis, 2018; Rashad, 2013a). Precursors are usually in powder form and may be occurring in natural pozzolans, calcined clays, or industrial by-products and wastes, such as granulated blast furnace slag,

granulated phosphorus slag, steel slag, coal fly ash, volcanic glass, zeolite, metakaolin, silica fume and non-ferrous slags (Provis, 2018; Shi et al., 2011). Depending on the precursor's Al and Ca content, AAM may be further classified as inorganic polymers or geopolymers (Figure 2.3), or simply as low-calcium (low-Ca) and high-calcium (high-Ca) AAM. As for activators, the most frequently used are sodium silicate, sodium hydroxide, sodium carbonate, potassium hydroxide, and potassium silicate (Rashad, 2013b). Hoy et al. (2018, 2016b) observed that the presence of sodium silicate in the alkali solution increased the speed of the alkaline activation. However, the ideal amount of activators may vary according to the type of precursor, and excess activator results in loss of strength (Adhikari et al., 2018).

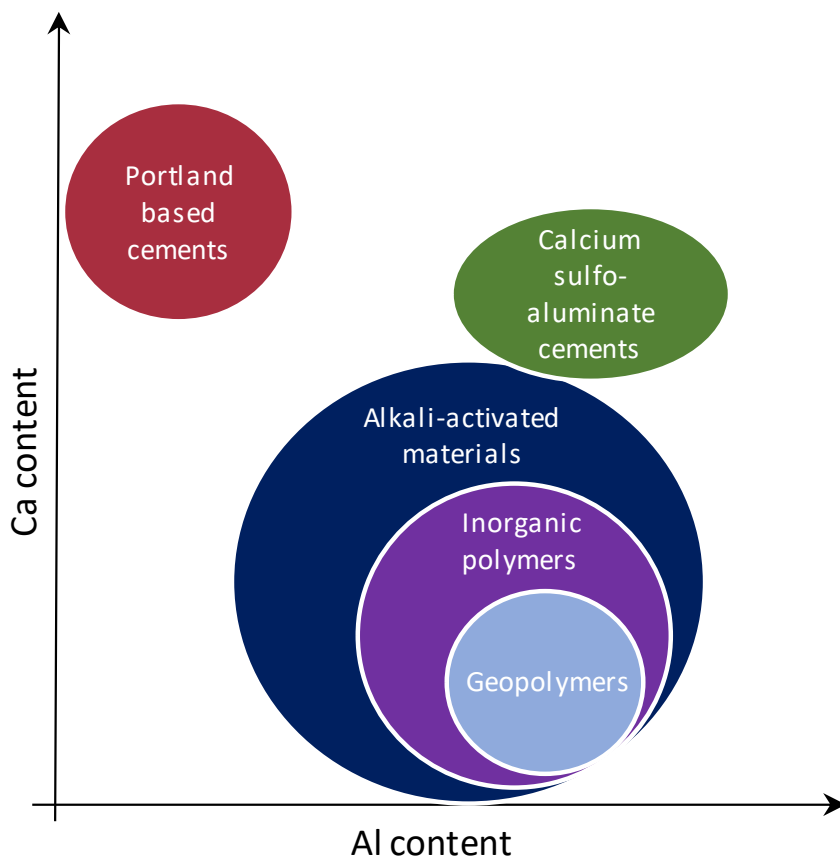


Figure 2.3. Classification of AAM and comparison with other systems (modified from Van Deventer et al., 2010)

- ***Ground Granulated Blast Furnace Slag (BFS) and Metakaolin (MK) based AAM***

High-Ca AAM is mainly represented by the alkali-activation of BFS, while low-Ca AAM is commonly produced with pulverised fly ash (PFA) and metakaolin (MK). This section will compare the activation of BFS and MK as examples of high and low-Ca systems.

BFS is a latent hydraulic material and, as such, it requires water and a minimal amount of a catalyst or activator to show cementitious properties. When mixed with PC, BFS is activated by the calcium hydroxide and alkalis formed during the hydration of the cement. In the absence of PC, the activation is carried out using an alkali solution made with an alkali hydroxide, silicate, carbonate, or sulphate, but combining sources (sodium hydroxide and sodium silicate) can yield even higher strength results (Fernández-Jiménez et al., 1999). Wang, Scrivener and Pratt (1994), employed individual activators and concluded that sodium silicate solution with silica modulus<sup>3</sup> from 1 to 1.5 achieved the best mechanical performance. When using sodium hydroxide, the authors recommended keeping the Na<sub>2</sub>O concentration within 3 and 5% by slag weight. They reported that lower Na<sub>2</sub>O percentages might delay the activation process, while higher values may result in efflorescence and brittleness.

The chemical process from alkali-activation is entirely different from the reactions involved in PC hydration. Many researchers have contributed to a better understanding of this chemical mechanism, but the activation process is not yet fully understood. A full description of the reaction mechanism is beyond the scope of this study and can be found elsewhere (Farhan et al., 2020; Garcia-Lodeiro et al., 2015; Provis and Bernal, 2014). Figure 2.4 outlines the key processes and products of alkali-activation.

The activation of any aluminosilicate starts with the dissolution of the solid particles by hydrolysis and produces aluminate and silicate species. The high pH of the medium accelerates the dissolution and quickly supersaturates the solution (Puertas et al., 2011). However, the activator's

---

<sup>3</sup> SiO<sub>2</sub>/M<sub>2</sub>O molar ratio, where M is an alkali metal.

pH plays a different role in calcium solubility (high-calcium systems). The high pH reduces the solubility of the calcium species as supersaturation is reached for portlandite (Provis and Bernal, 2014). This concentrated solution leads to the formation of a gel, and the systems continue to rearrange to form a three-dimensional aluminosilicate network (P. Duxson et al., 2007). During the nucleation step, ongoing reactions favour gel growth, and precipitation (Shi et al., 2011).

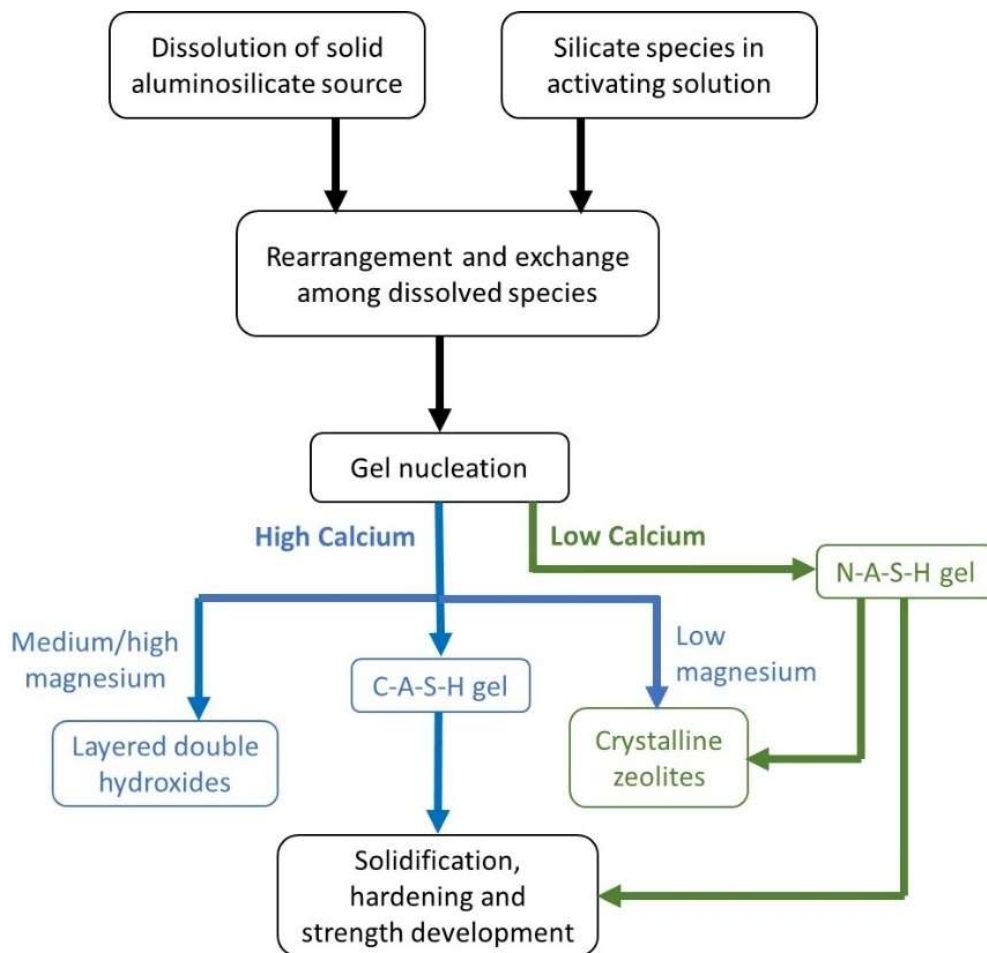


Figure 2.4. Process and reaction products of AAM – high and low calcium systems (modified from (Provis and Bernal, 2014) )

The main reaction product formed by alkaline activation of BFS is calcium (alumino)silicate hydrate (also known as C-A-S-H type gel), and secondary phases such as layered double hydroxides and a sodium aluminosilicate N-A-S-(H) type gel (can also show the substitution of

potassium) (Fernández-Jiménez et al., 2003; Provis, 2018; Provis and Bernal, 2014; Wang and Scrivener, 1995). The tetrahedrally coordinated silicate chains from the C-A-S-H gel are longer (compared to the C-S-H gel from PC), and there is a substitution of the bridging silicon by aluminium. This substitution caused a charge imbalance that is compensated by the alkali ions in the gel (Puertas et al., 2011).

According to the literature, an adequately designed alkali-activated slag shows improvements in many properties compared to PC – higher strength, more resistance to acids, sulphates, or chlorides and fire resistance (Shi et al., 2011). However, slag-based AAM may also present some issues such as rapid setting, high shrinkage, the formation of micro-cracks, the possibility of alkali-aggregate reaction and high efflorescence (Fernández-Jiménez et al., 1999). The addition of superplasticisers and water reducers designed for PC into AAM seems to have a negligible effect on workability and setting time (Shi et al., 2011).

Metakaolinite ( $\text{Al}_2\text{Si}_2\text{O}_7$ ) also known as metakaolin (MK) is a product from the dihydroxylation of an aluminosilicate clay mineral kaolinite ( $\text{Al}_2(\text{Si}_2\text{O}_5)(\text{OH})_4$ ) at a temperature of between 450 - 800°C. During calcination, the kaolinite releases  $\text{OH}^-$  from its structure, which becomes amorphous and reactive. MK has CaO as impurities; it is a system composed mainly of (Si+Al), while BFS is a (Si+Al+Ca) system (Li et al., 2010). Like other pozzolans, MK does not have cementitious properties, but when used with PC, it is a highly reactive pozzolan that reacts with the hydrated lime to form C-S-H (Ramachandran et al., 2002). The addition of MK to PC-based systems can improve the mechanical strength, reduce the pore structure and mitigate some chemical attacks, such as alkali-silica reaction (Ambroise et al., 1994; Komnitsas and Zaharaki, 2007).

MK is also suitable for alkali activation yielding a material with high compressive strength, elastic modulus and lower porosity. The best properties are achieved in the presence of soluble silicates with the silica moduli of the final solution between 1 and 2 (Provis and Bernal, 2014). The reaction sequence of low calcium systems (green path in Figure 2.4) is similar to the one for high calcium, but the main reaction product is an alkaline aluminosilicate hydrate (N-A-S-H gel) with zeolite-like secondary phases. The N-A-S-H gel is considered an amorphous three-dimensional

framework of both  $\text{SiO}_4$  and  $\text{AlO}_4$  tetrahedrally coordinated and randomly interlinked by shared O atoms. The metal cations from the alkali solution ( $\text{Na}^+$  or  $\text{K}^+$ ) compensate for the negative imbalance caused by the four-coordinated Al (Barbosa et al., 2000; Lecomte et al., 2006). The absence of (or low content) calcium hinders the formation of crystalline phases associated with expansions (ettringite and gypsum), and the end products have better chemical stability (Alcamand et al., 2018). When properly designed, the final polymeric product has a quicker setting time, higher compressive strength, better resistance to seawater and sulphate attack, and higher heat resistance than PC systems (Alcamand et al., 2018; Rashad, 2013a).

Nevertheless, the alkaline activation of MK represents a higher environmental impact than the activation of BFS. First, kaolin clay is a natural material, and its utilisation represents the depletion of natural resources. Secondly, the calcination of kaolinite demands the burning of combustible fuels, which then release  $\text{CO}_2$ . MK activation mainly requires sodium silicate to provide the soluble silica to accelerate the hardening; however, the production of silicates is itself a heavy environmental burden (Habert et al., 2011). Because of all that, BFS is the preferable aluminosilicate over MK, when the first is available. The mix of BFS and MK (binary system) is a potential solution to achieve an end material with high compressive strength, lower porosity (Borges et al., 2016) and lower shrinkage than alkali-activated slag (Li et al., 2019). Binary systems show improvement in properties while still reducing the amount of alkaline activator needed for neat MK activation. Figure 2.5 shows that the activation of blended MK/BFS favours the formation of a denser matrix composed of C-A-S-H and N-A-S-H gels, which improves the overall properties (Borges et al., 2016; Li et al., 2019).

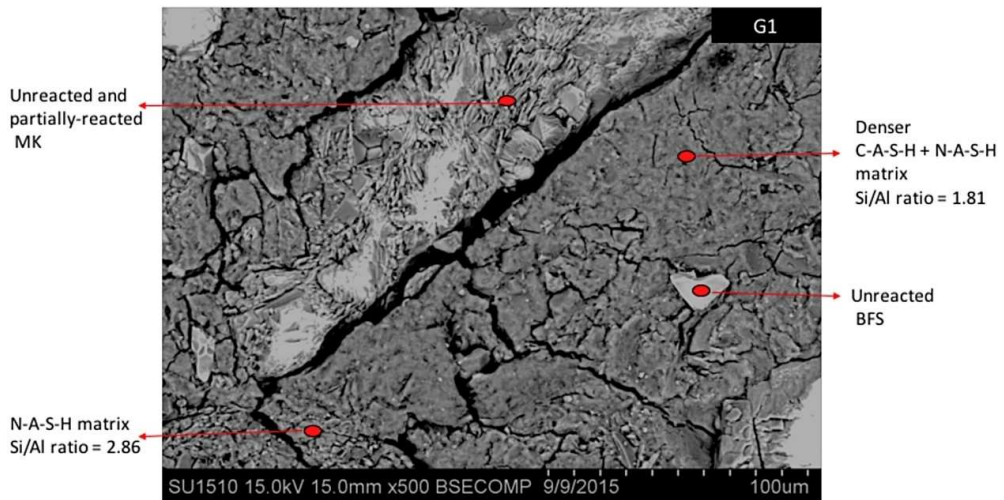


Figure 2.5. EDX spot analysis of MK+BFS systems (Borges et al., 2016)

### 2.2.5 RAP and alkali-activated materials

Many researchers have successfully studied the incorporation of RAP in base layers for pavement sections; for high replacement levels, the loss of mechanical properties needs to be compensated by using stabilisers, i.e. agents that increase the compressive and impact strength, as well as the overall integrity of the layers (reduction of swelling, shrinkage, abrasion) (Arulrajah et al., 2014; Avirneni et al., 2016). It is possible to stabilise RAP using materials such as lime, cement, fly ash, blast furnace slag, rice husk ash, sugar cane bagasse ash, among others (Adhikari et al., 2018; Consoli et al., 2018; Poltue et al., 2019; Singh et al., 2018a). The stabiliser's content varies depending on the type of stabiliser employed, but it usually ranges from 4% to 30% in mass of RAP (see Table 2.2). While the high dosage of Ca-rich stabilisers is discouraged - it causes shrinkage, cracking and failure of the pavement - the use of low-Ca stabiliser may not impair sufficient strength. Therefore, sometimes, it is possible to employ alkali activation to meet the strength requirement for base materials (Avirneni et al., 2016). The use of alkali activation in RAP base layers may help compensate for the strength loss.

Table 2.2 – Summary of the studies on alkali-activated matrices containing RAP (UCS: unconfined compressive strength)

Author	RAP: NA	Stabiliser		Alkali activator		UCS28 days (MPa)
		Type	Quantity	Type	Quantity	
Jallu et al. (2020)	60:40	PFA	20%	NaOH (3M) NaOH: Na <sub>2</sub> SiO <sub>3</sub> – 50:50 NaOH: Na <sub>2</sub> SiO <sub>3</sub> – 70:30	0.50 0.54	~6.2 ~6.5
Hoy et al. (2016b, 2016a)	100:0	PFA	20%	NaOH (10M) NaOH:Na <sub>2</sub> SiO <sub>3</sub> – 90:10 NaOH:Na <sub>2</sub> SiO <sub>3</sub> – 60:40 NaOH:Na <sub>2</sub> SiO <sub>3</sub> – 50:50	-	~3.9 ~4.0 ~4.9 ~5.6
Saride; Avirneni; Challapalli (2016)	80:20	PFA	20%-30%	NaOH	2-4%	~4.3 – 4.9
Avirneni; Peddinti; Saride (2016)	80:20		30%			~4.7 – 5.1
	60:40		20%			~4.6 – 5.7
	60:40		30%		2-4%	~5.0 – 5.4
Mohammadinia et al. (2016b)	100:0	PFA +BFS	4% 2%+2% 2%+2% 2%+2%	NaOH: Na <sub>2</sub> SiO <sub>3</sub> NaOH: Na <sub>2</sub> SiO <sub>3</sub> NaOH: Na <sub>2</sub> SiO <sub>3</sub> NaOH: Na <sub>2</sub> SiO <sub>3</sub>	L/B = 0.3-0.5 L/B = 0.3 L/B = 0.4 L/B = 0.5	~1.4 ~1.6 ~1.7 ~1.6
Mohammadinia et al. (2016a)	100:0	BFS	4%	NaOH: Na <sub>2</sub> SiO <sub>3</sub>	L/B = 0.3-0.5	~1.9
	100:0	PFA	4%-16%	NaOH (8M) Na <sub>2</sub> SiO <sub>3</sub> /NaOH = 2.5	L/B = 0.4	~1.2-1.4 (7 days)
Horpibulsuk (2017)	100:0	PFA	20%, 30% 20%, 30% 20%, 30% 20%, 30%	NaOH (10M) NaOH:Na <sub>2</sub> SiO <sub>3</sub> - 90:10 NaOH:Na <sub>2</sub> SiO <sub>3</sub> - 60:40 NaOH:Na <sub>2</sub> SiO <sub>3</sub> - 50:50	- - - -	~4 – 5 ~4 – 4.3 ~5 – 5.5 ~5.5 – 6



Author	RAP: NA	Stabiliser		Akali activator		UCS28 days (MPa)
		Type	Quantity	Type	Quantity	
Hoy et al. (2018)	100:0	BFS	10-20%	NaOH (8M)	-	~1.1 - 2.0
			10-20%	NaOH:Na <sub>2</sub> SiO <sub>3</sub> - 70:30	-	~1.0 - 2.3
			10-20%	NaOH:Na <sub>2</sub> SiO <sub>3</sub> - 60:40	-	~1.7 - 3.0
			10-20%	NaOH:Na <sub>2</sub> SiO <sub>3</sub> - 50:50	-	~1.5 - 2.2
Adhikari et al. (2018)	0:100	-	-	-	-	1.4
	0:100	PFA	15%-25%	-	-	1.6-5.38
	0:100	PC	5%-10%	NaOH (6-8M)	-	1.02-3.20
	15:85	PFA	0-25%	Na <sub>2</sub> SiO <sub>3</sub> /NaOH (0-0.5)	-	1.62-4.98
	25:75	-	-	-	-	-

The literature on the alkaline activation of base pavement layers containing RAP materials is still limited. Hoy et al. (Hoy et al., 2016b) and Horpibulsuk et al. (2017) presented results of alkali-activated base courses made with RAP and stabilised with high calcium ( $\text{CaO} > 10\%$ ) PFA. The SEM and XRD analysis indicate that the main activation products were C-A-S-H and N-A-S-H gels, and that the coexistence of both hydrates increased the strength, which was proportional to the  $\text{Na}_2\text{SiO}_3$  content. The absence of silicates resulted in low geopolymerisation for RAP-PFA systems, as in conventional alkali-activated concretes (Hoy et al., 2016b). The authors also found that C-S-H as a hydration product in systems with a higher calcium content such as those with BFS (Hoy et al., 2018).

These preliminary studies also conclude that similarly to the RAP-PC systems, the presence of the bitumen layer is detrimental to the binding of RAP to the matrix. In other words, the RAP particles presented better bonding to the matrix for exposed aggregate surfaces. Hence, better performance may be achieved if a milling procedure guarantees a higher exposed aggregate area (Saride et al., 2016).

While studying the incorporation of RAP and PFA on different types of soil for road base and subbase layers, Adhikari (2018) observed that an increase in the PFA and RAP content increased the strength of the geopolymer mixture up to 7 times compared with untreated soil. The elastic modulus and fracture energy also increased. However, when compared with PC stabilised samples, the alkali-activated ones were more flexible and presented lower compressive strength and stiffness (Mohammadinia et al., 2016b). Other authors also observed the positive effect of increasing the PFA content (Horpibulsuk et al., 2017; Mohammadinia et al., 2016a). Curing conditions also appear to have a significant impact on the mechanical properties, since it increases de dissociation (reactivity) of the phases. Alkali-activated RAP samples cured for seven days at  $40^\circ\text{C}$  presented approximately 70% higher strength than reference samples cured at room temperature (Mohammadinia et al., 2016a). However, high-temperature curing is not practical for on-site applications. The flexural behaviour of the RAP-AAM bases can be improved with the use of geogrids up to 2.54 times (Jallu et al., 2020).

Wet-dry cycles are commonly used to simulate weather changes over time and estimate durability. Avirneni et al. (2016) observed that activated PFA as stabilisers for RAP: NA mixes had an acceptable performance under aggressive wet/dry cycles, with less than 10% weight loss. Alkali-activated systems presented lower weight loss on wet-dry cycling than non-activated ones. After six wet/dry cycles, the formation of macro- and micro-cracks caused a strength reduction, which was more significant for lower NaOH contents (Hoy et al., 2017).

One large environmental concern when using wastes and alkali-activated materials is the possibility of contamination of soil and watercourses due to the leaching of alkalis and heavy metals. The durability of base layers may also be affected by the leaching of stabilisers during their service life. Preliminary studies comparing the leaching of stabilised RAP with and without alkali activation have concluded that the environmental impact on soil and groundwater is minimal. The studies assessed the leaching of heavy metals, pH, and sodium, concluding that the employment of an activator has reduced the leachability of metals from the aluminosilicate source. (Avirneni et al., 2016; Horpibulsuk et al., 2017; Hoy et al., 2016b)

## 2.3 Reflections from literature

Even with the current recycling efforts, the construction industry has been unable to consume all the produced RAP, and more recycling alternatives are needed. The use of RAP for unbound base layers represents a reduction in strength. Attempts to compensate for this reduction often mean:

1. Blending it with virgin aggregate, reduces the volume of recycled materials used and therefore reduces the sustainability prospect of the solution.
2. Using binders or stabilisation. PC will add an environmental burden to the solution (reference needed here or above in text); supplementary cementitious materials (such as PFA, BFS and rice husk ash) take a longer time to react and may not add sufficient strength.

The presence of the thin bitumen coating on the surface of the RAP aggregate is the main reason for the cementitious binder's inferior performance. The bitumen weakens the ITZ, making it larger and more porous. RAP beneficiation methods targeting the increase of the exposed aggregate surface could represent a significant gain in strength. While the more porous ITZ could represent a gain in freeze and thaw resistance, it also compromises durability by permitting the ingress of harmful substances. RAP beneficiation methods targeting the increase of the exposed aggregate surface could represent a significant gain in strength and durability of RAP-PC.

The literature on RAP with AAM is very scarce, and some important factors remain unanswered such as the effect of type of aluminosilicate, activator, RAP beneficiation, and gradation. Similar to RAP-PC, the porous ITZ is also a reason for durability concerns. However, it is unclear if different precursors and alkali solutions could improve the binding between the different ITZ sections. The use of a properly designed AAM may promote the recycling of RAP by increasing the early strength, creating a denser and more resistant (durability) matrix. The application of AAM is very similar to PC, and minor changes in the construction practice are expected. However, the costs associated with the transportation of the alkali solution must be considered.

### ***2.3.1 Potential, challenges and research gaps on RAP-AAM***

This section covers important topics that have not been addressed so far for the future development of RAP-incorporated alkali-activated materials. Nevertheless, they are essential to determine the potential application of those new materials by the pavement industry. The following section also highlights future research gaps.

- ***Cost and availability of local materials***

Different from the employment of lime or Portland cement as binders for the stabilisation of aggregates, AAM depends on the availability and costs of the alkaline solutions and precursors used (aluminosilicates). In that sense, the overall cost to develop RAP-AAM may surpass the benefits of

some countries. Sodium silicate and sodium hydroxide, the most common activators used in AAM, are expensive chemicals in some countries, where AAM has barely become viable for most the possible applications (Van Deventer et al., 2012). Each country may have to select the available sources of aluminosilicate. Calcium-rich materials (industrial by-products or wastes) are preferred because they tend to reduce the demand for alkaline solutions. So, the employment of blast-furnace slag or high-calcium PFA may be an option to consider. Agricultural residues such as rice husk ash or sugarcane bagasse ash may be viable and inexpensive options for developing countries (Brazil, India, and other Asian countries), as they are interesting raw materials for alkaline activation (Moraes et al., 2016; Sturm et al., 2016). However, they are usually low calcium and low alumina reactive materials, which therefore depend on another source of  $\text{Al}_2\text{O}_3$  and high amounts of activators.

The activation may be carried out using blended (or hybrid) systems, e.g., small amounts of lime or a reduced amount of PC to promote the activation with a minimum amount of alkalis and enhance the final properties (Tailby and MacKenzie, 2010; Temuujin et al., 2009). The study of those blended systems with RAP aggregates is not available, and it is a potential topic for investigation.

- ***Performance and durability of RAP-AAM***

The performance and durability of any RAP-AAM system are closely associated with the amount and gradation of RAP used as aggregates, together with any beneficiation methods employed to the former. These variables determine the adhesion and ultimately, the mechanical performance of RAP to AAM matrices. The choice of low calcium or high-calcium precursors (and consequently the amount and type of activators) may also play an important role in the mechanical and durability properties. None of these topics has been systematically addressed so far in the published literature and represent essential research needs before the implementation of RAP-AAM pavement layers.

Long-term or accelerated durability tests employed on current pavement layers are also required to determine the durability of RAP-AAM under mechanical stresses (fatigue, rutting resistance) (Van den bergh et al.,

2017) as well as weather conditions such as freeze-thaw cycling (Hoy et al., 2017). Needless to mention the importance of assessing the susceptibility to delamination of RAP-AAM concrete base from the asphalt surface layer in semi-rigid pavements, stabilising a comparison with traditional Portland cement concrete (Chabot et al., 2013).

Leaching of alkalis with consequent contamination of soil and groundwater are questions to be answered as well. Leaching is a function of the type of precursor and amount of alkalis used; in general, it should not present an issue if the alkali content is limited. On the other hand, alkali-activated matrices have proven to be suitable to encapsulate heavy metals and toxic waste (Ji and Pei, 2019); thus, the leaching of undesirable species could even reduce, including some contaminants in the RAP aggregates.

- ***Life cycle assessment (LCA) of RAP-AAM***

Another object of future research is the life cycle assessment of RAP-AAM pavement layers. The environmental impact of AAM as a replacement for PC has been widely discussed (Habert and Ouellet-Plamondon, 2016; Van Den Heede and De Belie, 2012), and the benefits are dependent on the precursor and amount of solution employed. The same applies to RAP-AAM, an LCA comparing RAP-AAM, traditional RAP-stabilised layers and Portland cement concrete base layers must be subject to future studies. LCA should be combined with the cost analysis to determine when RAP-AAM is viable. So far, it is not possible to say if the challenges to design and specifying RAP-AAM pavements would be both technically acceptable and economically feasible. Future research should definitively address these questions.

## **2.4 Conclusions**

This chapter presents the findings of a literature review on the use of RAP aggregates on cement-bound systems. The investigation was an overview of the impact caused by using RAP aggregates on Portland cement and alkali-activated matrices. The main objective was to identify if RAP-AAM could be a suitable base layer of pavements while also proving a more sustainable alternative (higher RAP replacement levels and lower environmental impact) than RAP-PC.

Similar to RAP-PC, the biggest challenge facing the use of RAP-AAM is how to overcome the binding issues caused by the presence of asphalt. The bitumen coating on the aggregates reduces the mechanical properties and durability due to increased permeability. This may be addressed by physical or chemical pre-treatments of the RAP aggregates or by improvements on the binder.

The amount of research on RAP-AAM is limited; most studies used only PFA as a precursor, and still little is known about mechanical and durability properties. It is necessary to address how important factors, such as the effect of the type of aluminosilicate (low calcium or high calcium), type and amount of activator, neat or hybrid systems, as well as gradation, and amount and beneficiation of RAP could help improve the binding properties and the overall final material.

The employment of alkali-activated matrices to RAP aggregates depends on the availability and cost of precursors for AAM. Local materials may include industrial and agricultural residues and wastes and soils, which could be a source of clay materials for alkaline activation. The use of local materials is of great importance when aiming for sustainable practice in the long term.

AAM may be used to stabilise RAP particles, or they could be part of an AAM-RAP concrete base. The amount of binder and alkaline materials in the former is much lower. The choice of the system determines the mechanical properties, durability and environmental impact, which should be carried out via LCA and compared with current solutions.

The use of RAP-AAM is very promising for pavement sections due to their high early strength and increased durability of the alkaline binder. An optimised mix design could help compensate for the reduction in strength caused by the use of RAP granules. In addition, the low strength requirement of foundation layers could represent a lower need for alkalis and consequently lower the environmental impact of this solution.

*This chapter is a slightly modified version of the paper “Cementitious binders and reclaimed asphalt aggregates for sustainable pavement base layers: Potential, challenges, and research needs” published by Construction and Building Materials in December 2020. It has been published on this thesis with the authorisation of the copyright holders.*



# BIBLIOGRAPHY

---

- Abraham, S.M., Ransinchung, G.D.R.N., 2019. Pore Structure Characteristics of RAP-Inclusive Cement Mortar and Cement Concrete Using Mercury Intrusion Porosimetry Technique. *Adv. Civ. Eng. Mater.* 8, 20180161. <https://doi.org/10.1520/acem20180161>
- Abraham, S.M., Ransinchung, G.D.R.N., 2018a. Strength and permeation characteristics of cement mortar with Reclaimed Asphalt Pavement Aggregates. *Constr. Build. Mater.* 167, 700–706. <https://doi.org/10.1016/j.conbuildmat.2018.02.075>
- Abraham, S.M., Ransinchung, G.D.R.N., 2018b. Influence of RAP aggregates on strength, durability and porosity of cement mortar. *Constr. Build. Mater.* 189, 1105–1112. <https://doi.org/10.1016/j.conbuildmat.2018.09.069>
- Adesanya, E., Perumal, P., Luukkonen, T., Yliniemi, J., Ohenoja, K., Kinnunen, P., Illikainen, M., 2021. Opportunities to improve sustainability of alkali-activated materials: A review of side-stream based activators. *J. Clean. Prod.* 286, 125558. <https://doi.org/10.1016/j.jclepro.2020.125558>
- Adhikari, S., Khattak, M.J., Adhikari, B., 2018. Mechanical characteristics of Soil-RAP-Geopolymer mixtures for road base and subbase layers. *Int. J. Pavement Eng.* 1–14. <https://doi.org/10.1080/10298436.2018.1492131>
- Alcamand, H.A., Borges, P.H.R., Silva, F.A., Trindade, A.C.C., 2018. The effect of matrix composition and calcium content on the sulfate durability of metakaolin and metakaolin/slag alkali-activated mortars. *Ceram. Int.* 44, 5037–5044. <https://doi.org/10.1016/j.ceramint.2017.12.102>
- Ambroise, J., Maximilien, S., Pera, J., 1994. Properties of Metakaolin blended cements. *Adv. Cem. Based Mater.* 1, 161–168. [https://doi.org/10.1016/1065-7355\(94\)90007-8](https://doi.org/10.1016/1065-7355(94)90007-8)
- Anthonissen, J., Van den bergh, W., Braet, J., 2016. Review and environmental impact assessment of green technologies for base

courses in bituminous pavements. *Environ. Impact Assess. Rev.* 60, 139–147. <https://doi.org/10.1016/j.eiar.2016.04.005>

Antunes, V., Freire, A.C., Neves, J., 2019. A review on the effect of RAP recycling on bituminous mixtures properties and the viability of multi-recycling. *Constr. Build. Mater.* 211, 453–469. <https://doi.org/10.1016/j.conbuildmat.2019.03.258>

Apeagyei, A.K., Diefenderfer, B.K., Diefenderfer, S.D., 2011. Rutting resistance of asphalt concrete mixtures that contain recycled asphalt pavement. *Transp. Res. Rec.* 9–16. <https://doi.org/10.3141/2208-02>

Arshad, M., Ahmed, M.F., 2017. Potential use of reclaimed asphalt pavement and recycled concrete aggregate in base/subbase layers of flexible pavements. *Constr. Build. Mater.* 151, 83–97. <https://doi.org/10.1016/j.conbuildmat.2017.06.028>

Arulrajah, A., Piratheepan, J., Disfani, M.M., 2014. Reclaimed asphalt pavement and recycled concrete aggregate blends in pavement subbases: Laboratory and field evaluation. *J. Mater. Civ. Eng.* [https://doi.org/10.1061/\(ASCE\)MT.1943-5533.0000850](https://doi.org/10.1061/(ASCE)MT.1943-5533.0000850)

Avirneni, D., Peddinti, P.R.T.T., Saride, S., 2016. Durability and long term performance of geopolymer stabilized reclaimed asphalt pavement base courses. *Constr. Build. Mater.* 121, 198–209. <https://doi.org/10.1016/j.conbuildmat.2016.05.162>

Barbosa, V.F.F., MacKenzie, K.J.D., Thaumaturgo, C., 2000. Synthesis and characterisation of materials based on inorganic polymers of alumina and silica: Sodium polysialate polymers. *Int. J. Inorg. Mater.* 2, 309–317. [https://doi.org/10.1016/S1466-6049\(00\)00041-6](https://doi.org/10.1016/S1466-6049(00)00041-6)

Bennert, T., Papp, J., Maher, A., Gucunski, N., 2000. Utilization of construction and demolition debris under traffic-type loading in base and subbase applications. *Transp. Res. Rec.* 2, 33–39. <https://doi.org/10.3141/1714-05>

Borges, P.H.R., Banthia, N., Alcamand, H.A., Vasconcelos, W.L., Nunes, E.H.M., 2016. Performance of blended metakaolin/blastfurnace slag alkali-activated mortars. *Cem. Concr. Compos.* 71, 42–52.

<https://doi.org/10.1016/j.cemconcomp.2016.04.008>

Brand, A.S., Roesler, J.R., 2017a. Bonding in cementitious materials with asphalt-coated particles: Part I – The interfacial transition zone. *Constr. Build. Mater.* 130, 171–181. <https://doi.org/10.1016/j.conbuildmat.2016.10.019>

Brand, A.S., Roesler, J.R., 2017b. Bonding in cementitious materials with asphalt-coated particles: Part II – Cement-asphalt chemical interactions. *Constr. Build. Mater.* 130, 182–192. <https://doi.org/10.1016/j.conbuildmat.2016.10.013>

Brand, A.S., Roesler, J.R., Al-Qadi, I.L., Shangguan, P., 2012. Fractionated Reclaimed Asphalt Pavement (FRAP) as a Coarse Aggregate Replacement in a Ternary Blended Concrete Pavement, University of Illinois.

Castañeda López, M.A., Fedrigo, W., Kleinert, T.R., Matuella, M.F., Núñez, W.P., Ceratti, J.A.P., 2018. Flexural fatigue evaluation of cement-treated mixtures of reclaimed asphalt pavement and crushed aggregates. *Constr. Build. Mater.* 158, 320–325. <https://doi.org/10.1016/j.conbuildmat.2017.10.003>

Chabot, A., Hun, M., Hammoum, F., 2013. Mechanical analysis of a mixed mode debonding test for “ composite” pavements. *Constr. Build. Mater.* 40, 1076–1087. <https://doi.org/10.1016/j.conbuildmat.2012.11.027>

Colbert, B., You, Z., 2012. The determination of mechanical performance of laboratory produced hot mix asphalt mixtures using controlled RAP and virgin aggregate size fractions. *Constr. Build. Mater.* 26, 655–662. <https://doi.org/10.1016/j.conbuildmat.2011.06.068>

Consoli, N.C., Giese, D.N., Leon, H.B., Mocelin, D.M., Wetzel, R., Marques, S.F.V., 2018. Sodium chloride as a catalyser for crushed reclaimed asphalt pavement – Fly ash – Carbide lime blends. *Transp. Geotech.* 15, 13–19. <https://doi.org/10.1016/j.trgeo.2018.02.001>

Cook, R.A., Hover, K.C., 1993. Mercury porosimetry of cement-based

materials and associated correction factors. *Constr. Build. Mater.* 7, 231–240. [https://doi.org/10.1016/0950-0618\(93\)90007-Y](https://doi.org/10.1016/0950-0618(93)90007-Y)

Debbarma, S., Ransinchung, G.D., Singh, S., 2019. Feasibility of roller compacted concrete pavement containing different fractions of reclaimed asphalt pavement. *Constr. Build. Mater.* 199, 508–525. <https://doi.org/10.1016/j.conbuildmat.2018.12.047>

Duxson, P., Fernández-Jiménez, A., Provis, J.L., Lukey, G.C., Palomo, A., Van Deventer, J.S.J., 2007. Geopolymer technology: The current state of the art. *J. Mater. Sci.* 42, 2917–2933. <https://doi.org/10.1007/s10853-006-0637-z>

Duxson, Peter, Provis, J.L., Lukey, G.C., van Deventer, J.S.J., 2007. The role of inorganic polymer technology in the development of “green concrete.” *Cem. Concr. Res.* 37, 1590–1597. <https://doi.org/10.1016/j.cemconres.2007.08.018>

EAPA, 2017. Asphalt in figures 2007 [WWW Document]. URL <https://eapa.org/asphalt-in-figures/> (accessed 1.30.20).

EAPA, 2008. Arguments to stimulate the government to promote asphalt reuse and recycling. *Eur. Asph. Pavement Assoc.* 1–14.

El Euch Ben Said, S., El Euch Khay, S., Loulizi, A., 2018. Experimental Investigation of PCC Incorporating RAP. *Int. J. Concr. Struct. Mater.* 12, 8. <https://doi.org/10.1186/s40069-018-0227-x>

El Euch Ben Said, S., Euch Khay, S. El, Achour, T., Loulizi, A., 2017. Modelling of the adhesion between reclaimed asphalt pavement aggregates and hydrated cement paste. *Constr. Build. Mater.* 152, 839–846. <https://doi.org/10.1016/j.conbuildmat.2017.07.078>

Farhan, K.Z., Johari, M.A.M., Demirboğa, R., 2020. Assessment of important parameters involved in the synthesis of geopolymer composites: A review. *Constr. Build. Mater.* 264. <https://doi.org/10.1016/j.conbuildmat.2020.120276>

Fernández-Jiménez, A., Palomo, J.G., Puertas, F., 1999. Alkali-activated slag mortars: Mechanical strength behaviour. *Cem. Concr. Res.* 29,

1313–1321. [https://doi.org/10.1016/S0008-8846\(99\)00154-4](https://doi.org/10.1016/S0008-8846(99)00154-4)

Fernández-Jiménez, A., Puertas, F., Sobrados, I., Sanz, J., 2003. Structure of calcium silicate hydrates formed in alkaline-activated slag: Influence of the type of alkaline activator. *J. Am. Ceram. Soc.* 86, 1389–1394. <https://doi.org/10.1111/j.1151-2916.2003.tb03481.x>

Gao, Y., Xu, J., Bai, E., Luo, X., Zhu, J., Nie, L., 2015. Static and dynamic mechanical properties of high early strength alkali activated slag concrete. *Ceram. Int.* 41, 12901–12909. <https://doi.org/10.1016/j.ceramint.2015.06.131>

Garcia-Lodeiro, I., Palomo, A., Fernández-Jiménez, A., 2015. An overview of the chemistry of alkali-activated cement-based binders. *Handb. Alkali-Activated Cem. Mortars Concr.* 19–47. <https://doi.org/10.1533/9781782422884.1.19>

Ghanizadeh, A.R., Rahrovan, M., Bafghi, K.B., 2018. The effect of cement and reclaimed asphalt pavement on the mechanical properties of stabilized base via full-depth reclamation. *Constr. Build. Mater.* 161, 165–174. <https://doi.org/10.1016/j.conbuildmat.2017.11.124>

Guo, S., Hu, J., Dai, Q., 2018. A critical review on the performance of portland cement concrete with recycled organic components. *J. Clean. Prod.* 188, 92–112. <https://doi.org/10.1016/j.jclepro.2018.03.244>

Habert, G., D'Espinose De Lacaillerie, J.B., Roussel, N., 2011. An environmental evaluation of geopolymer based concrete production: Reviewing current research trends. *J. Clean. Prod.* 19, 1229–1238. <https://doi.org/10.1016/j.jclepro.2011.03.012>

Habert, G., Ouellet-Plamondon, C., 2016. Recent update on the environmental impact of geopolymers. *RILEM Tech. Lett.* 1, 17. <https://doi.org/10.21809/rilemtechlett.v1.6>

Horpibulsuk, S., Hoy, M., Witchayaphong, P., Rachan, R., Arulrajah, A., 2017. Recycled asphalt pavement - Fly ash geopolymer as a sustainable stabilized pavement material. *IOP Conf. Ser. Mater. Sci.*

Eng. 273. <https://doi.org/10.1088/1757-899X/245/1/012005>

Hossiney, N., Sepuri, H.K., Mohan, M.K., H R, A., Govindaraju, S., Chyne, J., 2020. Alkali-activated concrete paver blocks made with recycled asphalt pavement (RAP) aggregates. *Case Stud. Constr. Mater.* 12, e00322. <https://doi.org/10.1016/j.cscm.2019.e00322>

Hossiney, N., Tia, M., Bergin, M.J., 2010. Concrete containing RAP for use in concrete pavement. *Int. J. Pavement Res. Technol.* 3, 251–258. [https://doi.org/10.6135/ijprt.org.tw/2010.3\(5\).251](https://doi.org/10.6135/ijprt.org.tw/2010.3(5).251)

Hoy, M., Horpibulsuk, S., Arulrajah, A., 2016a. Strength development of Recycled Asphalt Pavement - Fly ash geopolymer as a road construction material. *Constr. Build. Mater.* 117, 209–219. <https://doi.org/10.1016/j.conbuildmat.2016.04.136>

Hoy, M., Horpibulsuk, S., Arulrajah, A., Mohajerani, A., 2018. Strength and microstructural study of recycled asphalt pavement: Slag geopolymer as a pavement base material. *J. Mater. Civ. Eng.* 30. [https://doi.org/10.1061/\(ASCE\)MT.1943-5533.0002393](https://doi.org/10.1061/(ASCE)MT.1943-5533.0002393)

Hoy, M., Horpibulsuk, S., Rachan, R., Chinkulkijniwat, A., Arulrajah, A., 2016b. Recycled asphalt pavement – fly ash geopolymers as a sustainable pavement base material: Strength and toxic leaching investigations. *Sci. Total Environ.* 573, 19–26. <https://doi.org/10.1016/j.scitotenv.2016.08.078>

Hoy, M., Rachan, R., Horpibulsuk, S., Arulrajah, A., Mirzababaei, M., 2017. Effect of wetting – drying cycles on compressive strength and microstructure of recycled asphalt pavement – Fly ash geopolymer. *Constr. Build. Mater.* 144, 624–634. <https://doi.org/10.1016/j.conbuildmat.2017.03.243>

Huang, B., Shu, X., Li, G., 2005. Laboratory investigation of portland cement concrete containing recycled asphalt pavements. *Cem. Concr. Res.* 35, 2008–2013. <https://doi.org/10.1016/j.cemconres.2005.05.002>

Huang, Y., Bird, R.N., Heidrich, O., 2007. A review of the use of recycled solid waste materials in asphalt pavements. *Resour. Conserv.*

Recycl. 52, 58–73. <https://doi.org/10.1016/j.resconrec.2007.02.002>

Huang, Y., Hakim, B., Zammataro, S., 2013. Measuring the carbon footprint of road construction using CHANGER. *Int. J. Pavement Eng.* 14, 590–600. <https://doi.org/10.1080/10298436.2012.693180>

Jallu, M., Arulrajah, A., Saride, S., Evans, R., 2020. Flexural fatigue behavior of fly ash geopolymer stabilized-geogrid reinforced RAP bases. *Constr. Build. Mater.* 254, 119263. <https://doi.org/10.1016/j.conbuildmat.2020.119263>

Jamshidi, A., Kurumisawa, K., Nawa, T., Igarashi, T., 2016. Performance of pavements incorporating waste glass: The current state of the art. *Renew. Sustain. Energy Rev.* 64, 211–236. <https://doi.org/10.1016/j.rser.2016.06.012>

Ji, Z., Pei, Y., 2019. Bibliographic and visualized analysis of geopolymer research and its application in heavy metal immobilization: A review. *J. Environ. Manage.* 231, 256–267. <https://doi.org/10.1016/j.jenvman.2018.10.041>

Kang, X., Ge, L., Kang, G.C., Mathews, C., 2015a. Laboratory investigation of the strength, stiffness, and thermal conductivity of fly ash and lime kiln dust stabilised clay subgrade materials. *Road Mater. Pavement Des.* 16, 928–945. <https://doi.org/10.1080/14680629.2015.1028970>

Kang, X., Kang, G.-C., Chang, K.-T., Ge, L., 2015b. Chemically Stabilized Soft Clays for Road-Base Construction. *J. Mater. Civ. Eng.* 27, 04014199. [https://doi.org/10.1061/\(ASCE\)MT.1943-5533.0001156](https://doi.org/10.1061/(ASCE)MT.1943-5533.0001156)

Kisku, N., Joshi, H., Ansari, M., Panda, S.K., Nayak, S., Dutta, S.C., 2017. A critical review and assessment for usage of recycled aggregate as sustainable construction material. *Constr. Build. Mater.* 131, 721–740. <https://doi.org/10.1016/j.conbuildmat.2016.11.029>

Komnitsas, K., Zaharaki, D., 2007. Geopolymerisation: A review and prospects for the minerals industry. *Miner. Eng.* 20, 1261–1277. <https://doi.org/10.1016/J.MINENG.2007.07.011>

- Kumari, M., Ransinchung, G.D.R.N., Singh, S., 2018. A laboratory investigation on Dense Bituminous Macadam containing different fractions of coarse and fine RAP. *Constr. Build. Mater.* 191, 655–666. <https://doi.org/10.1016/j.conbuildmat.2018.10.017>
- Lecomte, I., Henrist, C., Liégeois, M., Maseri, F., Rulmont, A., Cloots, R., 2006. (Micro)-structural comparison between geopolymers, alkali-activated slag cement and Portland cement. *J. Eur. Ceram. Soc.* 26, 3789–3797. <https://doi.org/10.1016/j.jeurceramsoc.2005.12.021>
- Li, C., Sun, H., Li, L., 2010. A review: The comparison between alkali-activated slag (Si + Ca) and metakaolin (Si + Al) cements. *Cem. Concr. Res.* 40, 1341–1349. <https://doi.org/10.1016/j.cemconres.2010.03.020>
- Li, Z., Nedeljković, M., Chen, B., Ye, G., 2019. Mitigating the autogenous shrinkage of alkali-activated slag by metakaolin. *Cem. Concr. Res.* 122, 30–41. <https://doi.org/10.1016/j.cemconres.2019.04.016>
- Liew, Y.M., Heah, C.Y., Mohd Mustafa, A.B., Kamarudin, H., 2016. Structure and properties of clay-based geopolymer cements: A review. *Prog. Mater. Sci.* <https://doi.org/10.1016/j.pmatsci.2016.08.002>
- Lopes, M., Gabet, T., Bernucci, L., Mouillet, V., 2015. Durability of hot and warm asphalt mixtures containing high rates of reclaimed asphalt at laboratory scale. *Mater. Struct. Constr.* 48, 3937–3948. <https://doi.org/10.1617/s11527-014-0454-9>
- Margaritis, A., Blom, J., Van den bergh, W., 2019. Evaluating the mechanical performance of Flemish bituminous mixtures containing RA by statistical analysis. *Road Mater. Pavement Des.* 20, S725–S739. <https://doi.org/10.1080/14680629.2019.1628431>
- Miranda, T., Leitão, D., Oliveira, J., Corrêa-Silva, M., Araújo, N., Coelho, J., Fernández-Jiménez, A., Cristelo, N., 2020. Application of alkali-activated industrial wastes for the stabilisation of a full-scale (sub)base layer. *J. Clean. Prod.* 242, 118427. <https://doi.org/10.1016/j.jclepro.2019.118427>



- Mo, K.H., Alengaram, U.J., Jumaat, M.Z., 2016. Structural performance of reinforced geopolymer concrete members: A review. *Constr. Build. Mater.* 120, 251–264. <https://doi.org/10.1016/j.conbuildmat.2016.05.088>
- Mohammadinia, A., Arulrajah, A., Horpibulsuk, S., Chinkulkijniwat, A., 2017. Effect of fly ash on properties of crushed brick and reclaimed asphalt in pavement base/subbase applications. *J. Hazard. Mater.* 321, 547–556. <https://doi.org/10.1016/j.jhazmat.2016.09.039>
- Mohammadinia, A., Arulrajah, A., Sanjayan, J.G., Disfani, M.M., Bo, M.W., Darmawan, S., 2016a. Strength Development and Microfabric Structure of Construction and Demolition Aggregates Stabilized with Fly Ash–Based Geopolymers. *J. Mater. Civ. Eng.* 28, 04016141. [https://doi.org/10.1061/\(ASCE\)MT.1943-5533.0001652](https://doi.org/10.1061/(ASCE)MT.1943-5533.0001652)
- Mohammadinia, A., Arulrajah, A., Sanjayan, J.G., Disfani, M.M., Win Bo, M., Darmawan, S., 2016b. Stabilization of Demolition Materials for Pavement Base/Subbase Applications Using Fly Ash and Slag Geopolymers: Laboratory Investigation. *J. Mater. Civ. Eng.* 28. [https://doi.org/10.1061/\(asce\)mt.1943-5533.0001526](https://doi.org/10.1061/(asce)mt.1943-5533.0001526)
- Moraes, J.C.B., Tashima, M.M., Akasaki, J.L., Melges, J.L.P., Monzó, J., Borrachero, M. V., Soriano, L., Payá, J., 2016. Increasing the sustainability of alkali-activated binders: The use of sugar cane straw ash (SCSA). *Constr. Build. Mater.* 124, 148–154. <https://doi.org/10.1016/j.conbuildmat.2016.07.090>
- Papakonstantinou, C.G., 2018. Resonant column testing on Portland cement concrete containing recycled asphalt pavement (RAP) aggregates. *Constr. Build. Mater.* 173, 419–428. <https://doi.org/10.1016/j.conbuildmat.2018.03.256>
- Plati, C., 2019. Sustainability factors in pavement materials, design, and preservation strategies: A literature review. *Constr. Build. Mater.* 211, 539–555. <https://doi.org/10.1016/j.conbuildmat.2019.03.242>
- Poltue, T., Suddeepong, A., Horpibulsuk, S., Samingthong, W., Arulrajah, A., Rashid, A.S.A., 2019. Strength development of recycled concrete aggregate stabilized with fly ash-rice husk ash based geopolymer as pavement base material. *Road Mater. Pavement Des.* 1–12.

<https://doi.org/10.1080/14680629.2019.1593884>

Provis, J.L., 2018. Alkali-activated materials. *Cem. Concr. Res.* 114, 40–48. <https://doi.org/10.1016/j.cemconres.2017.02.009>

Provis, J.L., Bernal, S.A., 2014. Geopolymers and related alkali-activated materials. *Annu. Rev. Mater. Res.* 44, 299–330. <https://doi.org/10.1146/annurev-matsci-070813-113515>

Puertas, F., Palacios, M., Manzano, H., Dolado, J.S., Rico, A., Rodríguez, J., 2011. A model for the C-A-S-H gel formed in alkali-activated slag cements. *J. Eur. Ceram. Soc.* 31, 2043–2056. <https://doi.org/10.1016/j.jeurceramsoc.2011.04.036>

Rahman, S.S., Khattak, M.J., 2021. Mechanistic and microstructural characteristics of roller compacted geopolymer concrete using reclaimed asphalt pavement. *Int. J. Pavement Eng.* 0, 1–19. <https://doi.org/10.1080/10298436.2021.1945057>

Ramachandran, V.S., Paroli, R.M., Beaudoin, J.J., Delgado, A.H., 2002. Supplementary Cementing Materials and Other Additions. *Handb. Therm. Anal. Constr. Mater.* 293–353. <https://doi.org/10.1016/b978-081551487-9.50010-4>

Rashad, A.M., 2013a. Alkali-activated metakaolin: A short guide for civil Engineer-An overview. *Constr. Build. Mater.* <https://doi.org/10.1016/j.conbuildmat.2012.12.030>

Rashad, A.M., 2013b. A comprehensive overview about the influence of different additives on the properties of alkali-activated slag - A guide for Civil Engineer. *Constr. Build. Mater.* 47, 29–55. <https://doi.org/10.1016/j.conbuildmat.2013.04.011>

Saride, S., Avirneni, D., Challapalli, S., 2016. Micro-mechanical interaction of activated fly ash mortar and reclaimed asphalt pavement materials. *Constr. Build. Mater.* 123, 424–435. <https://doi.org/10.1016/j.conbuildmat.2016.07.016>

Seferoğlu, A.G., Seferoğlu, M.T., Akpınar, M.V., 2018. Experimental study on cement-treated and untreated RAP blended bases: Cyclic

plate loading test. *Constr. Build. Mater.* 182, 580–587.  
<https://doi.org/10.1016/j.conbuildmat.2018.06.160>

Settari, C., Debieb, F., Kadri, E.H., Boukendakdji, O., 2015. Assessing the effects of recycled asphalt pavement materials on the performance of roller compacted concrete. *Constr. Build. Mater.* 101, 617–621. <https://doi.org/10.1016/j.conbuildmat.2015.10.039>

Shatarat, N., Alhaq, A.A., Katkhuda, H., Jaber, M.A., 2019. Investigation of axial compressive behavior of reinforced concrete columns using Recycled Coarse Aggregate and Recycled Asphalt Pavement aggregate. *Constr. Build. Mater.* 217, 384–393.  
<https://doi.org/10.1016/j.conbuildmat.2019.05.085>

Shi, C., Ana, F.-J., Palomo, A., 2011. New cements for the 21st century: The pursuit of an alternative to Portland cement. *Cem. Concr. Res.* 41, 750–763. <https://doi.org/10.1016/j.cemconres.2011.03.016>

Shi, X., Grasley, Z., Hogancamp, J., Brescia-Norambuena, L., Mukhopadhyay, A., Zollinger, D., 2020. Microstructural, Mechanical, and Shrinkage Characteristics of Cement Mortar Containing Fine Reclaimed Asphalt Pavement. *J. Mater. Civ. Eng.* 32, 1–11.  
[https://doi.org/10.1061/\(ASCE\)MT.1943-5533.0003110](https://doi.org/10.1061/(ASCE)MT.1943-5533.0003110)

Shi, X., Mukhopadhyay, A., Liu, K.W., 2017. Mix design formulation and evaluation of portland cement concrete paving mixtures containing reclaimed asphalt pavement. *Constr. Build. Mater.* 152, 756–768.  
<https://doi.org/10.1016/j.conbuildmat.2017.06.174>

Singh, S., Ransinchung, G.D., Debbarma, S., Kumar, P., 2018a. Utilization of reclaimed asphalt pavement aggregates containing waste from Sugarcane Mill for production of concrete mixes. *J. Clean. Prod.* 174, 42–52.  
<https://doi.org/10.1016/j.jclepro.2017.10.179>

Singh, S., Ransinchung, G.D., Kumar, P., 2018b. Laboratory investigation of concrete pavements containing fine RAP aggregates. *J. Mater. Civ. Eng.* 30, 1–9.  
[https://doi.org/10.1061/\(ASCE\)MT.1943-5533.0002124](https://doi.org/10.1061/(ASCE)MT.1943-5533.0002124)

Singh, S., Ransinchung, G.D., Kumar, P., 2017. An economical processing technique to improve RAP inclusive concrete properties. *Constr. Build. Mater.* 148, 734–747. <https://doi.org/10.1016/j.conbuildmat.2017.05.030>

Singh, S., Ransinchung, G.D.R.N., 2018. Durability Properties of Pavement Quality Concrete Containing Fine RAP. *Adv. Civ. Eng. Mater.* 7, 20180012. <https://doi.org/10.1520/acem20180012>

Singh, S., Ransinchung, G.D.R.N., Monu, K., Kumar, P., 2018c. Laboratory investigation of RAP aggregates for dry lean concrete mixes. *Constr. Build. Mater.* 166, 808–816. <https://doi.org/10.1016/j.conbuildmat.2018.01.131>

Singh, S., Ransinchung, R.N.G.D., 2020. Laboratory and Field Evaluation of RAP for Cement Concrete Pavements. *J. Transp. Eng. Part B Pavements* 146, 1–11. <https://doi.org/10.1061/JPEODX.0000162>

Sturm, P., Gluth, G.J.G., Brouwers, H.J.H., Kühne, H.C., 2016. Synthesizing one-part geopolymers from rice husk ash. *Constr. Build. Mater.* 124, 961–966. <https://doi.org/10.1016/j.conbuildmat.2016.08.017>

Su, N., Xiao, F., Wang, J., Amirkhanian, S., 2017. Characterizations of base and subbase layers for Mechanistic-Empirical Pavement Design. *Constr. Build. Mater.* 152, 731–745. <https://doi.org/10.1016/j.conbuildmat.2017.07.060>

Su, Y.-M., Hossiney, N., Tia, M., Bergin, M., 2014. Mechanical Properties Assessment of Concrete Containing Reclaimed Asphalt Pavement Using the Superpave Indirect Tensile Strength Test. *J. Test. Eval.* 42, 20130093. <https://doi.org/10.1520/jte20130093>

Tailby, J., MacKenzie, K.J.D., 2010. Structure and mechanical properties of aluminosilicate geopolymer composites with Portland cement and its constituent minerals. *Cem. Concr. Res.* 40, 787–794. <https://doi.org/10.1016/j.cemconres.2009.12.003>

Temuujin, J., van Riessen, A., Williams, R., 2009. Influence of calcium

compounds on the mechanical properties of fly ash geopolymer pastes. J. Hazard. Mater. 167, 82–88. <https://doi.org/10.1016/j.jhazmat.2008.12.121>

Thakur, J.K., Han, J., Pokharel, S.K., Parsons, R.L., 2012. Performance of geocell-reinforced recycled asphalt pavement (RAP) bases over weak subgrade under cyclic plate loading. Geotext. Geomembranes 35, 14–24. <https://doi.org/10.1016/j.geotexmem.2012.06.004>

Thomas, R.J., Fellows, A.J., Sorensen, A.D., 2018. Durability analysis of recycled asphalt pavement as partial coarse aggregate replacement in a high-strength concrete mixture. J. Mater. Civ. Eng. 30, 1–7. [https://doi.org/10.1061/\(ASCE\)MT.1943-5533.0002262](https://doi.org/10.1061/(ASCE)MT.1943-5533.0002262)

Turner, L.K., Collins, F.G., 2013. Carbon dioxide equivalent (CO<sub>2</sub>-e) emissions: A comparison between geopolymer and OPC cement concrete. Constr. Build. Mater. 43, 125–130. <https://doi.org/10.1016/j.conbuildmat.2013.01.023>

Ullah, S., Tanyu, B.F., 2019. Methodology to develop design guidelines to construct unbound base course with reclaimed asphalt pavement (RAP). Constr. Build. Mater. 223, 463–476. <https://doi.org/10.1016/j.conbuildmat.2019.06.196>

Van den bergh, W., Kara, P., Anthonissen, J., Margaritis, A., Jacobs, G., Couscheir, K., 2017. Recommendations and strategies for using reclaimed asphalt pavement in the Flemish Region based on a first life cycle assessment research. IOP Conf. Ser. Mater. Sci. Eng. 236. <https://doi.org/10.1088/1757-899X/236/1/012088>

Van Den Heede, P., De Belie, N., 2012. Environmental impact and life cycle assessment (LCA) of traditional and “green” concretes: Literature review and theoretical calculations. Cem. Concr. Compos. 34, 431–442. <https://doi.org/10.1016/j.cemconcomp.2012.01.004>

Van Deventer, J.S.J., Provis, J.L., Duxson, P., 2012. Technical and commercial progress in the adoption of geopolymer cement. Miner. Eng. 29, 89–104. <https://doi.org/10.1016/j.mineng.2011.09.009>

Van Deventer, J.S.J., Provis, J.L., Duxson, P., Brice, D.G., 2010.

Chemical research and climate change as drivers in the commercial adoption of alkali activated materials. *Waste and Biomass Valorization* 1, 145–155. <https://doi.org/10.1007/s12649-010-9015-9>

Wang, S.-D., Scrivener, K.L., 1995. Hydration products of alkali activated slag cement. *Cem. Concr. Res.* 25, 561–571. [https://doi.org/10.1016/0008-8846\(95\)00045-E](https://doi.org/10.1016/0008-8846(95)00045-E)

Wang, S.-D., Scrivener, K.L., Pratt, P.L., 1994. Factors affecting the strength of alkali-activated slag. *Cem. Concr. Res.* 24, 1033–1043. [https://doi.org/10.1016/0008-8846\(94\)90026-4](https://doi.org/10.1016/0008-8846(94)90026-4)

Winslow, D.N., Diamond, S., 1969. A Mercury Porosimetry Study of the Evolution of Porosity in Portland Cement. *J Mater* 5, 564–585.

World Bank Group, 2018. GRIP (Global Roads Inventory Dataset) - 2018: Road Density | Data Catalog.

Yazoghli-Marzouk, O., Vulcano-Greullet, N., Cantegrit, L., Friteyre, L., Jullien, A., 2014. Recycling foundry sand in road construction-field assessment. *Constr. Build. Mater.* 61, 69–78. <https://doi.org/10.1016/j.conbuildmat.2014.02.055>

Zhang, K., Huchet, F., Hobbs, A., 2019. A review of thermal processes in the production and their influences on performance of asphalt mixtures with reclaimed asphalt pavement (RAP). *Constr. Build. Mater.* 206, 609–619. <https://doi.org/10.1016/j.conbuildmat.2019.02.057>

Zhao, S., Huang, B., Shu, X., Woods, M., 2013. Comparative evaluation of warm mix asphalt containing high percentages of reclaimed asphalt pavement. *Constr. Build. Mater.* 44, 92–100. <https://doi.org/10.1016/j.conbuildmat.2013.03.010>

# MATERIALS CHARACTERISATION & EXPERIMENTAL TECHNIQUES

---

## 3.1 Introduction

It is important to understand how each raw material impacts the property of RAP-AAM to design the final composite. Hence, depending on the specific objective, the research was conducted using pastes, mortars, or concrete specimens. In this thesis, the current technology to manufacture and test PC was used as much as possible.

The raw materials applied in this research can be divided into three categories: (i) binders, i.e., bituminous, cementitious, or supplementary material; (ii) activators, chemicals used to produce a solution; and (iii) aggregates, inert granular materials. Each of the raw materials will be presented in the following sections, including a detailed description of the production of each specimen.

Additionally, some test procedures to assess the properties of the specimens (fresh and hardened) were also explained in this chapter. Figure 3.1 summarizes the binders, activators, aggregates, and methods employed to characterise each type of raw material.

This chapter will present a more extensive overview of all raw materials and experimental procedures used in this research; however, each of the following chapters will include a shorter summary of the relevant information.

	binder	activator	aggregate	technique
PASTE	<ul style="list-style-type: none"> <li>• Slag</li> <li>• Metakaolin</li> </ul>	<ul style="list-style-type: none"> <li>• Water</li> <li>• Sodium silicate</li> <li>• Sodium hydroxide</li> </ul>	-	<ul style="list-style-type: none"> <li>• FTIR</li> </ul>
MORTAR	<ul style="list-style-type: none"> <li>• Slag</li> <li>• Metakaolin</li> </ul>	<ul style="list-style-type: none"> <li>• Water</li> <li>• Sodium silicate</li> <li>• Sodium hydroxide</li> </ul>	<ul style="list-style-type: none"> <li>• Natural</li> <li>• RAP</li> </ul>	<ul style="list-style-type: none"> <li>• Calorimetry</li> <li>• Shrinkage</li> <li>• Water absorption</li> <li>• Compressive strength</li> <li>• Flexural strength</li> <li>• SEM</li> <li>• CLSM</li> <li>• MIP</li> </ul>
CONCRETE	<ul style="list-style-type: none"> <li>• Slag</li> <li>• Metakaolin</li> <li>• Portland cement</li> </ul>	<ul style="list-style-type: none"> <li>• Water</li> <li>• Sodium hydroxide</li> </ul>	<ul style="list-style-type: none"> <li>• Natural</li> <li>• RAP</li> <li>• Lab-made RAP</li> </ul>	<ul style="list-style-type: none"> <li>• Compressive strength</li> <li>• Indirect tensile</li> <li>• Freeze &amp; thaw</li> </ul>

Figure 3.1. Materials and methods used in the research (FTIR – Fourier-transform infrared spectroscopy, SEM – Scanning electron microscopy, CLSM – Confocal laser scanning microscopy, MIP – Mercury intrusion porosimeter)

## 3.2 Materials

### 3.2.1 Binders & Precursors

#### 3.2.1.1 Ground granulated blast furnace slag

The main precursor used to prepare the alkali-activated mortars was a commercial ground granulated blast furnace slag (BFS) supplied by Ecocem (Moerdijk, The Netherlands). The chemical composition of BFS was determined by X-ray fluorescence (XRF) and given in Table 3.1. Approximately 80% of the BFS composition is CaO and SiO<sub>2</sub>. The basicity coefficient ( $\text{CaO} + \text{MgO}/\text{SiO}_2 + \text{Al}_2\text{O}_3$ ) is 1.03, and the BFS is therefore basic (Pavel et al., 2017; Wang et al., 1994).



Table 3.1. Chemical composition of BFS (XRF).

Main Oxides (%)							
CaO	SiO <sub>2</sub>	Al <sub>2</sub> O <sub>3</sub>	MgO	SO <sub>3</sub>	TiO <sub>2</sub>	Fe <sub>2</sub> O <sub>3</sub>	Mn <sub>2</sub> O <sub>3</sub>
42.68	37.31	10.38	6.55	1.49	0.7	0.36	0.33

Figure 3.2 shows the mineralogical composition of BFS which was determined by X-ray diffraction (XRD), using a Bruker D8 Advance with copper radiation (scanning at  $2\theta = 1^\circ$  per minute, step size 0.04). The XRD diffractogram presents the BFS as a predominantly amorphous material due to the absence of well-defined peaks. There is a single broad and diffuse peak  $2\theta \sim 32^\circ$ ; it corresponds to the short-range order of the CaO-Al<sub>2</sub>O<sub>3</sub>-MgO-SiO<sub>2</sub> glass structure (Wang and Scrivener, 1995). The particle size distribution of the BFS (Figure 3.3) was measured using a Mastersizer Hydro 2000G Particle Size Analyser using water dispersion. The equipment is designed to carry sub-micron analysis in the range of 0.02 to 2000  $\mu\text{m}$ . BFS has a medium particle size ( $d_{50}$ ) of 13.7  $\mu\text{m}$ , indicating that it is finely ground and suitable for alkaline activation.

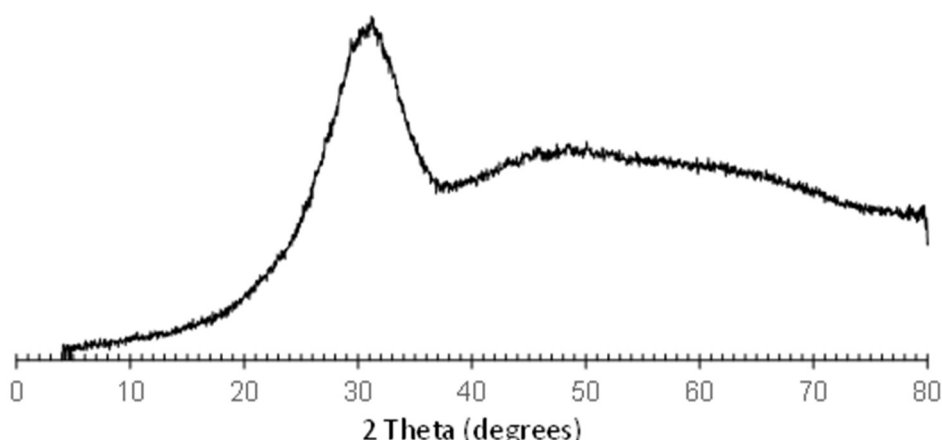


Figure 3.2. XRD pattern of BFS

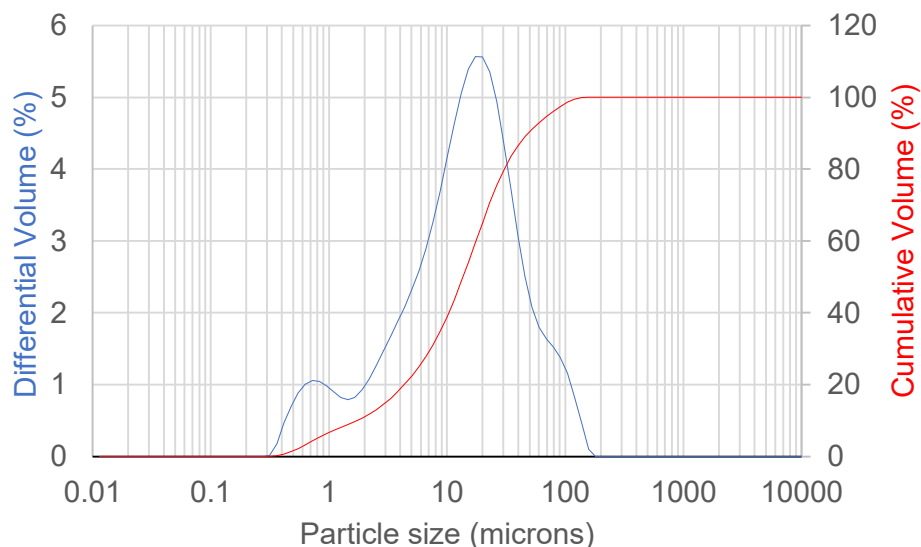


Figure 3.3. Particle size distribution of the BFS

### 3.2.1.2 Metakaolin

Some AAM formulations used in this research also employed MK as a precursor, replacing BFS in volume. The MK was provided by Caltra (Netherland). The chemical composition was determined by X-ray fluorescence (XRF) and given in Table 3.2. The mineralogical composition was determined by XRD using a Bruker D8 Advance with copper radiation scanning at  $2\theta = 1^\circ$  per minute, step size 0.04. The spectra of MK present kaolinite ( $\text{Al}_2\text{Si}_2\text{O}_5(\text{OH})_4$ ), quartz ( $\text{SiO}_2$ ) and rutile ( $\text{TiO}_2$ ) (Figure 3.4). The mineral presence in MK indicates material impurities and the incomplete calcination of kaolin clay. The particle size distribution of MK (Figure 3.5) was measured using Mastersizer Hydro 2000G Particle Size Analyser in water dispersion. The results show that MK has a mean diameter ( $d_{50}$ ) of  $2.5 \mu\text{m}$ , much smaller than BFS ( $13.7 \mu\text{m}$ ).

Table 3.2. Chemical Composition from MK

Main Oxides (%)							
CaO	SiO <sub>2</sub>	Al <sub>2</sub> O <sub>3</sub>	MgO	SO <sub>3</sub>	TiO <sub>2</sub>	Fe <sub>2</sub> O <sub>3</sub>	Mn <sub>2</sub> O <sub>3</sub>
0.20	46.47	47.42	-	-	1.64	0.63	0.04

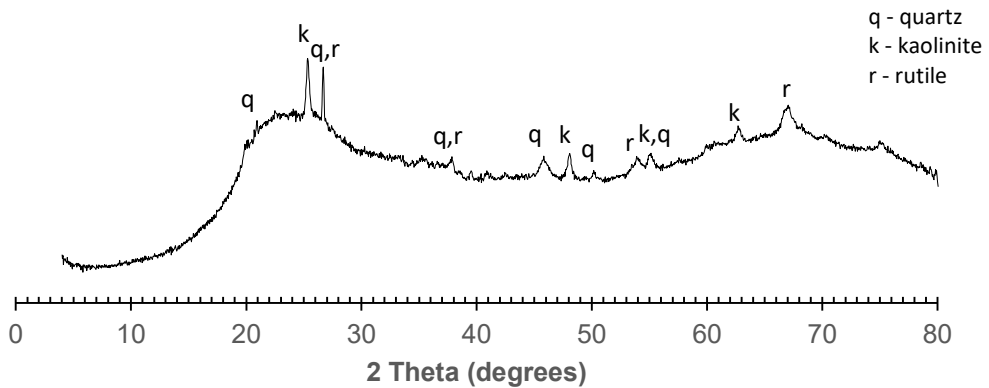


Figure 3.4. XRD pattern of MK

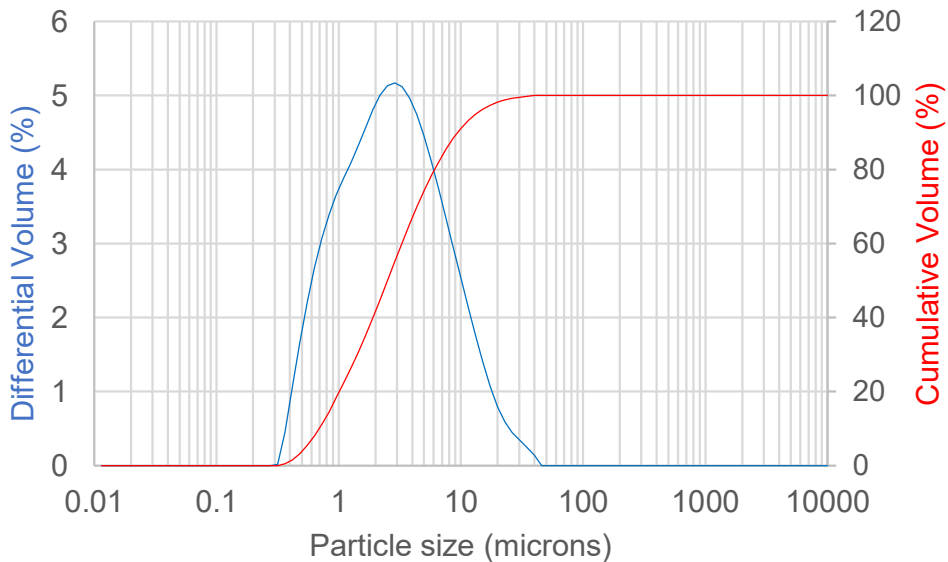


Figure 3.5. Particle size distribution of MK

### 3.2.1.3 Cement

A reference cement matrix with recycled aggregate (RAP1) was chosen during the study of concrete samples (Chapter 6). A commercial type CEM III/A 42.5 N LA supplied by LafargeHolcim was used to produce the reference concrete. The cement Blaine fineness was 389 m<sup>2</sup>/kg and the chemical composition is presented in Table 3.3 (as supplied by the manufacturer).

Table 3.3. Chemical Composition of cement

Main Oxides (%)							
CaO	SiO <sub>2</sub>	Al <sub>2</sub> O <sub>3</sub>	MgO	SO <sub>3</sub>	TiO <sub>2</sub>	Fe <sub>2</sub> O <sub>3</sub>	Mn <sub>2</sub> O <sub>3</sub>
52.0	25.8	8.2	4.5	3.3	-	2.6	-

### 3.2.2 Activators

The alkali solution used to activate the BFS was prepared by mixing (i) sodium hydroxide and deionized water; or (ii) sodium hydroxide, sodium silicate and deionized water. Both NaOH and Na<sub>2</sub>SiO<sub>3</sub> were supplied by VWR, Belgium. The sodium hydroxide (NaOH) used was commercial-grade in pellet form with 98% purity. The sodium silicate (Na<sub>2</sub>SiO<sub>3</sub>) was supplied in solution with an initial composition of 25.9 wt.% of sodium oxide (Na<sub>2</sub>O), 7.9 wt.% of silicon oxide (SiO<sub>2</sub>), and 66.2 wt.% H<sub>2</sub>O.

The activator was prepared by dissolving the NaOH flakes in deionized water. The mass of NaOH in the solution varied depending on the targeted concentration of Na<sub>2</sub>O used (wt.% BFS). For example, to activate 100g of BFS with 4% Na<sub>2</sub>O using only NaOH, one should use 5.21g of NaOH. Note that the mass of Na<sub>2</sub>O is a fraction of the mass of NaOH. The combination of sodium hydroxide and water is an exothermic reaction and therefore, the mix was always sealed and allowed to cool down to reach room temperature before use.

Some solutions were also prepared using sodium silicate. The amount of sodium silicate used was determined according to the targeted silica modulus (Ms) of the solution. The Ms ratio (Equation 3.1) of the solution was calculated considering the sodium oxide contribution from both sodium hydroxide and sodium silicate. The silicates were only added to the alkali solution after the solution reached room temperature to avoid the instability caused to the scale while measuring warm objects.

$$M_s = \frac{SiO_2}{Na_2O} \text{ (molar ratios)} \quad \text{Equation 3.1}$$

### 3.2.3 Aggregates

Several types of aggregates were used in this study – naturally sourced, recycled (RAP) and produced in the lab:

- Natural coarse aggregate, crushed, granite type.
- Natural siliceous fine aggregate, uncrushed.
- Local sourced RAP, mixed sourced aggregates and sized under 14mm, supplied by Willemen Infra Recycling (Figure 3.6). The particle origins were limestone, porphyry, gravel, and granite
- Lab-made RAP produced using natural aggregates.

Mortars were always produced using a single type of aggregate, either natural fine aggregates or the fines (<4mm) removed from the locally sourced RAP.

Depending on the objective of the specific study, each aggregate was used according to its supplied granulometry or by changing its particle size distribution to match a specific design. The modification of the gradation was performed by separating the material into different sizes by sieving and later selecting the exact amount of each fraction to use. Information regarding the gradation of each aggregate used can be found in each chapter of this thesis.



*Figure 3.6. RAP aggregates as collected*

#### **3.2.3.1 Fine natural aggregate (NA)**

The commercially available siliceous fine NA (Figure 3.7) is a poorly graded aggregate with over 85% of its particles between 0.25 and 0.125 mm. Figure 3.9 presents the particle size distribution of NA sand. The fineness modulus was equal to 2.82 and the specific gravity, measured by pycnometry, was 2.74. The NA was dried at 100°C for 24 hours and allowed to cool to room temperature prior to utilization in the formulations.



*Figure 3.7. Fine NA separated into fractions*

#### **3.2.3.2 Fine RAP aggregate**

The RAP aggregates were oven-dried at  $60 \pm 2$  °C for 72 h and sieved using a 4mm sieve to remove the coarse fraction. A lower drying temperature (compared to NA) was selected to avoid melting the bitumen adhered to the particles. The fine RAP aggregates presented a better particle size distribution compared to the fine NA and a coarser overall size (Figure 3.8 and Figure 3.9). The fineness modulus was equal to 4.53 and the specific gravity, measured by pycnometry, was 2.24. The bitumen content of the fine RAP fraction was 6.9%, determined by separating the binder using trichloroethylene solvent in a centrifuge as per the NBN EN 12697: 2020 method.



Figure 3.8. Fine RAP aggregates separated into fractions

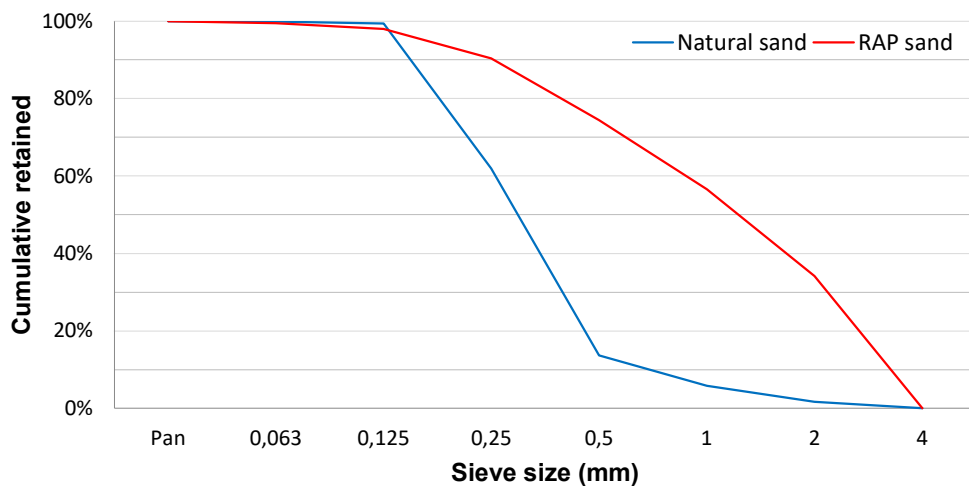


Figure 3.9. Fine aggregates particle size distribution

### 3.2.3.3 Coarse RAP aggregate

Three types of coarse RAP were used in the study. The first was locally sourced (RAP1) and supplied by Willemen Infra Recycling (Belgium). The fine fraction (<4mm) was removed and only the coarse fraction was used. RAP1 a had specific gravity of 2.53 and bitumen content of 4.8%. The former was oven-dried at  $60 \pm 2$  °C for 72h before mixing.

The other two RAP were produced in the laboratory, targeting a similar grading to RAP1 but with different bitumen content. The mixture used

limestone coarse aggregates (74%), round sand (13%), and filler (13%). The mixes used a bitumen with a penetration grade of 35/50. RAPL (L designates low and H high bitumen content) and RAPH presented the same gradation but different bitumen content, 4.5% and 5.7% respectively. After the mixing procedure, the trays containing the loose asphalt mixtures were kept in the oven for 5 days at 95° C to simulate field aging (Ferreira et al., 2021). After the aging procedure, the loose particles were further disaggregated by mixing in a concrete mixer and the fine fraction (under 4mm) was removed. RAPL and RAPH had a specific gravity of 2.48 and 2.66, respectively. Figure 3.10 shows the gradation of the coarse fraction and Table 3.4 summarizes the characteristics of the three RAP aggregates employed.

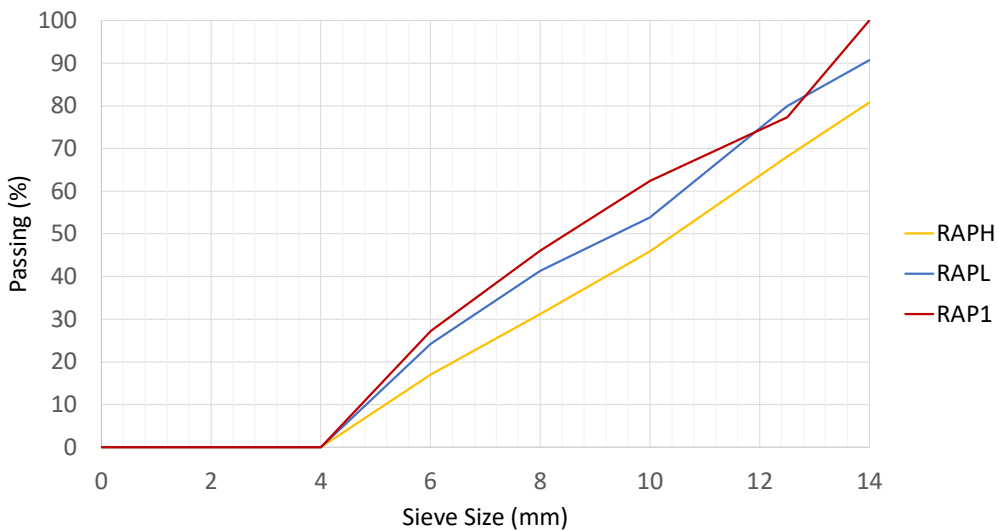


Figure 3.10. Sieve analysis of RAP1

Table 3.4. Characteristics of the RAP aggregates

Aggregate	Origin	Specific gravity	Bitumen content (%)
RAP1	Supplied	2.53	4.8
RAPL	Lab Manufactured	2.66	4.5
RAPH	Lab manufactured	2.48	5.7

The different RAP production methods and bitumen content may also contribute to the formation and amount of RAP aggregate clusters. Although the lab-made RAP aggregates had a similar white gradation



curve (i.e., particle size distribution before bitumen addition) the formation of clusters may result in different black gradation curves. The compaction of the RAP-containing lean concrete may separate or break these clusters. A comparative study (Chapter 6) on the effect of modified proctor compaction on the gradation of the RAP aggregates was performed by sieving the RAP before and after a dry proctor compaction routine.

### 3.3 Mixture proportions & procedures

#### 3.3.1 Pastes

The AAM paste samples were produced exclusively to be used in FTIR. The water/precursor ratio used was 0.4 to avoid water bleeding from the fresh paste. Naturally, mortars and concrete samples in this research had different water content due to the nature of the aggregates used. The paste samples were produced to assess selected mixes from Chapter 5, either 100%BFS or with 20% volume replacement of BFS by MK. In addition, the activator had 8% Na<sub>2</sub>O and Ms ratios of 0 or 1.

The paste samples were produced using the following procedure: (i) the alkali solution was prepared by mixing water, sodium hydroxide pellets, allowing it to cool to room temperature and later adding the sodium silicate; (ii) approximately 40g of precursors were added to a beaker and manually mixed with a spatula until homogeneous; (iii) the alkali solution was added to the beaker and the paste was mechanically mixed for approximate 2 minutes – no extra water was added during mixing; (iv) the paste was poured into acrylic dishes (Figure 3.11) and kept protected from moisture loss (i.e. with the lid on) at room temperature (20 °C ± 4 °C) until tested.



Figure 3.11. Alkali-activated paste

### 3.3.2 Mortars

Mortar samples were produced using either 100% NA or 100% RAP fine aggregate. Different alkali content and Ms ratio were used in this research. All mortars had fixed water to precursor (BFS and MK) ratio and aggregate to precursor ratios, 0.5 and 1.5, respectively. Mortars were used in Chapters 4 and 5 and the formulations employed in each chapter are described as follows.

In Chapter 4 the activation of 100% BFS using six different alkali solutions is investigated. Each solutions had different  $\text{Na}_2\text{O}$  content (4% or 6% by weight of BFS) and modulus of silica ( $\text{Ms} = \text{SiO}_2/\text{Na}_2\text{O}$  molar ratio) either 0, 0.5, or 1. The dosages were selected in accordance with the literature (Duran Atiş et al., 2009; Palacios and Puertas, 2005; Shi, 1996; Wang et al., 1994).

Table 3.5 summarizes the mortar compositions studied in Chapter 4. In the notation of the formulations, N denotes mortars made with natural aggregate and R using RAP. The first number shows the % $\text{Na}_2\text{O}$ , and the second (preceded by M) designates the modulus of silica. For example, mortar N4M1 denotes a mortar made with natural aggregate and activated with 4%  $\text{Na}_2\text{O}$  and  $\text{Ms} = 1$ . A total of 12 different compositions were produced.

*Table 3.5. AAM Mortar formulations studied in BFS systems (Chapter 4)*

Notation	Precursor	$\text{Na}_2\text{O}$ (wt.%)	Ms	Water/BFS	Aggr./BFS
N4M0; R4M0	100% BFS	4	0	0.5	1.5
N4M0.5; R4M0.5	100% BFS	4	0.5	0.5	1.5
N4M1; R4M1	100% BFS	4	1	0.5	1.5
N6M0; R6M0	100% BFS	6	0	0.5	1.5
N6M0.5; R6M0.5	100% BFS	6	0.5	0.5	1.5
N6M1; R6M1	100% BFS	6	1	0.5	1.5

The binder used to prepare the alkali-activated mortars was a commercial ground granulated blast furnace slag (BFS) and the alkaline solution composed of sodium hydroxide (NaOH), sodium silicate ( $\text{Na}_2\text{SiO}_3$ ), and demineralised water. The mortars were prepared with fine aggregates from either NA or RAP. The PSD curve of the RAP aggregate was

corrected to match the NA aggregate gradation so that the different PSD did not affect the results. In other words, all formulations were made with aggregates with the same PSD, given by the red and blue lines in Figure 3.12. Before sieving, the RAP was dry mixed in a concrete mixer for 15 min to disaggregate the granules further.

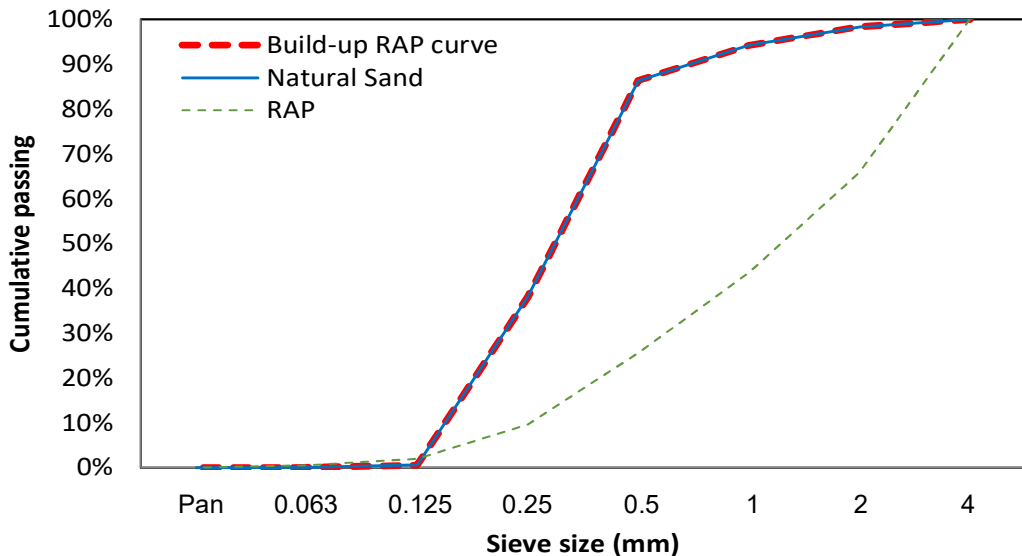


Figure 3.12. Aggregates particle size distribution.

Chapter 5 studied the replacement (vol.%) of BFS by MK. The mortar samples studied had different replacement levels (0, 5, 10, and 20% vol.). The alkali solution was produced with either 4% or 8% of  $\text{Na}_2\text{O}$  and two different silica moduli (either  $M_s = 0$  or 1); therefore,  $M_s=0$  (i.e.,  $\text{SiO}_2 = 0$ ) represents the formulations activated solely with  $\text{NaOH}$  and extra water. The  $\text{Na}_2\text{O}$  available in the solution comes from both  $\text{Na}_2\text{SiO}_3$  and  $\text{NaOH}$ . The  $\text{H}_2\text{O}$  from sodium silicate solution, from the dissociation of sodium hydroxide, and the extra water added were considered to calculate the water/precursor ratio, fixed at 0.5. The RAP/precursors ratio was also kept constant and equal to 1.5 (in mass) (Table 3.6).

Table 3.6. AAM Mortar formulations studied in RAP-AAM systems (Chapter 5)

Notation	Precursor (P)		Activator		Water/P	Aggr/P
	MK (vol%)	BFS (vol%)	Na <sub>2</sub> O (wt.%)	Ms		
R4-0	0	100	4	0	0.5	1.5
5MK4-0	5	95	4	0	0.5	1.5
R4-1	0	100	4	1	0.5	1.5
5MK4-1	5	95	4	1	0.5	1.5
R8-0	0	100	8	0	0.5	1.5
10MK8-0	10	90	8	0	0.5	1.5
20MK8-0	20	80	8	0	0.5	1.5
R8-1	0	100	8	1	0.5	1.5
10MK8-1	10	90	8	1	0.5	1.5
20MK8-1	20	80	8	1	0.5	1.5

The notation of the formulations describes the MK replacement level, the sodium content, and the silica modulus. For example, for sample 10MK8-1, the first two numbers are the MK replacement (10vol.%), 8 mean 8wt.% sodium oxide content (fixed for all mortars), and the last digit represents the silica modulus (either 0 or 1. R at the beginning of the mortar R8-0 and R8-1 indicates the reference mortars (without MK).

The mortar samples used in both Chapters 4 and 5 were produced using the following procedure: (i) the alkali solution (already at room temperature) and aggregates were mixed for 30 s using a 120L concrete mixer (Figure 3.13); (ii) the BFS was added during mixing for the following 30 s; (iii) the mixing continued for the following 30 s; (iv) the mixer was stopped to scrape the mixture off the sides of the bowl and switched on again on for 1.5 min (no extra water was added during mixing); (v) the samples were poured into pre-oiled moulds and compacted using a vibrating table. All samples were kept inside the mould for 24 h. After demoulding, the samples were placed wet sealed inside a plastic bag at room temperature (20 °C ± 4°C) until testing.



Figure 3.13. 120L concrete mixer (University of Antwerp)

### 3.3.3 Concrete

The last section of this research (Chapter 6) is focused on lean concrete mixtures; the mix composition selected was based on past studies from the EMIB research group (Niels, 2015). The reference sample (RC) was produced with cement (PC), while in the alkali-activated samples (NR, LB, HB), PC was replaced with a 9/1 BFS/MK (vol.%) precursor activated with 8%  $\text{Na}_2\text{O}$  solution (binder wt.%). All concretes were produced using a mix of fine natural aggregates (NA) and coarse RAP aggregates (all raw materials were added at room temperature). The three alkali-activated concretes used different types of coarse RAP aggregates, as described in section 3.2.3.3. Table 3.7 shows the mix composition of the reference and the alkali-activated concrete.

Table 3.7. Lean concrete mix proportion (kg/m<sup>3</sup>)

Notation	Binder			Solution		Aggregates			
	PC	BFS	MK	NaOH	Water	Fine	RAP1	RAPL	RAPH
<b>RC</b>	122	-	-	-	132	730	1217	-	-
<b>NR</b>	-	110	11	12.7	130	730	1217	-	-
<b>LB</b>	-	110	11	12.7	130	730	-	1217	-
<b>HB</b>	-	110	11	12.7	130	730	-	-	1217

For the preparation of the AAM, NaOH and water were mixed in advance and allowed to cool down to room temperature. The mixing procedure for the lean concrete samples was: (i) The weighted aggregates and binders were added into a mixer (Figure 3.13) and dry-mixed for 2min; (ii) the solution was poured while still mixing and mixed for another 2 min, until uniformly mixed (no extra water was added during mixing); (iii) the specimens were manually compacted using a proctor rammer (4.50±0.04 kg) dropped from a height of (457±3mm). For the latter, the number of blows and layers were selected in a way that the compaction energy would be between 0.56-0.63 MJ/m<sup>3</sup> as defined by NBN EN 13286-2:2010 (Table 3.8).

Table 3.8. Proctor compaction

Sample Shape	Size (mm)	Proctor compaction		Energy MJ/m <sup>3</sup>
		Layers	Blows	
Cube	100 x 100	2	15	0.60
Cylinder	100 x 200	3	15	0.58
Cylinder	150 x 300	6	25	0.57

The proctor rammer was also used to determine the maximum dry density (MDD) and optimum moisture content (OMC) of the RAP-AMM concretes (NR, LB, and HB), using modified proctor compaction as per NBN EN 13286-2:2010. The main objective was to observe the impact of the different production methods and bitumen content on MDD and OMC.

All lean concrete samples were demoulded after 24h and cured and sealed in a plastic bag at room temperature until testing (Figure 3.14).



*Figure 3.14. Lean concrete samples sealed and ready for storage (University of Antwerp)*

### **3.4 Experimental methodologies**

This section describes the procedures for experiments most frequently used in this research. It is divided into the characterization of pastes, mortars and lean concretes.

#### **3.4.1 Characterisation of pastes**

Fourier Transform Infrared (FTIR, Figure 3.15) was the only technique that required the use of pastes. It may be used to determine the structure of materials (chemical bonds that lead to structural identification). Herein, FTIR was performed to investigate the change of chemical groups during activation of AMM with NaOH ( $M_s = 0$ ) and NaOH+Na<sub>2</sub>SiO<sub>3</sub> ( $M_s = 1$ ) and BFS replacement with only 20%MK. Therefore, no fine aggregate (either natural or RAP) was used. The spectra of raw materials (BFS and MK) were included for comparison.



*Figure 3.15. FTIR instrument (University of Antwerp)*

FTIR was carried out in pastes as described in section 3.3.1. The 7 days old pastes were crushed using a pestle and mortar, and the fraction passing 63 microns sieve was immediately used for FTIR. The measurements were performed with a Thermo Scientific Nicolet iS™ 10 FTIR Spectrometer. The infrared analyses were performed using a diamond ATR crystal with a resolution of  $4.0\text{ cm}^{-1}$  and the wavelength range of  $4000\text{--}500\text{ cm}^{-1}$ .

## **3.4.2 Characterisation of mortars**

### **3.4.2.1 Calorimetry**

An isothermal calorimeter (Figure 3.16, TAM air, TA Instruments) was used to investigate the reaction kinetics of the alkali-activated mortars. The equipment was set at a constant temperature of  $20\text{ }^{\circ}\text{C}$ . Approximately 15 g of mortar were mechanically mixed inside a glass ampoule for 1.5 min using a hand mixer. The hand mixer had a small spatula attached to reach inside the glass ampoule. The ampoule containing the mortar was carefully placed inside the calorimeter approximately 3 min after the mixing procedure initiation. The heat production was recorded for up to seven days.





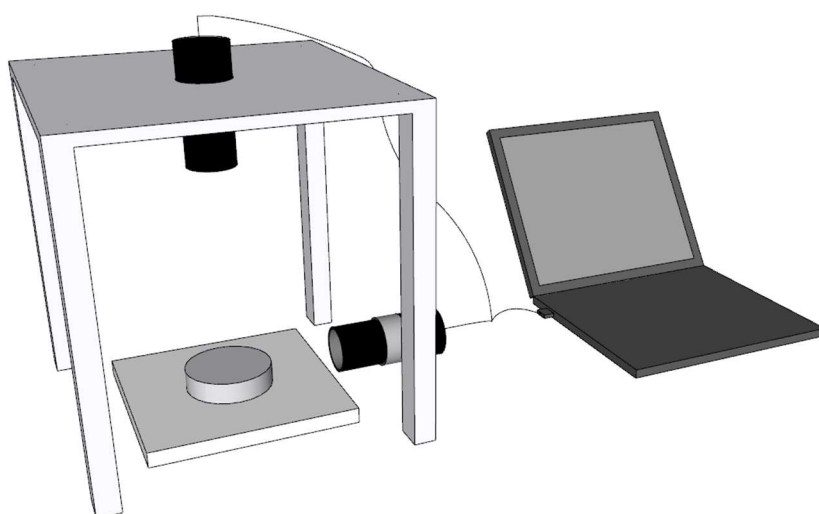
Figure 3.16. Isothermal calorimetry and glass ampoule (University of Antwerp)

### 3.4.2.2 Shrinkage assessment

The shrinkage of the mortars was measured using a digital image assessment, in which a set of cameras inside a black room records the volume changes of the sample (Figure 3.17). After mixing, the fresh samples were carefully placed in a PVC ring mould (diameter  $61 \pm 1 \text{ mm}$  and height  $1.7 \pm 0.1 \text{ mm}$ ). After approximately 40 minutes, the mould was removed, and the cameras would start capturing the image every 15 minutes for seven days. The images were then uploaded to an imaging processing software, where the total area of the sample (and the shrinkage over time) was calculated. The shrinkage strain ( $S$ , Equation 3.2) was calculated by dividing the area of the sample ( $A_t$ ) by the area of the sample at the beginning of the reading ( $A_0$ ).

$$S (\text{mm}^2/\text{mm}^2) = A_t/A_0$$

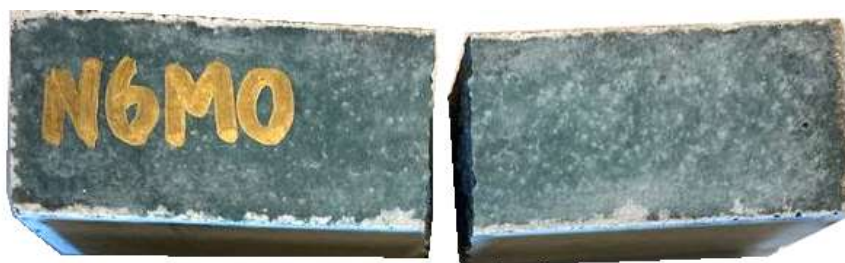
Equation 3.2



*Figure 3.17. Digital Imaging Setup*

#### **3.4.2.3 Flexural strength and compressive strength**

For the mortar samples, flexural and compressive strength were measured at specified ages (between 1 and 60 days old) following NBN EN 196-1: 2016. Three prismatic samples ( $4 \times 4 \times 16$  cm) were used at each age. The samples were kept sealed at room temperature until tested. All samples were first tested for flexural strength (Figure 3.18), and later each of the broken halves of the same sample was tested for compressive strength, as recommended by the standard method.



*Figure 3.18. Prismatic mortar sample after flexural strength test*

#### **3.4.2.4 Mercury Intrusion Porosimetry (MIP)**

Mercury Intrusion Porosimetry (MIP) was used to assess the pore size distribution using a Quantachrome PoreMaster-60 (Figure 3.19), with low pressure ranging from 1.5 to 300 kPa and high pressure from 140 kPa to 420 MPa. The study assumed a contact angle of  $140^\circ$  and the surface tension of mercury of 0.48 N/m. Thin slices of the centre of uncrushed 4x4x16 mm prisms were sawed (about 4 mm thick) and dried at  $60^\circ\text{C}$  for 72 h before testing (Figure 3.20). The low temperature of the drying regime was selected to avoid degrading (melting) the bitumen layer on the surface of the RAP aggregates and was applied to samples produced with RAP aggregates and NA.



*Figure 3.19. MIP equipment (Cefet-MG)*



Figure 3.20. Example of samples prepared for MIP

#### 3.4.2.5 Apparent porosity

The apparent porosity ( $p$ , Equation 3.3) was determined using a modified vacuum saturation method described by RILEM CPC 11.3:1984. The technique consists of weighing the samples in three different conditions: dry ( $w_1$ ), saturated underwater ( $w_2$ ), and saturated surface dry ( $w_3$ ). To measure  $w_2$  and  $w_3$ , the samples were saturated underwater and vacuumed for 24 hours. To avoid the problems with partial saturation of the samples, they were reduced in size. The samples were oven-dried at  $60 \pm 5^\circ\text{C}$  until constant weight (approximately three days) to calculate the dry weight. A lower drying temperature was employed to avoid melting the bitumen present on the surface of the RAP aggregates. Four samples of each formulation were tested, and the average and standard deviation were reported. The samples were tested at 3, 7, 28 days.

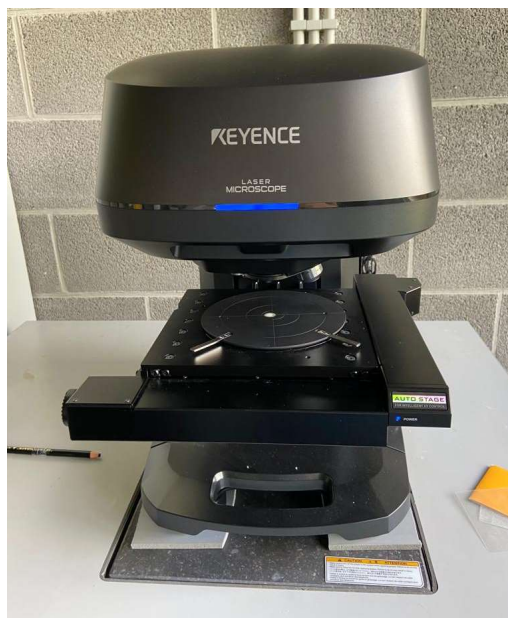
$$p = \frac{w_3 - w_1}{w_3 - w_2} \quad \text{Equation 3.3}$$

#### 3.4.2.6 Microstructure analysis

Scanning electron microscopy (SEM) is a valuable technique to characterise the microstructure of AAM. However, since it can only produce black and white images, it can be challenging to visualise the transitions between the mastic-aggregate and the mastic-AAM matrix when RAP is used as aggregate. A combination of SEM with Confocal Laser Scanning Microscopy (CLSM) was employed in this thesis to observe the microstructure of RAP-AAM.

SEM on Backscattering Electron Image was performed either using a Hitachi TM3000 benchtop microscope (from Cefet-MG for research in Chapter 4) or a Coxem EM 30P benchtop microscope using a 15 kV as accelerating voltage (from University of Antwerp for research in Chapter 5). In both cases, SEM was used to assess the porosity of samples mainly at the interface transition zone (ITZ) between AAM matrices and NA or RAP aggregates. The only reason for using different SEM was to accommodate laboratory maintenance schedules.

CLSM is an optical imaging technique that enables live coloured three-dimension images. A Keyence VK-X1000 Confocal Microscope (Figure 3.21) was first used to assess the particle shape of both aggregates (natural and RAP) and determine the amount of bitumen covering the RAP particles quantitatively. The latter was calculated by image analysis after treatment of 3 stitched CLSM images (corresponding to 49 images) with the software ImageJ. CLSM was also employed on cut and broken samples of selective mortar formulations to assess the ITZ between matrix and aggregates.



*Figure 3.21. Confocal laser scanning microscope(University of Antwerp)*

The mortar samples for microscopy were mounted on an epoxy resin and later ground using a sequence of SiC paper (120, 320, 2400, 4000 grit and diamond film) and 10nm carbon coating (Figure 3.22).



*Figure 3.22. Sample prepared for microscopy*

### **3.4.3 Characterisation of concretes**

#### **3.4.3.1 Compressive and splitting tensile strength**

The compressive strength of the 100x100 mm concrete cubes was determined based on the NBN EN 13286-41:2021 at a loading rate of 0.4MPa/s. Three specimens of each composition were tested at both 7 and 28 days. The ultrasonic pulse velocity (UPV) of the samples was recorded before crushing.

The indirect tensile strength was measured on 100x200 mm cylinders as per NBN EN 13286-42:2003 at a 0.2 MPa/s loading rate. Three specimens of each composition were tested at the same age (7 and 28 days).

#### **3.4.3.2 Modulus of elasticity and ultrasonic pulse velocity (UPV)**

The static modulus of elasticity was performed on cylindrical specimens (150 x 300 mm) as prescribed in EN12390-13:2021. The test was performed for two specimens of each formulation at 28 days. The compressive strength ( $f_c$ ) was estimated from a relationship between cubes and cylinders. The samples were cyclically loaded following method A described in the procedure at a rate of 0.4 MPa as follows.

Three preloading cycles were carried out with stresses ranging from 0.5MPa to 0.15fc followed by three loading cycles with stresses ranging from 0.15fc to 0.33fc. Three electronic universal compressometers-extensometers were attached to the specimens and used to measure the deformation in compression and to obtain the average strain undergone by the cylinders during the test.

UPV technique may be used to determine the dynamic modulus of elasticity. It is a non-destructive test that determines the propagation velocity of longitudinal stress waves generated by a transducer through a concrete sample. Each transducer was placed on opposite faces of the specimens (direct transmission) and the pulse velocity was recorded. Concretes with higher pulse velocities are considered more homogeneous and with higher quality, while lower velocities indicate the presence of cracks and voids (Saboo et al., 2020). The dynamic modulus of elasticity ( $E_d$ ) can be estimated from Equation 3.1, as proposed by ASTM C-597. In Equation 3.4,  $V$  is the velocity of the wave propagation,  $\rho$  is the density of the concrete, and  $\mu$  is the Poisson's ratio.

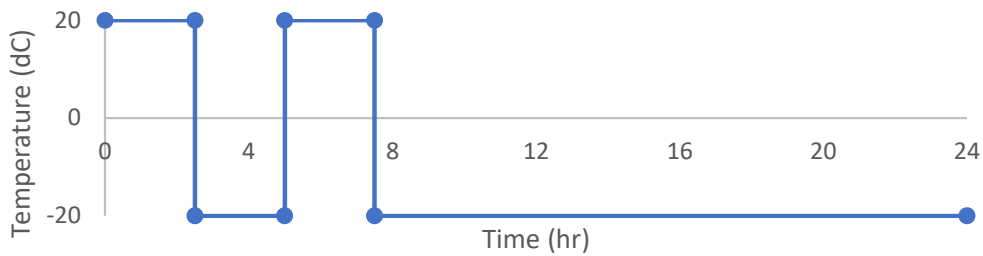
$$E_d = \frac{\rho V^2 (1+\mu)(1-2\mu)}{(1-\mu)} \quad \text{Equation 3.4}$$

Previous studies in RAP-PC systems indicated that concrete samples produced with high RAP replacement (>60%) have a Poisson ration ranging from 0.21-0.30 (Ghazy et al., 2022; Nabil Hossiney, 2012; Saboo et al., 2020; Su et al., 2014; Tia et al., 2012). The Poisson's ratio was assumed 0.25 in this research.

### **3.4.3.3 Freeze and Thaw (F&T)**

The F&T procedure adopted in this research is a modified version of ASTM C666. Three samples from each composition were subjected to freeze and thaw cycles after 14 days of curing. The samples were initially placed in a water bath (at room temperature) for 48 hours. After this period, the excess water was removed using a damp cloth, and the samples' weight and pulse velocity was recorded. Each sample was then carefully wrapped and sealed with a plastic sheet to prevent water loss/gain during the experiment. During 24 hours two complete freeze and thaw cycles were performed. The samples were manually moved

from the freezing chamber at  $-20^{\circ}\text{C}$  to the thawing bath at  $+20^{\circ}\text{C}$ . The samples were kept frozen during the nights and weekends (Figure 3.23). The samples had their weight and pulse velocity measured after 18 and 36 cycles. At the end of the experiment, the F&T and reference samples were tested for compressive strength.



*Figure 3.23. F&T cycles in 24 hours*



# BIBLIOGRAPHY

---

Duran Atış, C., Bilim, C., Çelik, Ö., Karahan, O., 2009. Influence of activator on the strength and drying shrinkage of alkali-activated slag mortar. *Constr. Build. Mater.* 23, 548–555. <https://doi.org/10.1016/J.CONBUILDMAT.2007.10.011>

Ferreira, W.L.G., Castelo Branco, V.T.F., Vasconcelos, K., Bhasin, A., Sreeram, A., 2021. The impact of aging heterogeneities within RAP binder on recycled asphalt mixture design. *Constr. Build. Mater.* 300, 124260. <https://doi.org/10.1016/J.CONBUILDMAT.2021.124260>

Ghazy, M.F., Abd Elaty, M.A.A., Abo-Elenain, M.T., 2022. Characteristics and optimization of cement concrete mixes with recycled asphalt pavement aggregates. *Innov. Infrastruct. Solut.* 7, 1–15. <https://doi.org/10.1007/s41062-021-00651-5>

Nabil Hossiney, 2012. Evaluation of Concrete Mixtures Containing Rap for Use in Concrete Pavements. a Diss. Present. To Grad. Sch. Univ. Florida Partial Fulfillment Requir. Degree Dr. Philos. <https://doi.org/10.1017/CBO9781107415324.004>

NBN EN 12697: 2020, n.d. Bituminous mixtures - Test methods - Part 1: Soluble binder content.

NBN EN 196-1: 2016, n.d. Methods of testing cement - Part 1: Determination of strength.

Niels, M., 2015. Vergelijkend onderzoek naar schraal beton en zandcement bij labo- en werfomstandigheden. Universiteit Antwerpen.

Palacios, M., Puertas, F., 2005. Effect of superplasticizer and shrinkage-reducing admixtures on alkali-activated slag pastes and mortars. *Cem. Concr. Res.* 35, 1358–1367. <https://doi.org/10.1016/j.cemconres.2004.10.014>

Pavel, K., Oleg, P., Hryhorii, V., Serhii, L., 2017. The Development of Alkali-activated Cement Mixtures for Fast Rehabilitation and Strengthening of Concrete Structures. *Procedia Eng.* 195, 142–146. <https://doi.org/10.1016/j.proeng.2017.04.536>

RILEM CPC 11.3:1984, 1984. Water Absorption by Immersion Under Vacuum.pdf.

Saboo, N., Nirmal Prasad, A., Sukhija, M., Chaudhary, M., Chandrappa, A.K., 2020. Effect of the use of recycled asphalt pavement (RAP) aggregates on the performance of pervious paver blocks (PPB). *Constr. Build. Mater.* 262, 120581. <https://doi.org/10.1016/j.conbuildmat.2020.120581>

Shi, C., 1996. Strength, pore structure and permeability of alkali-activated slag mortars. *Cem. Concr. Res.* 26, 1789–1799. [https://doi.org/10.1016/S0008-8846\(96\)00174-3](https://doi.org/10.1016/S0008-8846(96)00174-3)

Su, Y.-M., Hossiney, N., Tia, M., Bergin, M., 2014. Mechanical Properties Assessment of Concrete Containing Reclaimed Asphalt Pavement Using the Superpave Indirect Tensile Strength Test. *J. Test. Eval.* 42, 20130093. <https://doi.org/10.1520/jte20130093>

Tia, M., Hossiney, N., Su, Y.-M., Chen, Y., Do, T.A., 2012. Use of reclaimed asphalt pavement in concrete pavement slabs. Gainesville.

Wang, S.-D., Scrivener, K.L., 1995. Hydration products of alkali activated slag cement. *Cem. Concr. Res.* 25, 561–571. [https://doi.org/10.1016/0008-8846\(95\)00045-E](https://doi.org/10.1016/0008-8846(95)00045-E)

Wang, S.-D., Scrivener, K.L., Pratt, P.L., 1994. Factors affecting the strength of alkali-activated slag. *Cem. Concr. Res.* 24, 1033–1043. [https://doi.org/10.1016/0008-8846\(94\)90026-4](https://doi.org/10.1016/0008-8846(94)90026-4)

# THE EFFECT OF RAP AGGREGATES ON ALKALI- ACTIVATED MORTARS

---

The detrimental effect caused by the bitumen coating on strength and porosity has limited the use of RAP on traditional cementitious systems based on Portland cement (PC). The use of RAP with alternative binders, such as alkali-activated materials (AAM) is still scarce.

This **experimental study** investigates the potential use of RAP to substitute natural aggregates (NA) in mortars produced with AAM. The binder was prepared using ground granulated blast furnace slag (BFS), activated sodium hydroxide and sodium silicate. The assessed properties of 100% RAP-AAM were hydration kinetics (Isothermal Calorimetry), pore size distribution (Mercury Intrusion Porosimetry), mechanical performance (Compressive and Flexural strength), and microstructure analysis (Scanning Electron Microscopy and Confocal Laser Scanning Microscopy).

The results show that RAP aggregates do not compromise the reaction of the matrices; however, it causes a significant strength loss: the compressive strength of RAP-mortars was 54% lower than reference NA-mortar at 28 days. The higher porosity at the interface transition zone of RAP-AAM is the main responsible for the lower strength performance.

Increasing silicate dosages improves alkaline activation, but it has little impact on the adhesion between aggregate and bitumen. Despite the poorer mechanical performance, 100% RAP-AAM still yields enough strength to promote this recycled material in engineering applications.

## 4.1 Introduction

A better understanding of how RAP aggregates impact the properties of AAM could enable the use of these materials as pavement layers and offer another possibility for recycling RAP. This chapter investigates the potential use of fine RAP to substitute NA in alkali-activated mortars. The main objective is to determine how the aggregate replacement affects the properties of AAM prepared and determine the ideal activator.

The three main research topics from this chapter are: (i) the impact of the alkali content and RAP addition on the reaction of AAM; (ii) the effect of the alkali concentration on the mechanical properties (compressive and flexural strength) of the mortars containing RAP; (iii) the effect of RAP aggregates on the microstructure and porosity of the mortars.

AAM was produced using ground granulated blast furnace slag (BFS) activated with 4% or 6% Na<sub>2</sub>O (wt. BFS) combined with a modulus of silica (Ms) equal to 0, 0.5 and 1.0. The assessed properties of 100% RAP-AAM were hydration kinetics (Isothermal Calorimetry), pore size distribution (Mercury Intrusion Porosimetry), and mechanical performance at 1, 3, 7, 28 and 60 days (Compressive and Flexural strength). The microstructure was assessed via a combination of Confocal Laser Scanning Microscopy (CLSM) with Scanning Electron Microscopy (SEM) in the characterization of alkali-activated materials containing RAP aggregates.

## 4.2 Experimental summary

The complete description of the material and methods used in this chapter is available in Chapter 3. Table 5.1 shows a summary of the type of specimens produced and their composition. All mortar samples were produced using a 1:1.5 precursor: aggregate ratio and water/precursor of

0.5. Samples starting with “N” were produced using natural aggregates (NA), while “R” means that the aggregate used was fine RAP (< 4 mm).

The aggregates used, both NA and RAP, were previously sieved, separated into fractions (using 4mm, 2mm, 1mm, 0.5mm, 0.25mm, 0.125mm and 0.063mm sieves) and the same gradation was used for each aggregate type.

*Table 5.1. Composition studied*

<b>Notation</b>	<b>Precursor</b>	<b>Na<sub>2</sub>O (%)</b>	<b>Ms</b>	<b>Aggregate</b>
N4MO / R4MO	100% BFS	4	0	NA / RAP
N4M0.5 / R4M0.5	100% BFS	4	0.5	NA / RAP
N4M1 / R4M1	100% BFS	4	1	NA / RAP
N6M0 / R6M0	100% BFS	6	0	NA / RAP
N6M0.5 / R6M0.5	100% BFS	6	0.5	NA / RAP
N6M1 / R6M1	100% BFS	6	1	NA / RAP

For each of the 12 compositions studied 17 prismatic (4x 4x 16 cm) samples were produced, thus a total of 204 specimens. Three specimens were tested for flexural strength at each age (1, 3, 7, 28 and 60 days) and the same specimens were later tested for compressive strength. The spare specimens were left untested and used for MIP and microscopy. Small pieces of the core of the specimens were sawed and used for the tests.

## 4.3 Results & Discussion

### 4.3.1 Isothermal Calorimetry

Figure 5.1 and Figure 5.2 present the results of the isothermal calorimetry when, respectively, natural aggregates and RAP aggregates were employed. Time 0 hrs represents the start of the test at the equipment (with zero samples loaded). All mortars showed a sharp main peak at the beginning of the curve ( $60 \pm 10$  min of testing). This reaction is only partially captured due to the time it takes to mix, load, and equilibrate the specimen in the instrument. After the initial peak, the specimens prepared without silicates (N4M0 and N6M0) show an almost immediate second

increase in heat flow, while the specimens with silicates (N4M1 and N6M1) show a slow reduction before the next flow peak.

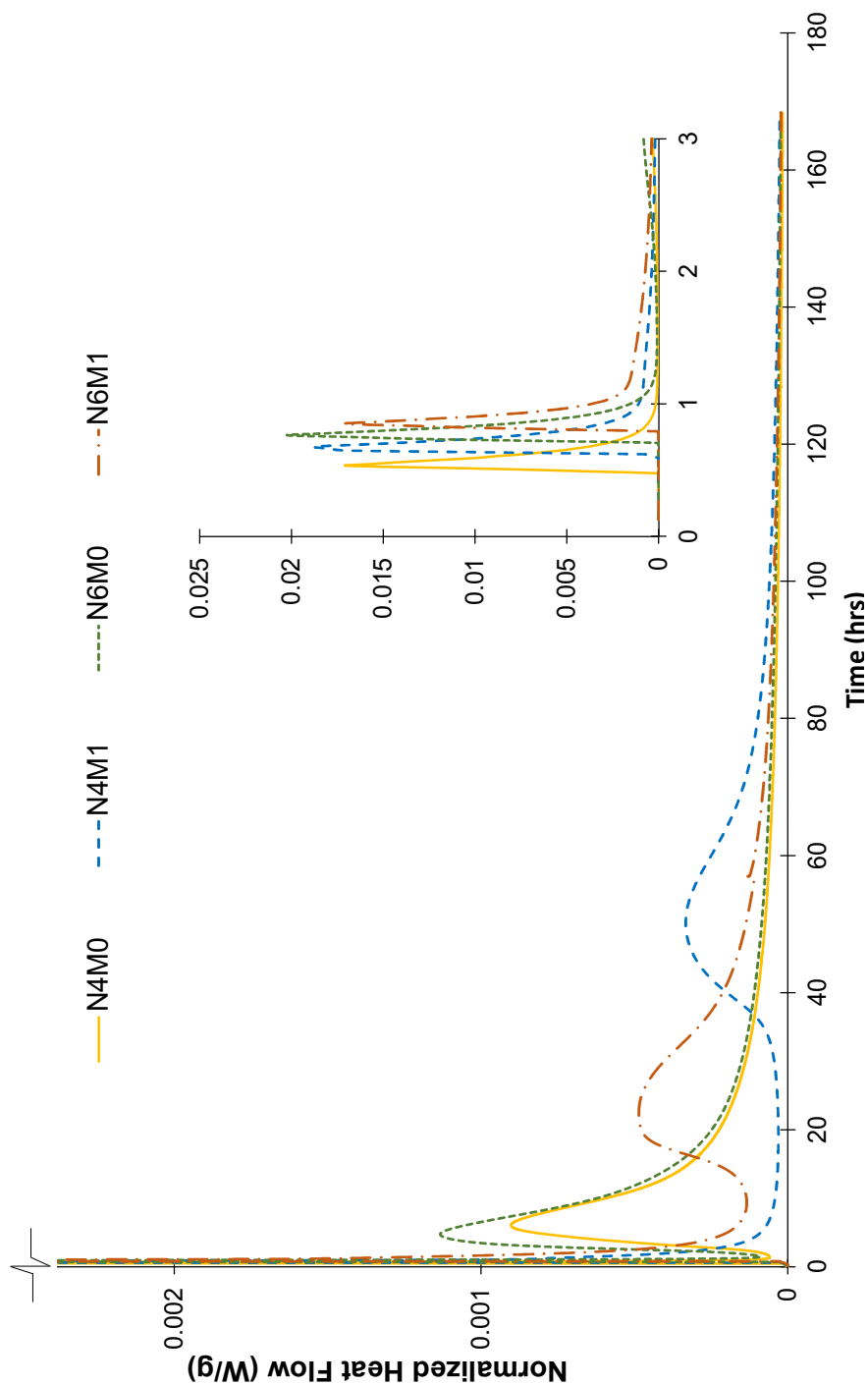


Figure 5.1. Effect of activators on heat evolution of natural aggregate mortars specimens

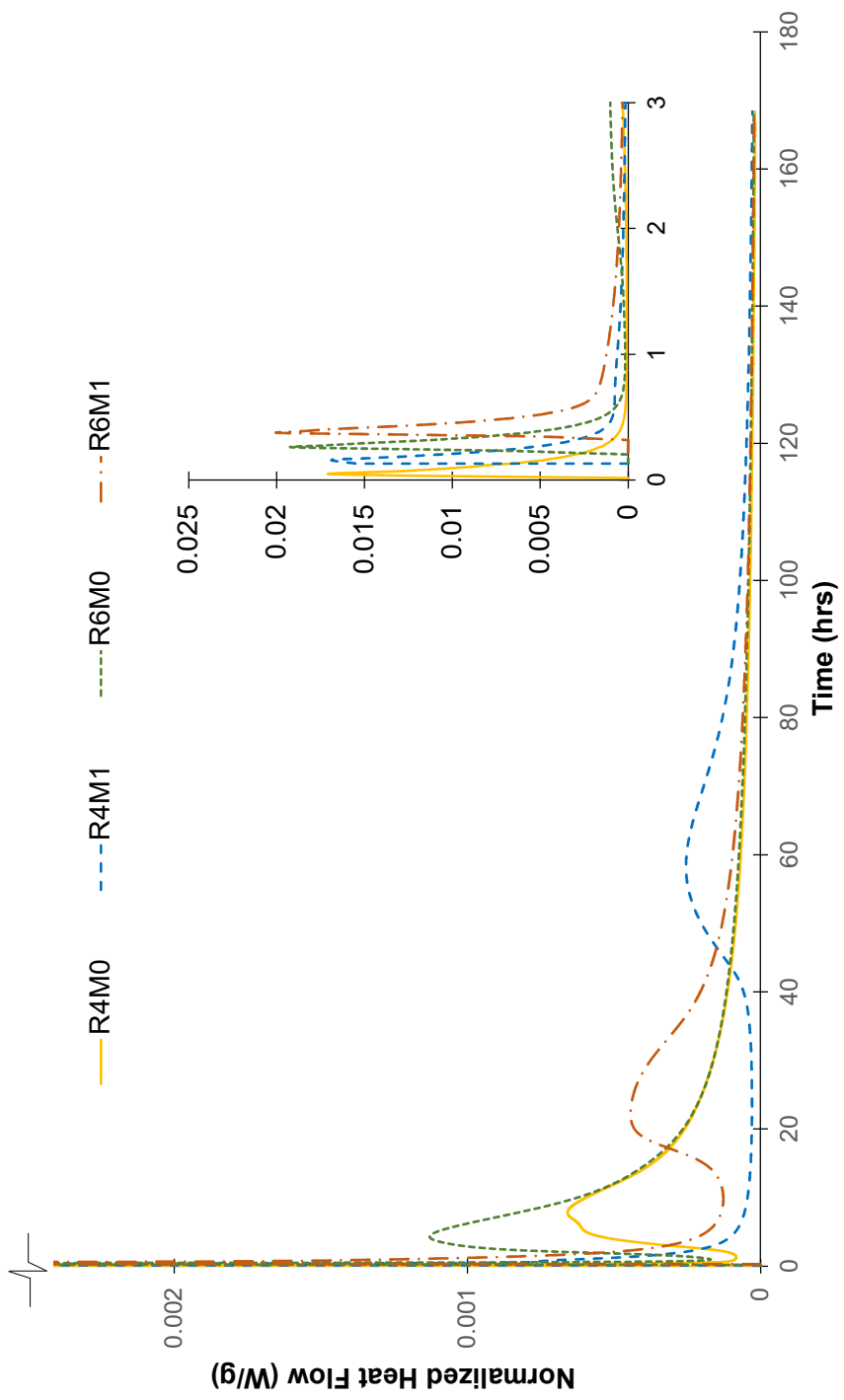


Figure 5.2. Effect of activators on heat evolution of RAP aggregate mortars specimens

The complex mechanism involved in the alkaline activation of BFS is not yet fully understood and is often summarised firstly as the breakdown of the structure, followed by polycondensation and precipitation of the reaction products (Fernandez-Jimenez et al., 1998; Liu et al., 2018). The heat changes of BFS can be described in five steps. There is a sharp peak at the first few minutes of the reaction associated with the partial dissolution of the slag. This is followed by an induction period with low reactivity until the next peak. The second peak comprises the third and fourth steps, called acceleration and deceleration, where massive precipitation of the reaction products occurs. The final step is called decay, and it is a low reactivity period until the end of the reaction (Huanhai et al., 1993; Liu et al., 2018).

The type of alkalis used in the activator has an important role in each of the steps. The high intensity at the beginning of the reaction and the impact of the specimen preparation makes it difficult to detect and compare the first peak. The effect of the activators on steps two to five can be seen more clearly.

When the activator is NaOH (samples N4M0 and N6M0), the induction period is extremely short, and the second peak of the curve (associated with the formation of hydrated products such as C-A-S-H gel) is more intense and shorter in duration (Fernandez-Jimenez et al., 1998; Gebregziabihier et al., 2016; Kashani et al., 2014). Specimens with sodium silicate (N4M1 and N6M1) show a delayed second peak (after the induction period) that is correlated to the workability retention typically from the employment of water glass (Kashani et al., 2014). In both systems (NaOH or NaOH + Na<sub>2</sub>SiO<sub>3</sub>), the induction period is highly reduced by increasing sodium oxide, which aligns with previous research (Gebregziabihier et al., 2016; Liu et al., 2018). The peaks are also higher when more Na<sub>2</sub>O is used when comparing N6M1 with N4M1, and N6M0 with N4M0. This indicates that OH<sup>-</sup> has an accelerating effect on the dissolution and hydration of the slag (Liu et al., 2018).

When natural aggregates are replaced with RAP particles (Figure 5.2), the heat changes of the samples follow a similar trend. This result indicates that the bitumen coating on the RAP aggregates does not alter the hydration reaction of the alkali-activated binder at any of the concentrations studied. Figure 5.3 summarises the cumulative heat of all



formulations, and it is a better way to show some minor differences between the curves with NA and RAP. In other words, bitumen has a high heat capacity; thus, RAP-containing mortars yield a smaller temperature rise compared with NA mortars. Similar results were observed with RAP aggregates on Portland cement matrices (El Euch Ben Said et al., 2018; Shi et al., 2020).

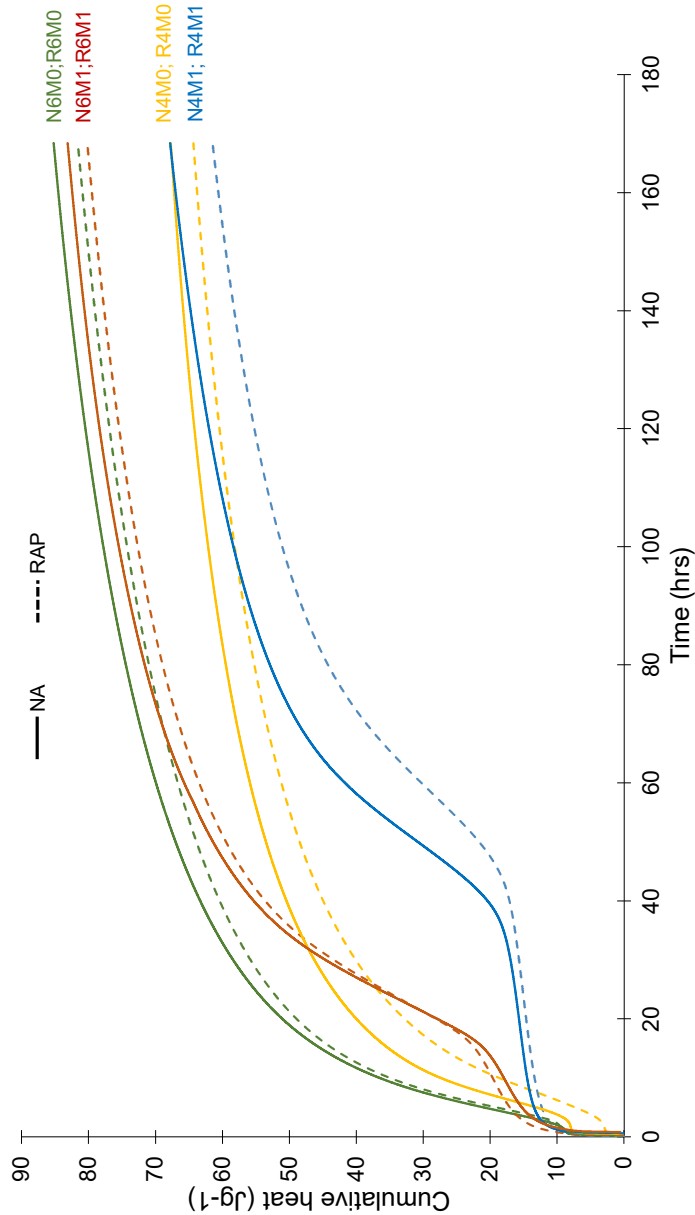


Figure 5.3. Cumulative heat of alkali-activated mortar specimens

The higher  $\text{Na}_2\text{O}$  content (6% wt. against 4% wt. slag) generates more heat during the activation, irrespective of the type of aggregate used (Figure 5.3). The effect on mechanical performance will be discussed in the following section.

The calorimetry results indicate that the bitumen presence on the RAP particle has little to no impact on alkali-activation kinetics and that the alkali-activated gel could yield similar strength in the presence of NA or RAP. The gel strength is partly responsible for the RAP-AAM composite strength, together with other factors such as aggregate strength, adhesion and ITZ.

### ***4.3.2 Compressive and Flexural Strength***

Figure 5.4 shows the average results for compressive strength of the mortars produced with NA and RAP, while Figure 5.5 shows the flexural strength results. The error bars indicate the standard deviation. The mortars containing RAP aggregates are represented as hatched bars alongside their counterpart mortar made with natural aggregates as a solid bar.

It is possible to notice that the increase in  $\text{Na}_2\text{O}$  from 4% to 6% had a negligible impact on flexural and compressive strength at all ages when  $M_s = 0$  (NaOH-activated formulations). Wang et al. (1994) studied neat NaOH-activated slags; they concluded that above a certain value of  $\text{Na}_2\text{O}\%$ , it is not recommended to increase the alkali dosage as it will not bring any significant increase in strength and might be followed by some negative properties such as efflorescence and brittleness. According to Komnitsas and Zaharaki (2007), KOH-activated slag in the absence of silicates takes longer to solidify, and an increase in the alkali concentration will not bring significant changes to the compressive strength (will not exceed 25 MPa at two days).

A better strength performance from the combined source of activation (sodium silicate + sodium hydroxide) is in accordance with the literature (Fernández-Jiménez et al., 1999; Palacios and Puertas, 2005). At later ages (7 and 28 days), there is a significant increase in compressive strength with sodium silicate—the more sodium silicate is used, the

higher the compressive strength results (Figure 5.4). However, the addition of sodium silicate ( $M_s > 0$ ) does not have a positive effect at early ages (1 day) for all mixes. BFS activated with  $\text{Na}_2\text{O} = 4\%$ , and  $M_s = 1.0$  did not sufficiently react for the 1-day assessment, while the others showed a slight increase in compressive strength. Early strength is an important property for pavement layer materials as it may reduce construction time and allow a faster opening for traffic.

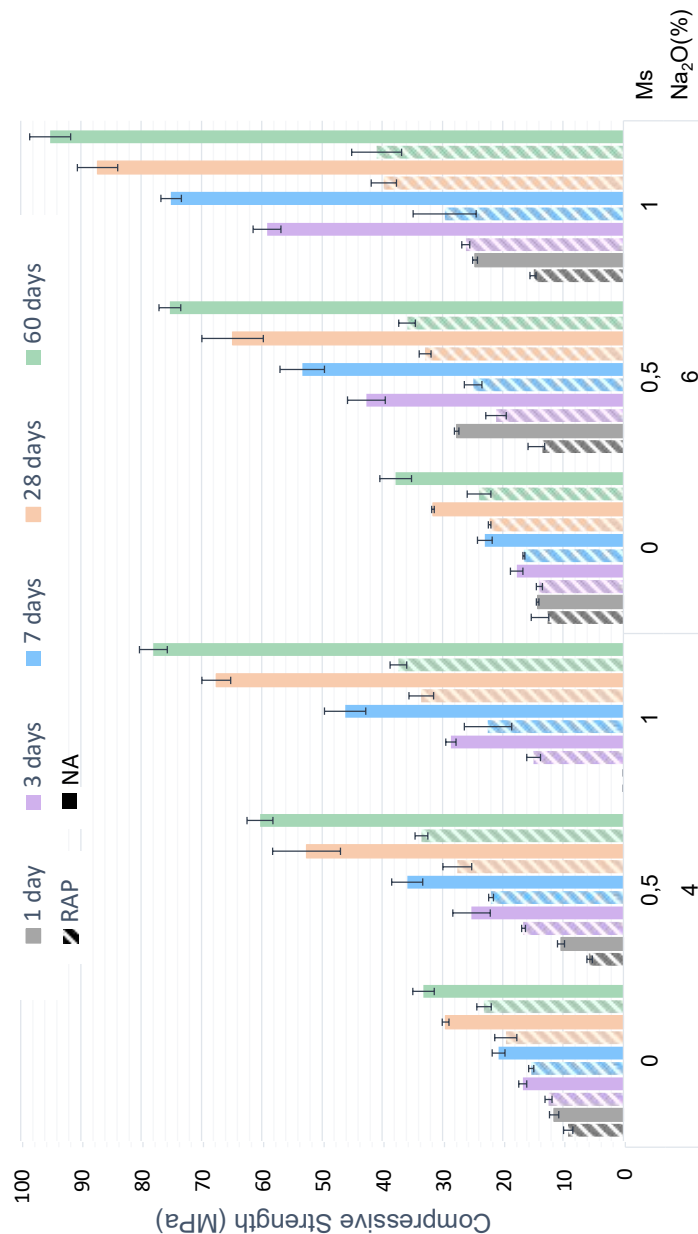


Figure 5.4. Compressive strength of mortars.

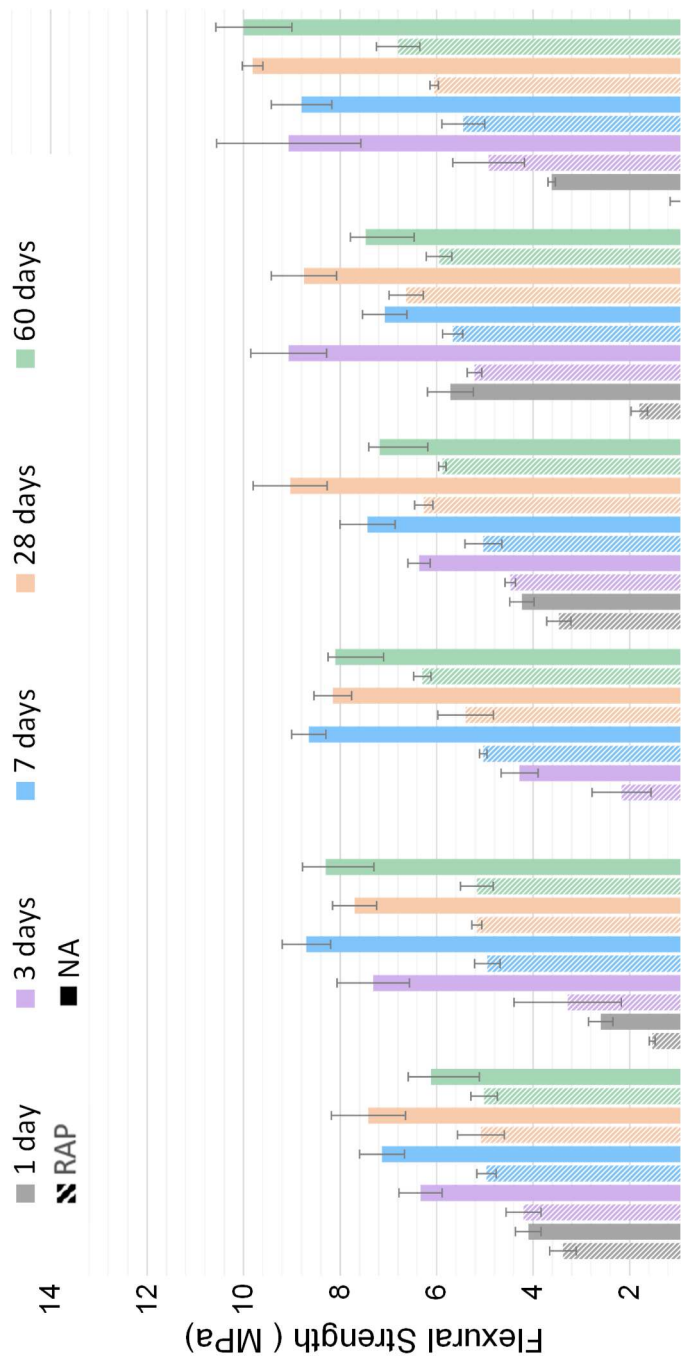


Figure 5.5.Flexural strength of mortars.

The increase in activator dosages was less significant (15% to 43% lower at 28 days) on flexural strength on mortars produced with both NA and RAP (Figure 9). Ageing also played a less important role, as after three days, the results showed little difference (taking into account the standard deviation). The high standard deviation of the samples is likely due to flaws in the mortar's paste, such as air-entrained pores. These flaws allow for the propagation of cracks and compromise the results. The apparent decrease in flexural strength at 60 days is likely to be related to that.

The substitution of NA for RAP caused a significant reduction in the mortars' compressive and flexural strength. A similar result was reported for Portland cement (Abraham and Ransinchung, 2018; Shi et al., 2020) and alkali-activated (Hossiney et al., 2020) matrices. The RAP aggregates compromised samples' ability to gain strength over time; it is possible to observe that the difference in strength between the NA-based and the RAP-based mortars increases as the age of the samples. The addition of sodium silicate promotes a rise in compressive strength, but this is less significant for RAP-AAM. Figure 5.6 shows the impact of increasing the Ms ratio on compressive strength gain and loss. In this figure, 0% represents the strength found for Ms = 0. In general, adding sodium silicate to the RAP systems had half of the effect on compressive strength compared with NA systems. For example, the 28 days compressive strength of NA-based mortar rose 178% when the Ms ratio increased from 0 to 1 (at 6% Na<sub>2</sub>O), and the RAP-mortar increased 79%.

The inability of RAP-mortars to gain strength compared with NA-mortars is likely due to the binding between aggregates and binders and will be further discussed in Section 0.

Despite the reductions in strength, it is possible to observe that RAP mortars presented sufficient compressive strength even for pavement layers (i.e., higher than 20 MPa at 28 days). The use of sodium silicate should be kept to a minimum or avoided since it has limited efficiency. RAP coarse aggregates may further improve the strength if aiming for a lean concrete base course in semi-rigid pavements or surface layers in rigid pavement.

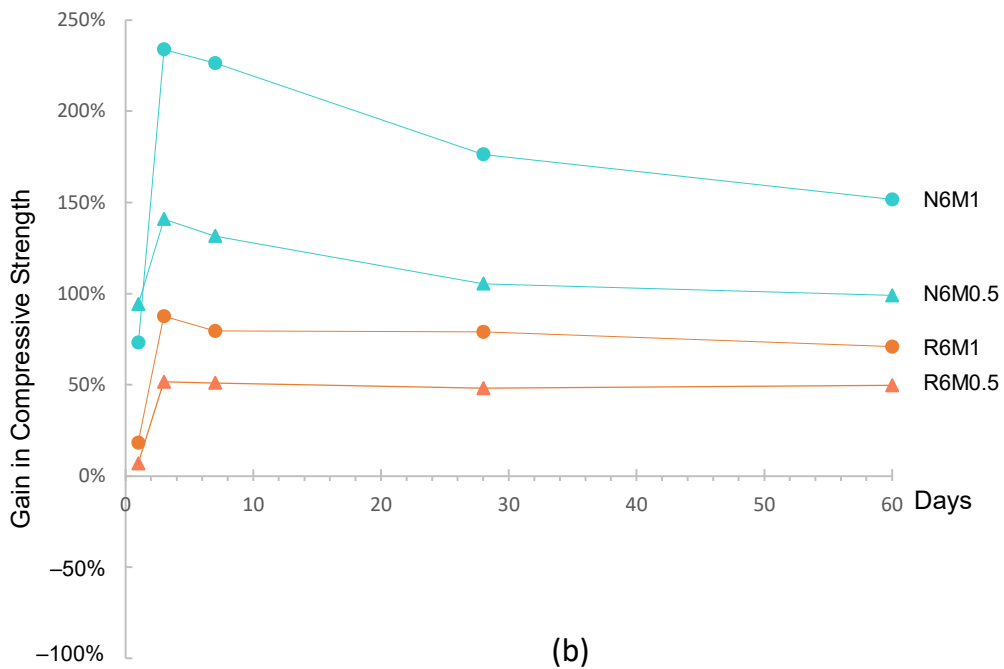
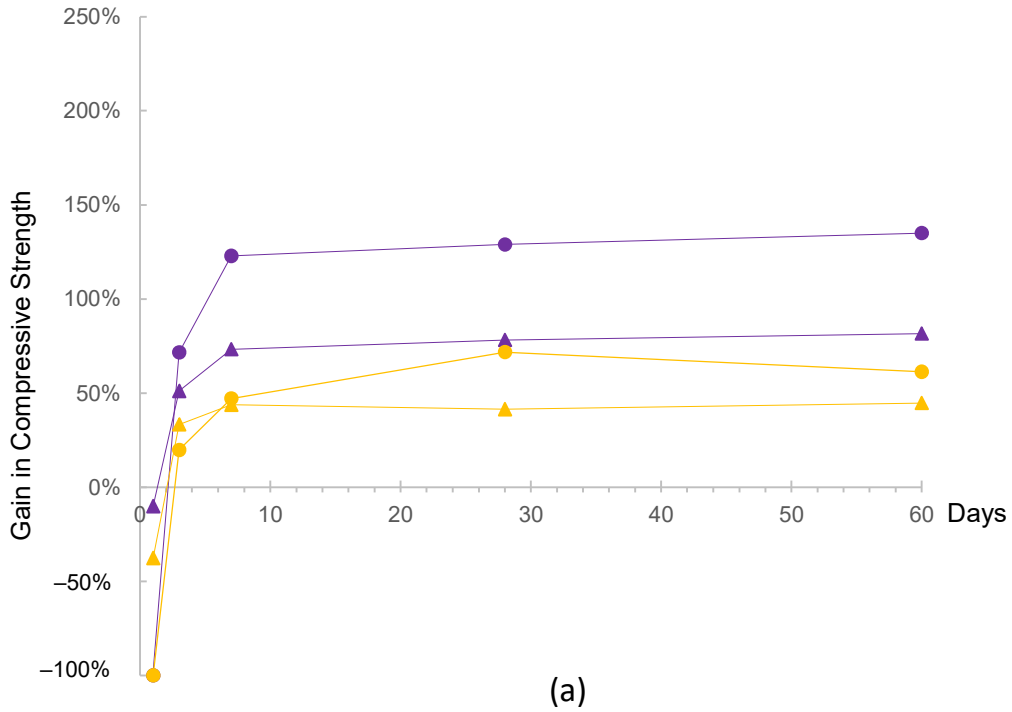


Figure 5.6. Gain and Strength loss in compressive strength due to the increase in Ms for (a) mortars with 4% Na<sub>2</sub>O and (b) mortars with 6% Na<sub>2</sub>O.

### 4.3.3 Mercury Intrusion Porosimetry

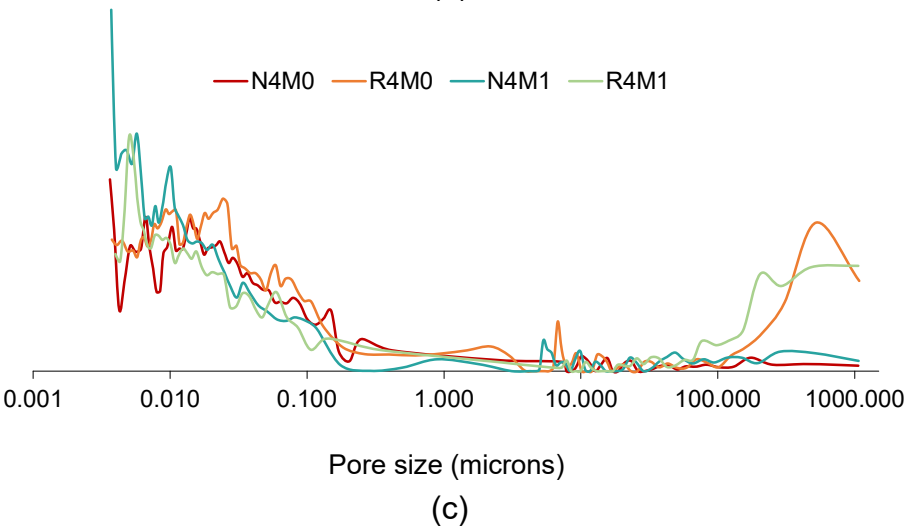
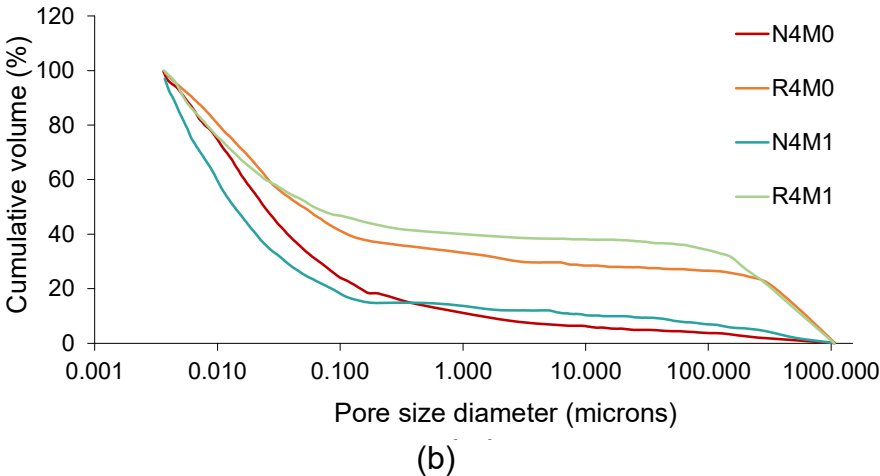
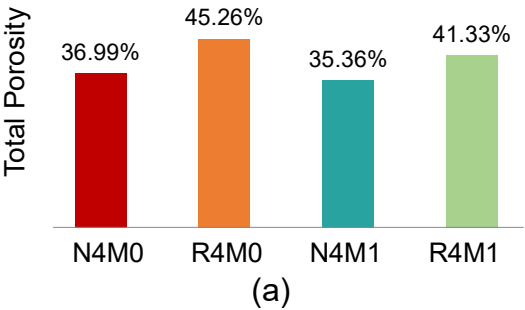
Figure 5.7 presents the results of pore size distribution via MIP. It is important to highlight that this technique has some shortcomings. The high-pressure intrusion may alter the microstructure of cementitious materials, the technique base assumption that all pores are cylindrical and the fact that the pore entrance, rather than the pore itself, is measured (also known as the bottle-neck effect) (Diamond, 2000). Because of that, small variations in formulations might not be detected using MIP. Nevertheless, the latter has been extensively used to characterise cement-based materials, including AAM (Abraham and Ransinchung, 2019; Borges et al., 2016; Gao et al., 2021). The results presented in Figure 5.7 are for four formulations (N4M0, R4M0, N4M1 and R4M1). Therefore, the effect of the type of aggregate and the presence of sodium silicate can be discussed.

It is possible to see that the total MIP porosity of the activated mortars increased with the substitution of natural aggregates with RAP and decreased slightly with soluble silicates (Figure 5.7a). This is in accordance with the compressive strength findings—the use of soluble silicates increases the compressive strength of the samples while the substitution of RAP decreases. The lower porosity and higher strength of the mortar specimens in the presence of silicates are attributed to a higher degree of BFS activation, thus forming a denser pore structure (Shi et al., 2018).

The cumulative intrusion curves (Figure 5.7b) have different shapes according to the types of aggregate used. The mortars containing RAP (orange and light green curves) have coarse porosity, with more than 20% pores above 100  $\mu\text{m}$ . The cumulative curves did not change much for different Ms in the activator (M0 and M1), which shows that the aggregate type affects the pore size distribution more than the matrix.

Pore distribution (Figure 5.7c,d) showed a predominance of micropores ( $<0.1 \mu\text{m}$ ), 59.0% and 53.5%, respectively, for R4M0 and R4M1 and 79.5% and 82.9%, for N4M0 and N4M1. The significant increase in macropores ( $>10 \mu\text{m}$ ) for RAP mortars is confirmed, i.e., 28.7% and 37.9% against 6.2% and 10.5% for mortars with NA (Figure 5.7d). The increased presence of macropores can be attributed to both air

entrapment and increased porosity of the ITZ. The first could indicate that RAP better performs in freezing and thawing and salt decay (Abraham and Ransinchung, 2019). The latter explains the reductions in the mechanical performance of RAP mortars discussed in Section 4.3.2.





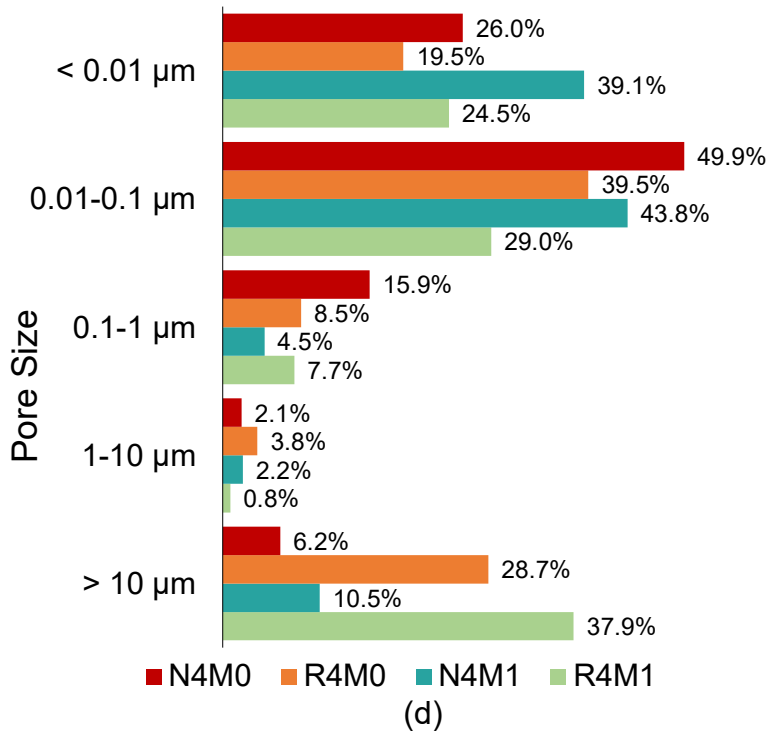


Figure 5.7. MIP results: (a) total porosity, (b) cumulative intrusion curve, (c,d) pore size distribution of RAP-AAM mortars

In summary, the MIP results are a clear indication that the increase in total porosity and pore sizes caused by the replacement of NA with RAP is directly related to the reduction in strength observed. The increased porosity is likely to concentrate around the RAP aggregate particles due to the more porous nature of the recycled aggregate and wall effect. This increased porosity may also affect the permeability and durability of the RAP-AAM by allowing the ingress of harmful solutions.

#### 4.3.4 Microstructure Observation of the Mortars

Figure 5.8 shows the aggregate particles used in this research, as visualised by CLSM. The natural aggregates (Figure 5.8a) have a round shape, while the RAP aggregates (Figure 5.8b) are slightly angular. There is a significant difference in each RAP grain; some are heavily coated (such as the one inside the red circles), while others have little or no bitumen (highlighted by an arrow). The heavily coated grains also seem to form a cluster of smaller particles bonded by the bitumen. The

image analysis (Figure 5.9) resulted in an average of 72.9% ( $\pm 9.6\%$ ) RAP particles covered.


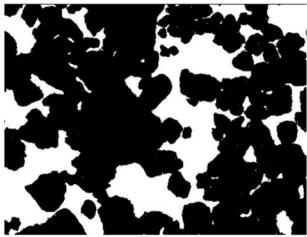
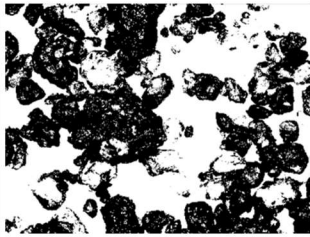








(a)



(b)

*Figure 5.8.Fine aggregates (a) natural (b) RAP.*

		
Original Image	Grains – Area: 4063736	Asphalt – Area: 2926718
		
Original Image	Grains – Area: 95737	Asphalt – Area: 60605
		
Original Image	Grains – Area: 756133	Asphalt – Area: 631059

*Figure 5.9. ImageJ analysis of bitumen content of the RAP grains.*

Figure 5.10 shows the images obtained for specimen N4M0. From the sawed specimen (Figure 5.10a), it is possible to observe the aggregate clusters and note the large quantities of bitumen adhered to the grains (i.e. asphalt mortar), while other sections show only the bitumen with little to no aggregates. RAP-AAM is a composite material and the interaction between each constituent determines the mortar's mechanical behaviour. The presence of clusters of asphalt mortar (large quantities of bitumen) should significantly impact the material's final strength. These clusters may reduce the strength of the composite since asphalt has inferior mechanical properties compared with natural aggregates.

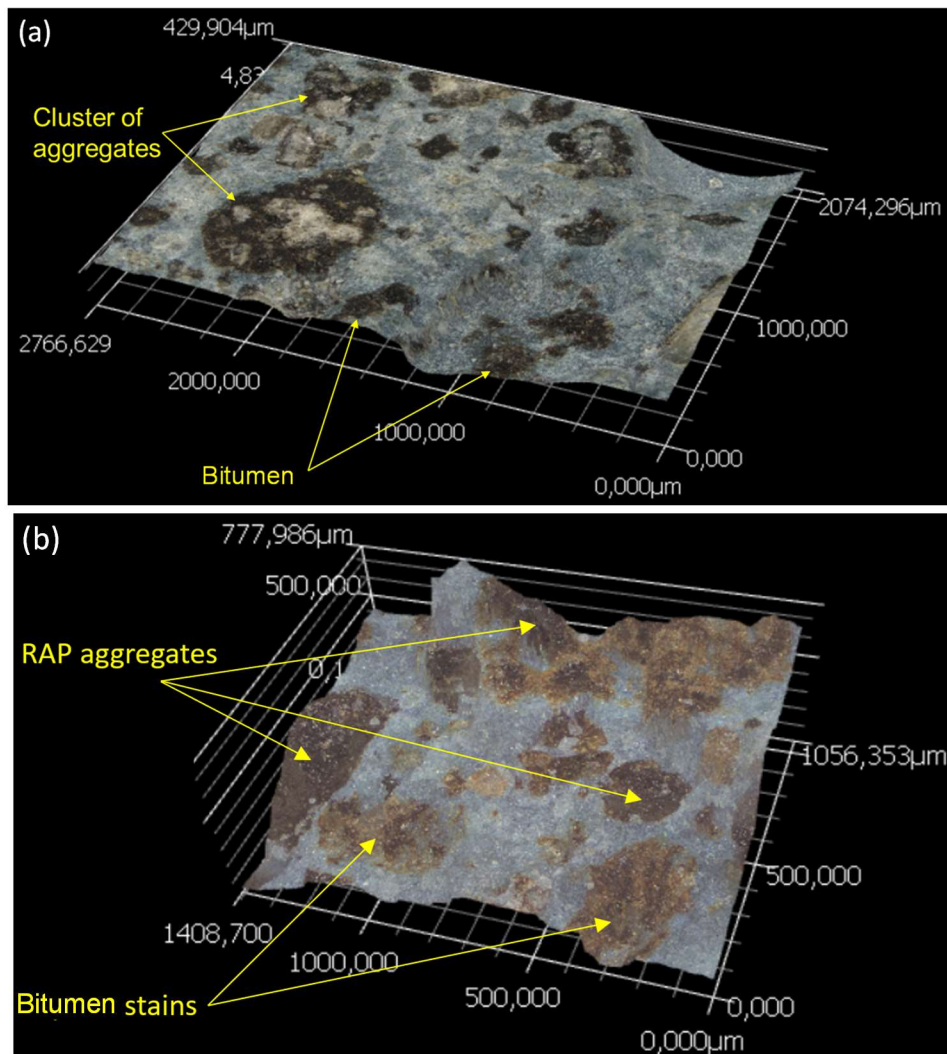


Figure 5.10. Mortar specimen R4M0 (a) sawed, (b) broken.

The broken specimen (Figure 5.10b) has a more irregular surface, and also part of the bitumen appears dissolved into the matrix (leaving asphalt stains). This image shows, in particular, that the fracture of the specimens predominantly happened at the interface with the asphalt layer. This suggests that the poor adhesion between aggregates and bitumen (within the asphalt mortar) could also be responsible for the reduced compressive strength when RAP is used.

The clear distinction between the cementitious matrix, aggregates, bitumen and their distribution in the microstructure is a special feature

that CLSM allows in characterising RAP-based composites. This distinction is not so evident in SEM. On the other hand, CLSM presents poor interface transition zone images (ITZ); the latter is better analysed via SEM.

Secondary backscattered electron images on SEM of the mortars incorporating NA and RAP aggregates are shown in Figure 5.11 and Figure 5.12. It is possible to observe large aggregate grains and the alkali-activated gel containing unhydrated slag particles. Figure 5.11a, and b show, respectively, for NA and RAP, the interface between aggregates and the matrix. There is a negligible increase in porosity at the interface between the NA aggregates and the matrix in Figure 5.11a. In other words, the ITZ is unclear and not easy to delineate (see dashed lines) in NA-based AAM.

The ITZ is easier to identify in Figure 5.11b; it is much enlarged and more porous when NA is replaced by RAP, which was also observed by (Brand and Roesler, 2017) for PC-based matrices. The worsening of the ITZ may explain the high porosity and the loss in strength observed in Section 4.3.2. For the latter, two explanations are possible: the bitumen coating reduces the roughness of the aggregates (and consequently the physical interlocking) and hinders any chemical bonding between matrix and aggregate (El Euch Ben Said et al., 2018).

Figure 5.12 shows the cracking pattern of the specimens. Images (a) and (b) were taken from specimens with NA and specimens (c) and (d) with RAP. The alkaline solution of specimens (a) and (c) contained only NaOH, while specimens (b) and (d) had also sodium silicate. All specimens showed cracking around aggregate particles with connections to the activated slag paste. The cracking pattern has increased in the presence of sodium silicate; however, it is impossible to observe any increase in cracking with the employment of RAP aggregates. The presence of microcracks in transition zones of RAP and PC matrices was observed by (El Euch Ben Said et al., 2017; Sachet et al., 2013). Alkali-activated slag matrices have higher shrinkage than PC matrices (Collins and Sanjayan, 2000). However, it is unclear if the cracks observed result from the higher shrinkage of the gel or if it is due to the specimen's preparation.



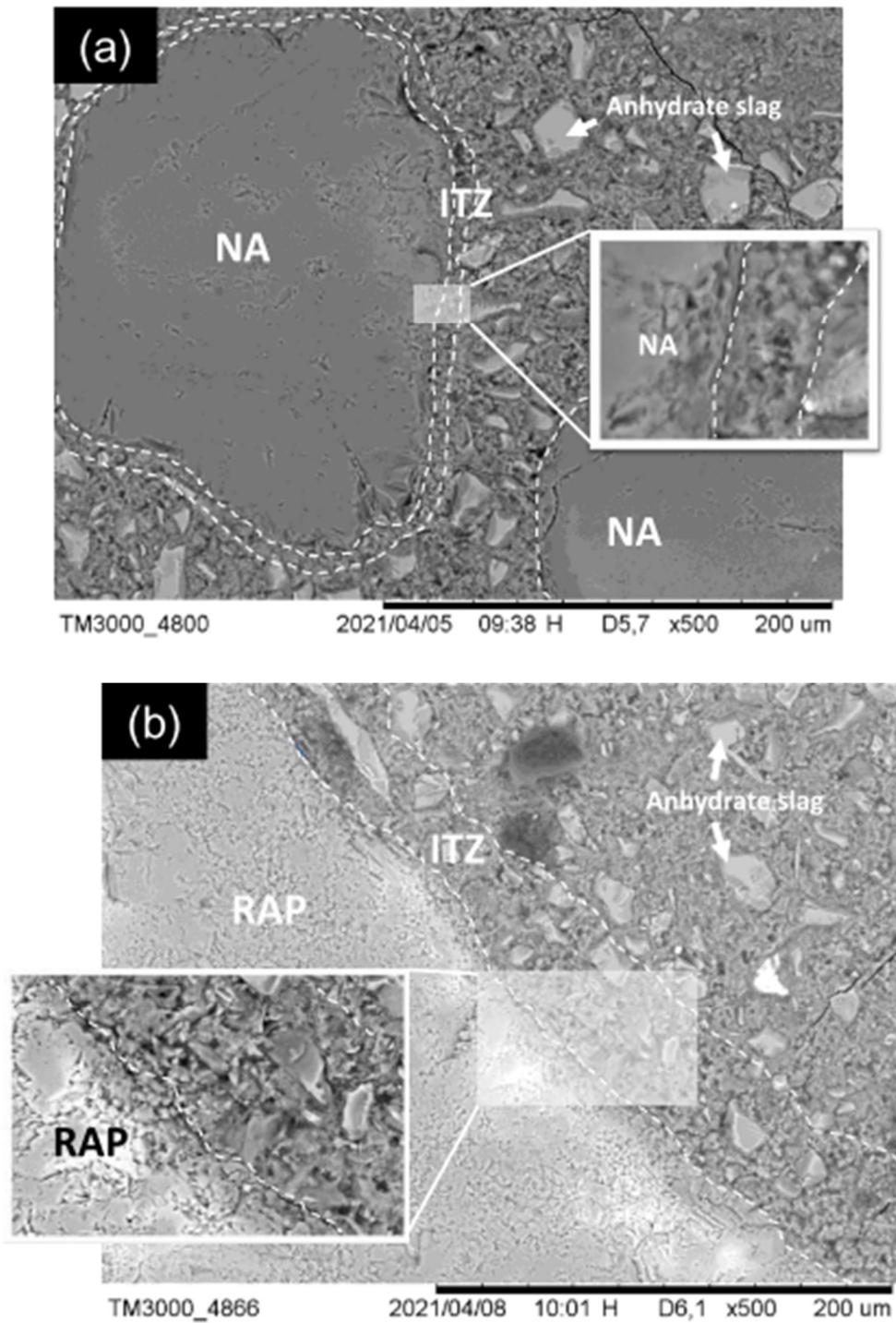
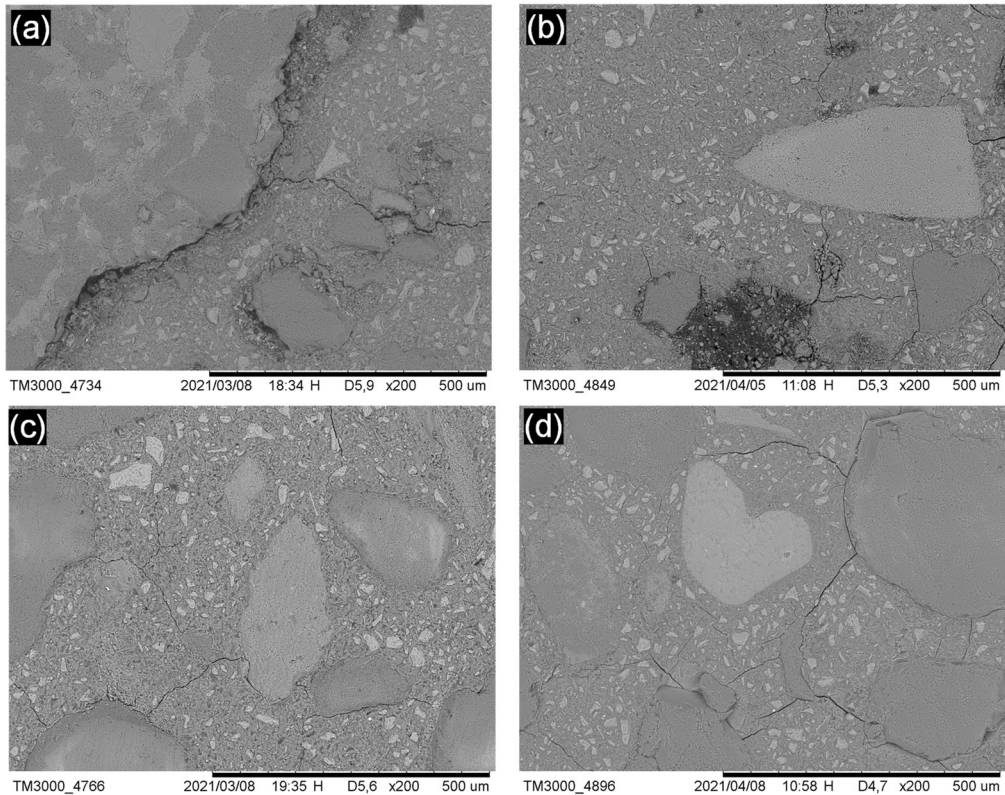


Figure 5.11. SEM Images of mortars (a) N4M1, (b)R4M1.



*Figure 5.12. Evolution of cracking of mortars (a) N6M0, (b) N6M1, (c) R6M0, (d) R6M1. 5.*

The microscopy results confirm the presence of a more porous and larger ITZ (as suggested in Section 4.3.3). It also highlights the presence of clusters within the material. The clusters are weak regions with a high concentration of bitumen from where cracks may appear and propagate, reducing the strength of the composite.

## 4.4 Conclusions

This study investigated the effect of different activator dosages on the properties and microstructure of RAP—alkali-activated slag mortars (AAM). Natural aggregates (NA) were used as a reference. The following conclusions are demonstrated:

- The calorimetry studies showed that 4% to 6%  $\text{Na}_2\text{O}$  (wt. slag) content in the activator increased the heat output of all studied AAM. The

presence of RAP aggregates and the bitumen coating of the RAP particles did not compromise the reaction of the matrices.

- The substitution of NA for RAP caused a significant reduction in both the compressive and flexural strength of the mortars—on average, 44% and 31% at 28 days, respectively. The RAP aggregates compromised samples' ability to gain strength likely due to poor binding between bitumen and matrix/aggregates and weaker ITZ.

- The addition of sodium silicate promotes a rise in compressive strength but is less for RAP-AAM. While the compressive strength of NA mortars increased up to 234% with sodium silicate, the strength of RAP mortars increased to a maximum of 88%.

- MIP results showed that samples prepared with RAP aggregates contained up to 9.3% more pores than samples prepared with NA. The pore content increase was concentrated in the macropores ( $>10\text{ }\mu\text{m}$ ). As pores' presence is directly related to strength, these findings explain the loss in strength caused by recycled aggregates (RAP). To overcome this, a better mix design with more fines or a pre-treatment of RAP particles should be investigated.

- Confocal Laser Scanning Microscopy (CLSM) is a helpful tool to identify the bitumen and its irregular distribution among the RAP aggregates. Some RAP particles have extremely little to no bitumen coating, whereas others (particularly the clusters) had an extremely high bitumen concentration. CLSM is also important to visualise the RAP distribution in the AAM mortars (sawed specimens). This technique also shows that the broken specimens fractured at the bitumen layer, suggesting poor adhesion between aggregates and bitumen. This is linked to reduced mechanical performance. SEM is preferable to see the interface between aggregates and matrices and confirm that RAP-AAM contains a larger and porous ITZ than NA-AAM.

- Overall, it is possible to conclude that, although silicates increase the alkaline activation, it has little or no impact on the adhesion between aggregate and bitumen. Therefore, soluble silicates should be limited to low quantities in RAP-AAM. Any improvements in the matrix are unlikely



to avoid adhesion issues that compromise the mechanical performance. Despite the reduction in strength caused by the increased porosity and poor binding to the matrix, it is still possible to achieve sufficient strength with RAP-AAS for many engineering applications.

**Highlights:**

1. Higher alkali content ( $\text{Na}_2\text{O}$  and  $\text{Ms}$ ) increased the mechanical strength of both NA-AAM and RAP-AAM systems. However, the increase was less significant for RAP-AAM. Therefore, RAP-AAM will need more activators than NA-AAM for similar strength, suggesting that RAP-AAM is more suitable for applications that demand lower strength requirements, such as pavement base layers. For pavement applications, RAP-AAM mortars yielded sufficient strength with little and no sodium silicate.
2. Although the presence of mastic on top of RAP granules caused a significant decrease in compressive and flexural strength, there is no indication that mastic interferes with the AAM's reaction kinetics.
3. Observations of fractured specimens indicate that the loss in mechanical properties is due to poor adhesion between RAP aggregates and cementitious matrix and higher porosity in the interface.

*This Chapter is a modified version of the paper “The Effect of Reclaimed Asphalt Pavement (RAP) Aggregates on the Reaction, Mechanical Properties, and Microstructure of Alkali-Activated Slag” published in CivilEng, MDPI in September 2021. It has been published on this thesis with the authorisation of the copyright holders.*

# BIBLIOGRAPHY

---

Abraham, S.M., Ransinchung, G.D.R.N., 2019. Pore Structure Characteristics of RAP-Inclusive Cement Mortar and Cement Concrete Using Mercury Intrusion Porosimetry Technique. *Adv. Civ. Eng. Mater.* 8, 20180161. <https://doi.org/10.1520/acem20180161>

Abraham, S.M., Ransinchung, G.D.R.N., 2018. Influence of RAP aggregates on strength, durability and porosity of cement mortar. *Constr. Build. Mater.* 189, 1105–1112. <https://doi.org/10.1016/j.conbuildmat.2018.09.069>

Borges, P.H.R., Banthia, N., Alcamand, H.A., Vasconcelos, W.L., Nunes, E.H.M., 2016. Performance of blended metakaolin/blast furnace slag alkali-activated mortars. *Cem. Concr. Compos.* 71, 42–52. <https://doi.org/10.1016/j.cemconcomp.2016.04.008>

Brand, A.S., Roesler, J.R., 2017. Bonding in cementitious materials with asphalt-coated particles: Part II – Cement-asphalt chemical interactions. *Constr. Build. Mater.* 130, 182–192. <https://doi.org/10.1016/j.conbuildmat.2016.10.013>

Collins, F., Sanjayan, J.G., 2000. Cracking tendency of alkali-activated slag concrete subjected to restrained shrinkage. *Cem. Concr. Res.* 30, 791–798. [https://doi.org/10.1016/S0008-8846\(00\)00243-X](https://doi.org/10.1016/S0008-8846(00)00243-X)

Diamond, S., 2000. Mercury porosimetry. An inappropriate method for the measurement of pore size distributions in cement-based materials. *Cem. Concr. Res.* 30, 1517–1525. [https://doi.org/10.1016/S0008-8846\(00\)00370-7](https://doi.org/10.1016/S0008-8846(00)00370-7)

El Euch Ben Said, S., El Euch Khay, S., Loulizi, A., 2018. Experimental Investigation of PCC Incorporating RAP. *Int. J. Concr. Struct. Mater.* 12. <https://doi.org/10.1186/s40069-018-0227-x>

El Euch Ben Said, S., Euch Khay, S. El, Achour, T., Loulizi, A., 2017. Modelling of the adhesion between reclaimed asphalt pavement

aggregates and hydrated cement paste. *Constr. Build. Mater.* 152, 839–846. <https://doi.org/10.1016/j.conbuildmat.2017.07.078>

Fernández-Jiménez, A., Palomo, J.G., Puertas, F., 1999. Alkali-activated slag mortars: Mechanical strength behaviour. *Cem. Concr. Res.* 29, 1313–1321. [https://doi.org/10.1016/S0008-8846\(99\)00154-4](https://doi.org/10.1016/S0008-8846(99)00154-4)

Fernandez-Jimenez, A., Puertas, F., Arteaga, A., 1998. Determination of kinetic equations of alkaline activation of blast furnace slag by means of calorimetric data. *J. Therm. Anal. Calorim.* <https://doi.org/10.1023/A:1010172204297>

Gao, Y., Wu, K., Yuan, Q., 2021. Limited fractal behavior in cement paste upon mercury intrusion porosimetry test: Analysis and models. *Constr. Build. Mater.* 276, 122231. <https://doi.org/10.1016/j.conbuildmat.2020.122231>

Gebregziabihier, B.S., Thomas, R.J., Peethamparan, S., 2016. Temperature and activator effect on early-age reaction kinetics of alkali-activated slag binders. *Constr. Build. Mater.* 113, 783–793. <https://doi.org/10.1016/j.conbuildmat.2016.03.098>

Hossiney, N., Sepuri, H.K., Mohan, M.K., H R, A., Govindaraju, S., Chyne, J., 2020. Alkali-activated concrete paver blocks made with recycled asphalt pavement (RAP) aggregates. *Case Stud. Constr. Mater.* 12, e00322. <https://doi.org/10.1016/j.cscm.2019.e00322>

Huanhai, Z., Xuequan, W., Zhongzi, X., Mingshu, T., 1993. Kinetic study on hydration of alkali-activated slag. *Cem. Concr. Res.* 23, 1253–1258. [https://doi.org/10.1016/0008-8846\(93\)90062-E](https://doi.org/10.1016/0008-8846(93)90062-E)

Kashani, A., Provis, J.L., Qiao, G.G., Van Deventer, J.S.J., 2014. The interrelationship between surface chemistry and rheology in alkali activated slag paste. *Constr. Build. Mater.* 65, 583–591. <https://doi.org/10.1016/j.conbuildmat.2014.04.127>

Komnitsas, K., Zaharaki, D., 2007. Geopolymerisation: A review and prospects for the minerals industry. *Miner. Eng.* 20, 1261–1277. <https://doi.org/10.1016/J.MINENG.2007.07.011>

Liu, S., Li, Q., Han, W., 2018. Effect of various alkalis on hydration properties of alkali-activated slag cements. *J. Therm. Anal. Calorim.* 131, 3093–3104. <https://doi.org/10.1007/s10973-017-6789-z>

Palacios, M., Puertas, F., 2005. Effect of superplasticizer and shrinkage-reducing admixtures on alkali-activated slag pastes and mortars. *Cem. Concr. Res.* 35, 1358–1367. <https://doi.org/10.1016/j.cemconres.2004.10.014>

Sachet, T., Balbo, J.T., Bonsembiante, F.T., 2013. Rendering the loss of strength in dry concretes with addition of milled asphalt through microscopic analysis. *Rev. IBRACON Estruturas e Mater.* 6, 933–954. <https://doi.org/10.1590/s1983-41952013000600006>

Shi, X., Grasley, Z., Hogancamp, J., Brescia-Norambuena, L., Mukhopadhyay, A., Zollinger, D., 2020. Microstructural, Mechanical, and Shrinkage Characteristics of Cement Mortar Containing Fine Reclaimed Asphalt Pavement. *J. Mater. Civ. Eng.* 32, 1–11. [https://doi.org/10.1061/\(ASCE\)MT.1943-5533.0003110](https://doi.org/10.1061/(ASCE)MT.1943-5533.0003110)

Shi, Z., Shi, C., Wan, S., Zhang, Z., 2018. Effects of alkali dosage and silicate modulus on alkali-silica reaction in alkali-activated slag mortars. *Cem. Concr. Res.* 111, 104–115. <https://doi.org/10.1016/J.CEMCONRES.2018.06.005>

Wang, S.-D., Scrivener, K.L., Pratt, P.L., 1994. Factors affecting the strength of alkali-activated slag. *Cem. Concr. Res.* 24, 1033–1043. [https://doi.org/10.1016/0008-8846\(94\)90026-4](https://doi.org/10.1016/0008-8846(94)90026-4)

# 5

## BLENDING RAP-AAM: MECHANICAL & MICROSTRUCTURAL PROPERTIES

---

This **experimental chapter** investigates blended AAM-RAP mortars produced with ground granulated blast furnace slag (BFS) and metakaolin (MK). The objective of this chapter is to determine the role of MK in the mechanical and durability property of RAP-AAM.

Initially, two low-alkali compositions from Chapter 4 (4 wt.%  $\text{Na}_2\text{O}$  and  $M_s = 0$  and 1) with 5%, 10% volume replacement of BFS with MK were produced. MK replacement considerably reduced the early strength of samples with 5% replacement and samples with 10% replacement even had no strength after 3 days. Alternative systems with 8%  $\text{Na}_2\text{O}$  (% wt. of binder), either using NaOH ( $M_s = 0$ ) or NaOH and  $\text{Na}_2\text{SiO}_3$  as activators ( $M_s = 1$ ), and 10% and 20% vol MK replacement were used. The fresh mortars were subjected to isothermal calorimetry until 48 h of hydration and shrinkage evaluation for 72 h. The hardened RAP-AAM were tested under flexion and compression at 3, 7 and 28 days. The apparent porosity was determined at the same ages. The microstructure was observed at 28 days using a combination of confocal and scanning electron microscopy.

Results have shown that the employment of MK slowed down the reaction and significantly impacted the early strength results of RAP-AAM, but not at later ages. The low early strength development may be compensated

by employing silicates, but this choice tends to increase the shrinkage. Best results were achieved with 8%  $\text{Na}_2\text{O}$ ,  $M_s = 0$ , 1:9 MK: BFS. This option will reduce the shrinkage and will not affect the porosity of the composites, despite the lower early strength.

## 5.1 Introduction

Some limitations of the alkaline activation of slag (AAS) have been pointed out over the years, related to a higher tendency to carbonation and shrinkage (Bakharev et al., 2001; Behfarnia and Rostami, 2017; Mastali et al., 2018; Zhang et al., 2022). Shrinkage of AAS depends on the type of activator and its dosage; the former is generally higher when sodium silicate is employed, exactly when higher mechanical strength is targeted (Ballekere Kumarappa et al., 2018; Lee et al., 2014).

Pavements are extremely sensitive to shrinkage effects (Fedrigo et al., 2017; Wang et al., 2020) and AAS-RAP base layers may suffer from extensive cracking. Blended AAM may be effective to reduce the shrinkage issues related to AAS. Some studies (Fu et al., 2021; Li et al., 2019) report that the partial replacement of BFS with MK is an alternative to mitigating the shrinkage of AAS, as the binary blends tend to make the matrices denser and alter the reaction products (combination of N-A-S-H gel from the activation of MK with C-A-S-H formed in AAS).

This chapter aims to study the mechanical properties and shrinkage of AAM-RAP systems, as a function of the composition of the activator ( $\text{NaOH}$  or a combination of  $\text{NaOH}$  and  $\text{Na}_2\text{SiO}_3$ ). At the same time, assess the impact of MK replacement of BFS as a means to improve the mechanical performance and reduce shrinkage, towards the development of AAM-RAP mixes for pavement application.

A preliminary test assessed the strength development of two compositions from Chapter 4 (R4-0 and R4-1) with 0%, 5% and 10% BFS replaced by MK (volume replacement). In early hydration studies, mechanical and microstructure assessment was performed on activated samples with 8% $\text{Na}_2\text{O}$  (% wt. of binder), either using  $\text{NaOH}$  ( $M_s = 0$ ) or  $\text{NaOH}$  and  $\text{Na}_2\text{SiO}_3$  as activators ( $M_s = 1$ ). MK replaced BFS in 0%, 10% and 20% vol.

The fresh mortars (composition presented in Chapter 3) were subjected to isothermal calorimetry until 48 h of hydration and shrinkage evaluation for 72 h. The hardened RAP-AAM were tested under flexion and compression at 3, 7 and 28 days. The apparent porosity was determined at the same ages. Fourier Transform Infrared (FTIR) was employed to determine the structure of materials (chemical bonds that lead to the structural identification). The microstructure was observed at 28 days using a combination of confocal and scanning electron microscopy.

## 5.2 Experimental Summary

The complete description of the material and methods used in this chapter is available in Chapter 3. Table 5.1 summarises the different compositions studied. All mortar samples were produced using RAP aggregates, 1:1.5 precursor: aggregate ratio and water/precursor of 0.5. Samples with “R” used BFS as a precursor, while samples with “MK” had part of the BFS replaced by MK. The number preceding the letters “MK” indicates the replacement level (vol.%).

*Table 5.1. Compositions studied*

Notation	Precursor (P)		Activator	
	MK (vol%)	BFS (vol%)	Na <sub>2</sub> O (wt%)	Ms
R4-0	0	100	4	0
5MK4-0	5	95	4	0
R4-1	0	100	4	1
5MK4-1	5	95	4	1
R8-0	0	100	8	0
10MK8-0	10	90	8	0
20MK8-0	20	80	8	0
R8-1	0	100	8	1
10MK8-1	10	90	8	1
20MK8-1	20	80	8	1

Each composition produced 11 prismatic specimens (4 x 4 x 16 cm), totaling 110 samples. For mechanical assessment, three prismatic specimens (4 x 4 x 16 cm) were produced for each testing age (3, 7 and 28 days). The specimens were first tested for flexural strength and the

same specimens were tested for compressive strength afterwards. Untested prisms were sawed and used for apparent porosity and microscopy. Fresh mortar was used for calorimetry and shrinkage.

## 5.3 Results & Discussion

### 5.3.1 Preliminary study on 4%Na<sub>2</sub>O activated samples

An initial experiment investigated the effect of MK replacement (0%, 5% and 10% of BFS volume) on samples activated with 4%Na<sub>2</sub>O and silica modulus of 0 and 1. The reference compositions (R4-0 and R4-1) were selected from the study performed in Chapter 4. Figure 5.1 and Figure 5.2 presents the compressive flexural strength development of the samples from 3 to 28 days. The increase in MK replacement levels sharply reduced the early strength (compressive and flexural) of the samples. The highest replacement levels studied (10% replacement, samples 10MK4-0 and 10MK4-1) had zero strength after 3 days, and at later ages (28 days) the strength was less than half of the reference sample. Samples 5MK4-0 and 5MK4-1 (with 5% MK) showed an improvement in compressive and flexural strength at 7 days and similar performance to the reference samples, and at 28 days most samples had higher strength than their reference.

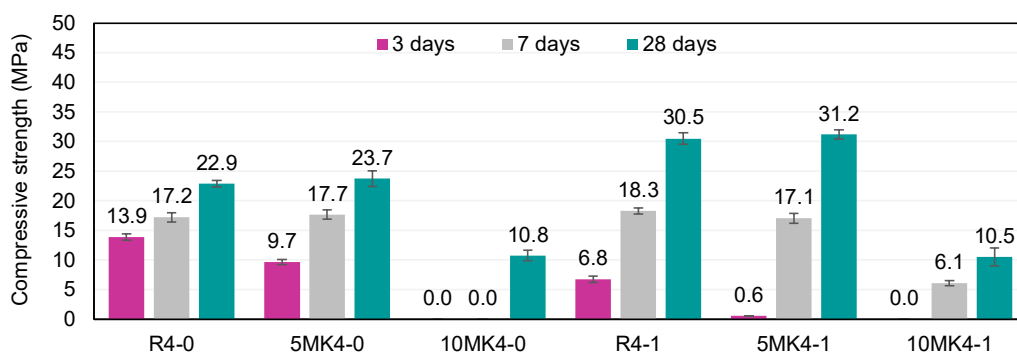
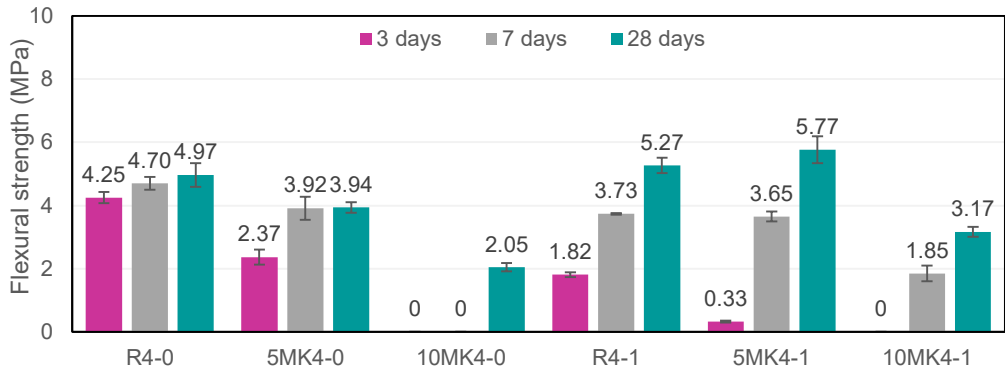


Figure 5.1. Compressive strength of blended samples activated with 4%Na<sub>2</sub>O





*Figure 5.2. Flexural strength of blended samples activated with 4%Na<sub>2</sub>O*

The calorimetry results of the mortars are presented in Figure 5.3 and Figure 5.4. The sharp peak at the start of the experiment was only partially captured. The second and main peak is related to the precipitation of the reaction products (Fernandez-Jimenez et al., 1998; Huanhai et al., 1993). Samples with sodium silicate (R4-1, 5MK4-1 and 10MK4-1) have a delayed second peak due to the workability retention and the reduced availability of OH<sup>-</sup> (Kashani et al., 2014; Liu et al., 2018). Replacing BFS with MK decreased the intensity and delayed the second peak. The delayed second peak formation refers to the reduced early strength observed in Figure 5.1 and Figure 5.2 and was also observed elsewhere (Fu et al., 2021). At the end of the experiment, the cumulative heat (Figure 5.4) of samples with 5% MK replacement was near the reference samples while the samples with 10% MK replacement were much lower

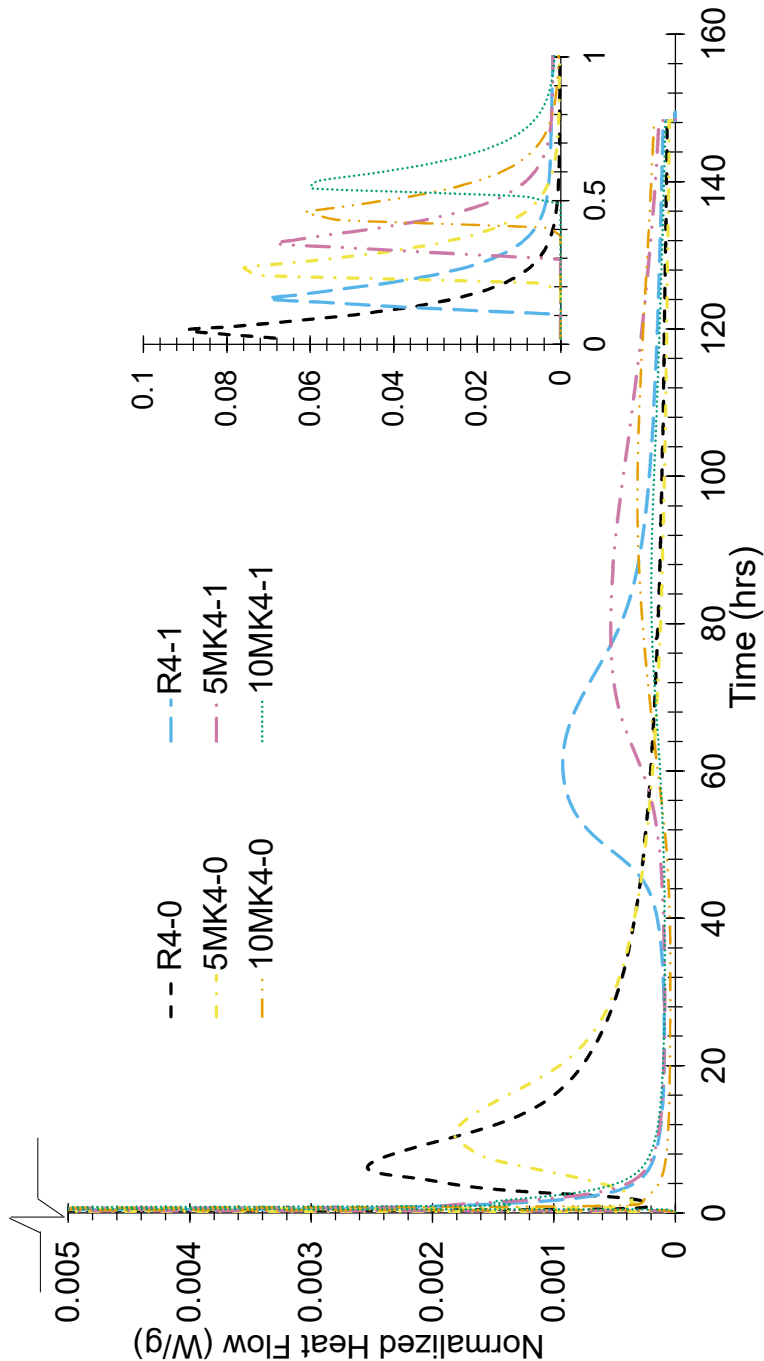


Figure 5.3. Heat release of RAP-AAM activated with 4%Na<sub>2</sub>O and initial peak in detail

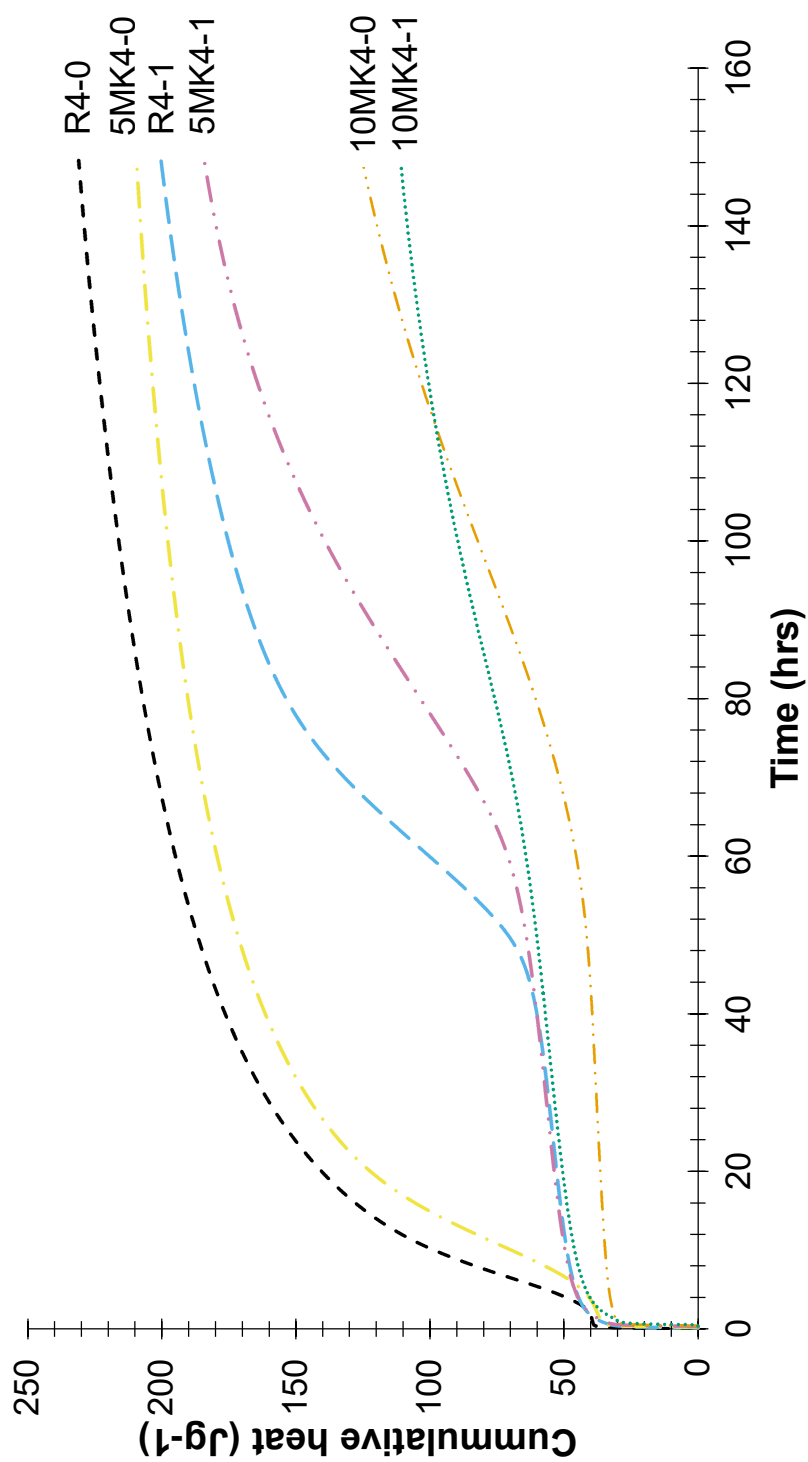


Figure 5.4. Cumulative heat release of the RAP-AAM activated with 4%Na<sub>2</sub>O

The BFS replacement with MK on samples with low alkali content (4%Na<sub>2</sub>O) showed a sharp reduction in compressive strength due to the delayed formation of main reaction products. Such low strength at 3 days is undesirable for engineering applications (including pavement) and could compromise the experimental design, therefore, a higher alkali concentration (8% Na<sub>2</sub>O) was chosen to continue the study of blended RAP-AAM.

### **5.3.2 Study on 8%Na<sub>2</sub>O activated samples**

#### **5.3.2.1 Calorimetry**

The heat output and cumulative heat of the studied AAM are shown in Figure 5.5 and Figure 5.6. The sharp peaks at the beginning of the curves (up to 1h of testing – zoomed area in Figure 5.5) refer to the wetting and partial dissolution of the BFS and the temperature stabilization of the externally mixed specimens. The initial peak is followed by an induction period with low reactivity until a second peak. The second (main) peak corresponds to the massive precipitation of reaction products. Afterwards, there is a period of low reactivity until the reaction reaches the end (Fernandez-Jimenez et al., 1998; Huanhai et al., 1993).

The activator type plays a significant role in the intensity of the main peak. Mortars activated only with NaOH presented a more intense main peak when compared with those activated with Na<sub>2</sub>SiO<sub>3</sub> + NaOH. These findings are in accordance with other studies (Costa et al., 2021; Fernandez-Jimenez et al., 1998; Gebregziabihier et al., 2016; Kashani et al., 2014), which relate the use of silicates with workability retention and a consequent delay of the main peak.

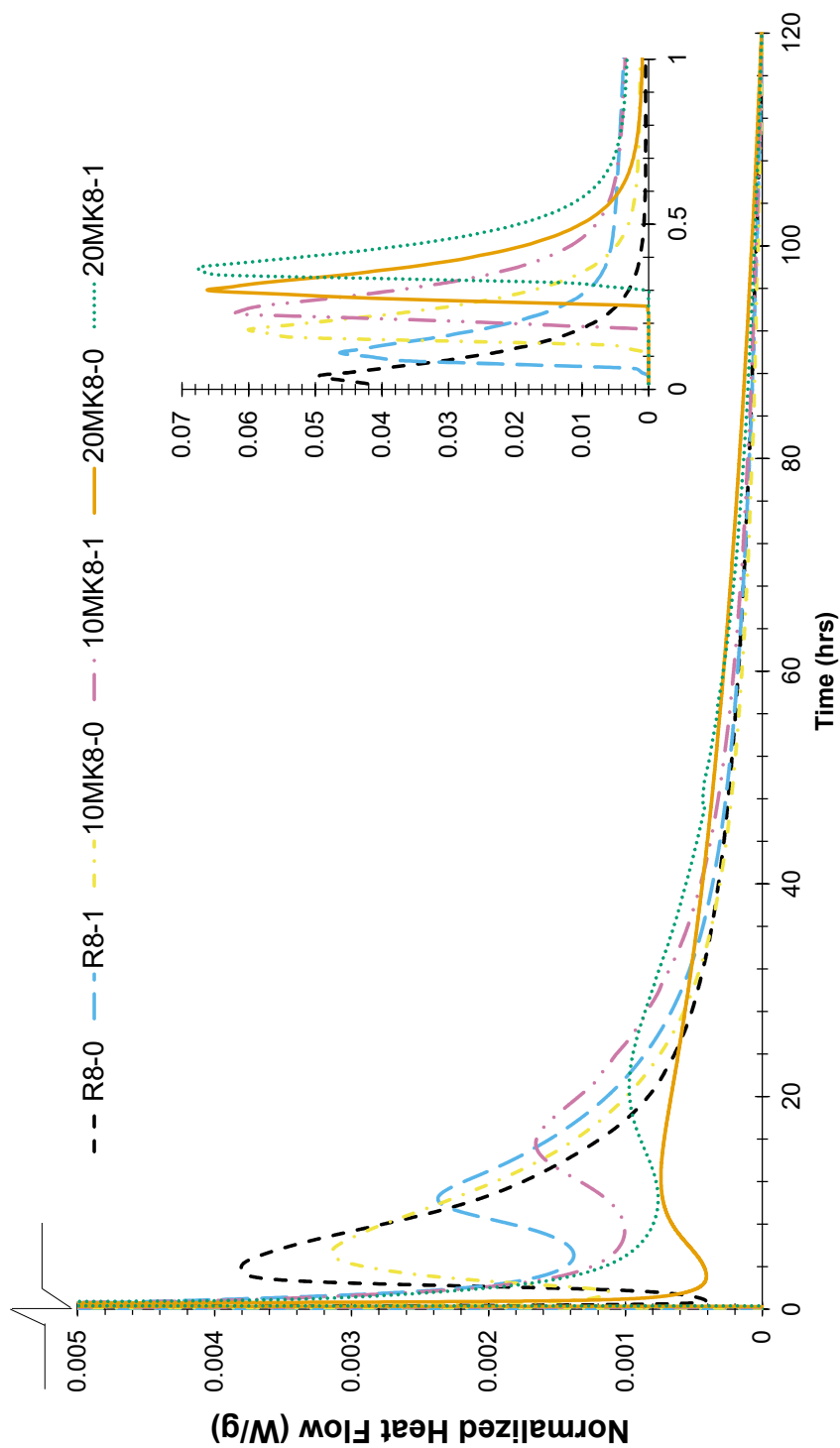


Figure 5.5. Heat release of RAP-AAM activated with 8%  $\text{Na}_2\text{O}$  and initial peak in detail

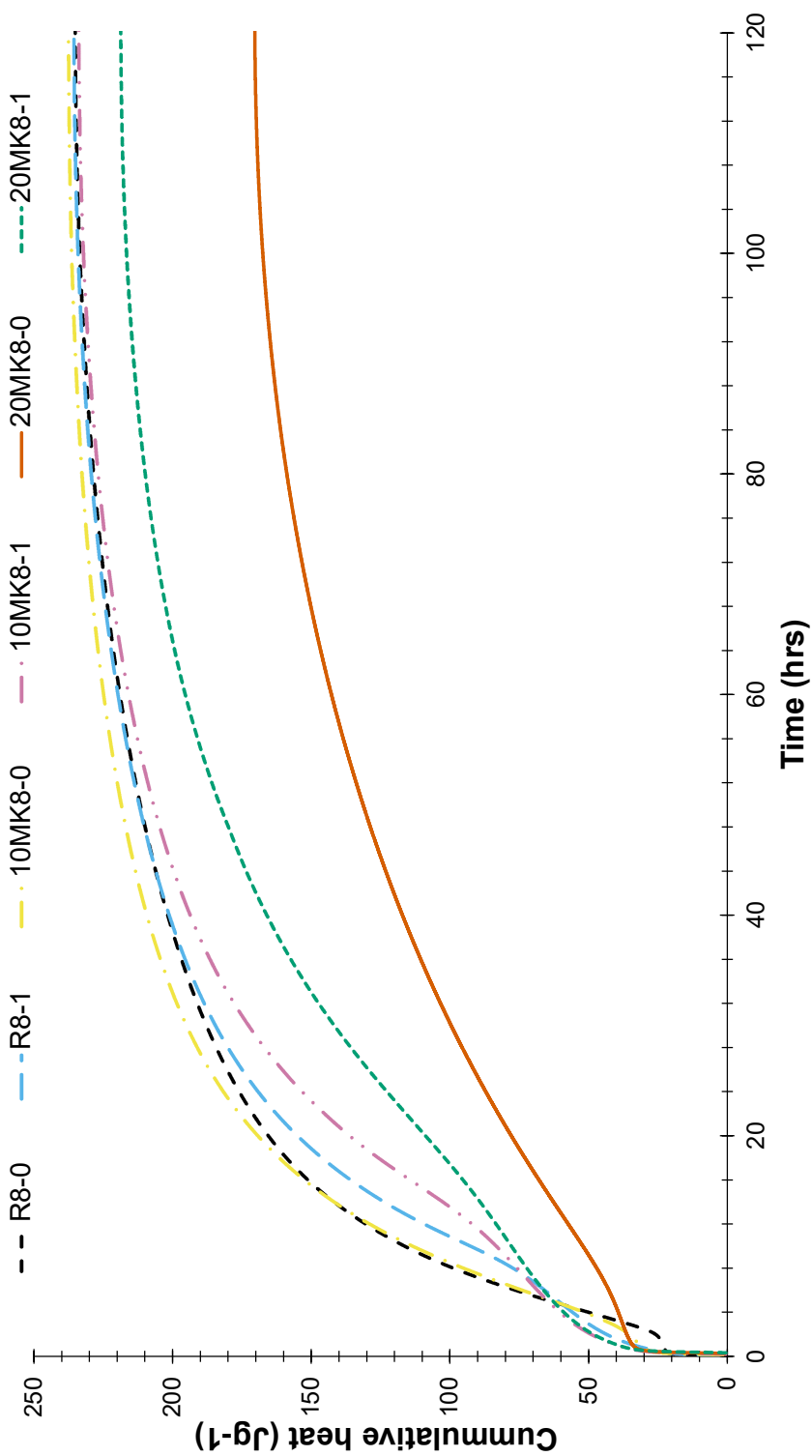


Figure 5.6. Cumulative heat release of the RAP-AAM

The replacement of part of the BFS with MK also caused a reduction in the intensity and delay of the main peak. The impact of MK in the formation of reaction products was also observed by (Li et al., 2019). The effect gets more significant with the increase in the replacement level (0%, 10% and 20%). The cumulative heat flow of the mortars (Figure 5.6) shows very little difference in total heat released after 120 h for mortars containing 0% and 10% MK irrespectively of the type of activation system used. However, samples with 20% MK replacement had a significantly lower cumulative heat release. This is in line with the findings of Li et al. (2020, 2019) and supports the suggestion that the presence of MK can reduce the reaction rate at early. The RAP particles in the mortars presented no apparent effect on the calorimetry results.

### **5.3.2.2 Shrinkage**

The shrinkage in cementitious systems can be classified as plastic, autogenous (or chemical), drying and carbonation (Zhang et al., 2022). Plastic shrinkage occurs during the fresh state due to water evaporation. Autogenous shrinkage is the volume change induced by the self-desiccation during hydration. Drying shrinkage is due to the loss of moisture in the gel pores. Carbonation shrinkage occurs when CO<sub>2</sub> penetrates the specimen. According to Zhang et al. (2022), the primary mechanism controlling the shrinkage in AAM is autogenous and drying shrinkage.

Image analysis of the samples at 15 minutes intervals was recorded and the amount of shrinkage was measured (Figure 5.7). The result presented in Figure 5.8 refers to the plastic, autogenous and drying shrinkage of all mortars after being left at room temperature (15 – 20°C and 40-60 RH). Indeed, the samples were not old enough to expect carbonation shrinkage. All mortars presented high shrinking at early ages, followed by a slight gain in volume quickly tailed by a second and less expressive loss in volume. The samples behaved in a linear pattern at later ages to apparent stability.

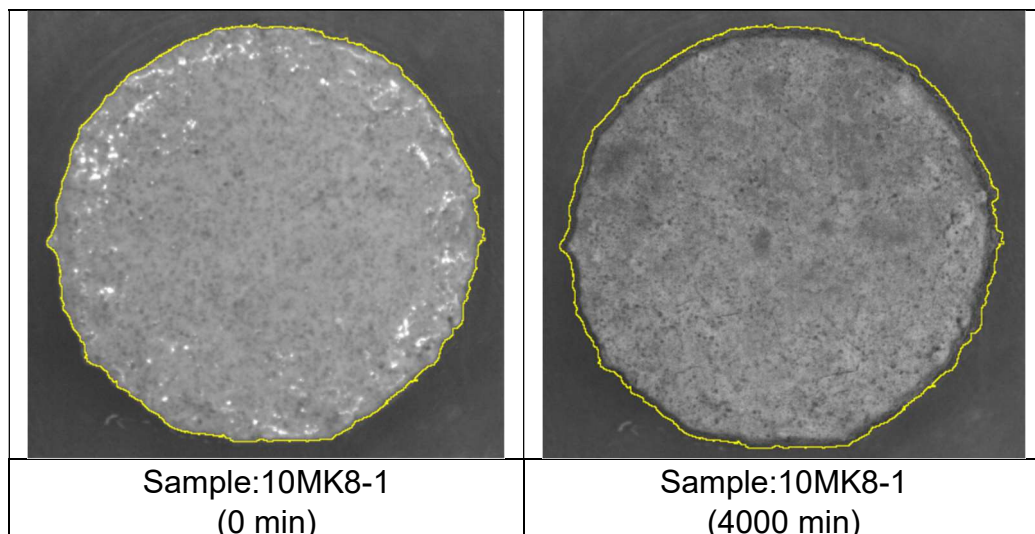


Figure 5.7. Shrinkage image of sample 10MK8-1 at time 0 and 4000 minutes

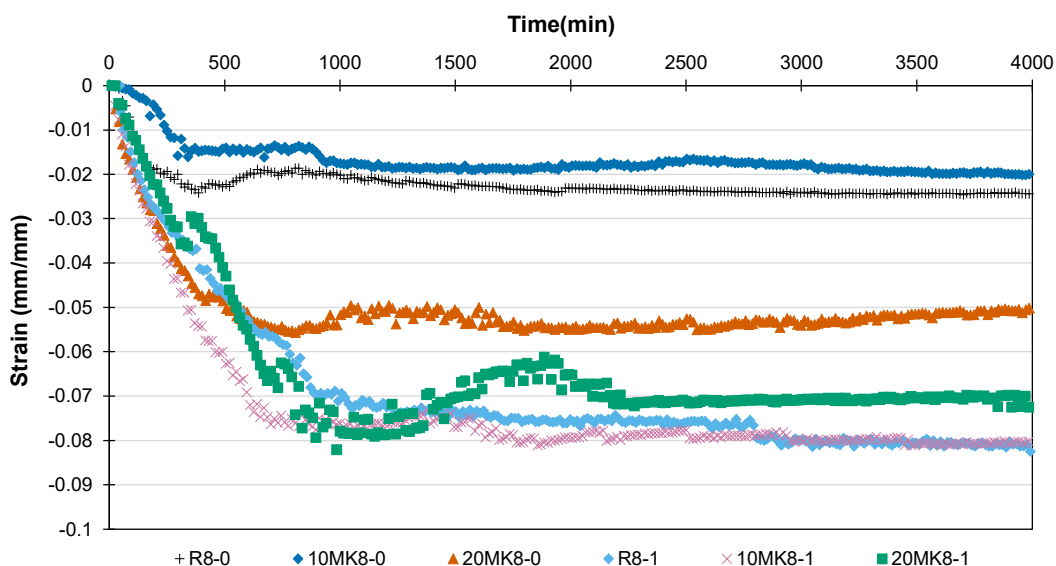


Figure 5.8. Shrinkage of RAP-AAM

- **Effect of the type of activator**

In general, higher shrinkage was exhibited by the RAP-AAM prepared with sodium silicate (R8-1, 10MK8-1 and 20MK8-1). This finding is in accordance with the literature (Duran Atiş et al., 2009; Melo Neto et al.,



2008). The main parameters controlling the shrinkage of AAS are activators species and dosage, BFS fineness and curing condition (Melo Neto et al., 2008). An increase in shrinkage is expected when higher dosages of the activator are used, especially in the presence of sodium silicate. Melo Neto et al. (2008) linked the increase of sodium silicate with increased mesopores and a higher degree of hydration and therefore higher shrinkage due to self-desiccation and chemical reaction. Figure 5.8 shows that the volume stabilisation in RAP-AAM activated with  $\text{NaOH} + \text{Na}_2\text{SiO}_3$  takes place after around 1000 minutes of testing.

On the other hand, the samples activated with  $\text{NaOH}$  (R8-0, 10MK8-0 and 20 MK8-0) had a similar shrinkage pattern, with volume stabilization at an earlier time (around 300-500 min). The shrinkage observed by digital imaging also appears to have a good correlation with the calorimetry tests. The main heat release peaks for samples R8-0 and 10MK8-0 took place at approximately 5 hours (300 minutes), the same time when the sharp shrinking curve stabilises. A similar trend can be observed for the other curves, suggesting a strong correlation between shrinking and acceleration. Other authors have also observed a good correlation between autogenous / drying shrinkage with the acceleration period of AAM (Melo Neto et al., 2008).

- **Effect of the MK addition**

The employment of 10 vol.% MK had a small effect on shrinkage (compared 100% BFS), irrespective on the activator used. Specimens without silicates (R8-0 and 10MK8-0) had a slight shrinkage reduction with the use of 10% MK and samples with silicates (R8-1 and 10MK8-1) showed almost no impact.

A different situation takes place when 20% MK is used in the mortars i.e., distinctive, and opposite trends in the final shrinkage depending on the activator employed. The mortar 20MK8-0 ( $\text{NaOH}$ , no silicate) presented higher shrinkage than the reference R8-0 and 10MK8-0 all over the test. In contrary, 20MK8-1 (activated with  $\text{NaOH} + \text{Na}_2\text{SiO}_3$ ) slightly improved the final shrinkage compared with R8-1 and 10MK8-1 (-0.07 against -0.08 at 4000h).

Li et al. (2019) and Fu et al. (2021) studied the replacement of BFS with MK in AMM with high alkaline content (6-9% NaOH and  $M_s = 0.76-1.0$ ). The authors pointed out sizeable autogenous shrinkage for 100% BFS and a significant reduction for formulations with 10% and 20% MK replacement (up to 60% reduction in 1 day). Herein, the reductions in the presence of sodium silicate were observed to a much lesser extent (10% shrinkage reductions from R8-1 to 20MK8-1. This difference in results could be due to the different nature of the raw materials, the different activation levels, or (most likely) due to the different observation methods.

Moreover, the results presented herein show that MK may improve shrinkage mitigation, but it is the absence of silicates that seems to represent the sharpest gain. When comparing mortars with the same binder composition, either 100% BFS, 90/10 BFS/MK or 80/20 BFS/MK, RAP-AMM activated with NaOH presented 75%, 70% and 29% lower shrinkage than its counterpart (NaOH +  $\text{Na}_2\text{SiO}_3$ ) at 4000h, respectively. These findings suggest that the filler effect combined with increased reaction products could be the driving force behind the reduction in shrinkage for samples without silicates.

### **5.3.3 FTIR**

The spectra of the unreacted raw material are presented in Figure 5.9. It is possible to observe in the BFS a minimal vibration at approximately  $1500\text{cm}^{-1}$ , possibly associated with the asymmetric stretching of O-C-O bonds in carbonate. Broadband centred at about  $930\text{cm}^{-1}$  is linked with the asymmetric stretching vibration of Si-O-T bonds (T: tetrahedral Si or Al), followed by a small shoulder at  $854\text{cm}^{-1}$  likely related to the vibration of Al-O bonds of  $\text{AlO}_4$  groups, and at  $680\text{cm}^{-1}$  a vibration attributed to the bending vibration mode of the Al-O-Si bonds (Bernal et al., 2012; Ismail et al., 2014; Palacios and Puertas, 2005). The unreacted MK spectrum shows a broad band at  $1074\text{cm}^{-1}$  linked with the asymmetric stretching of Si-O-Si, and the other two vibrations at  $791\text{cm}^{-1}$  and  $451\text{cm}^{-1}$ , associated with the bending of Al-O-Si and Si-O (Barbosa et al., 2000; Gao et al., 2020).

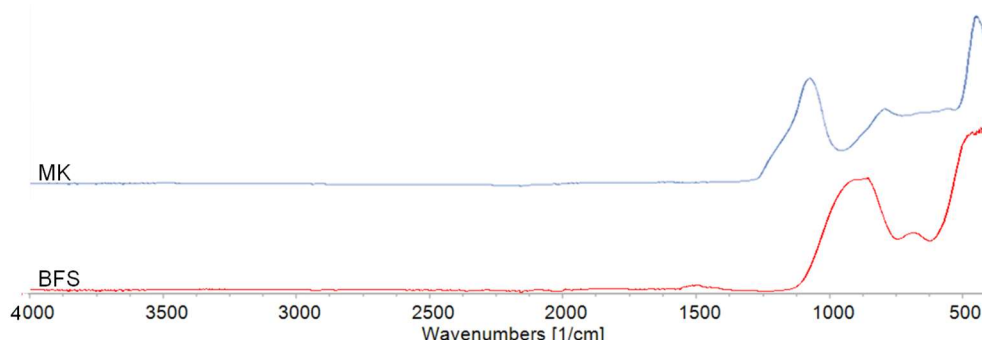
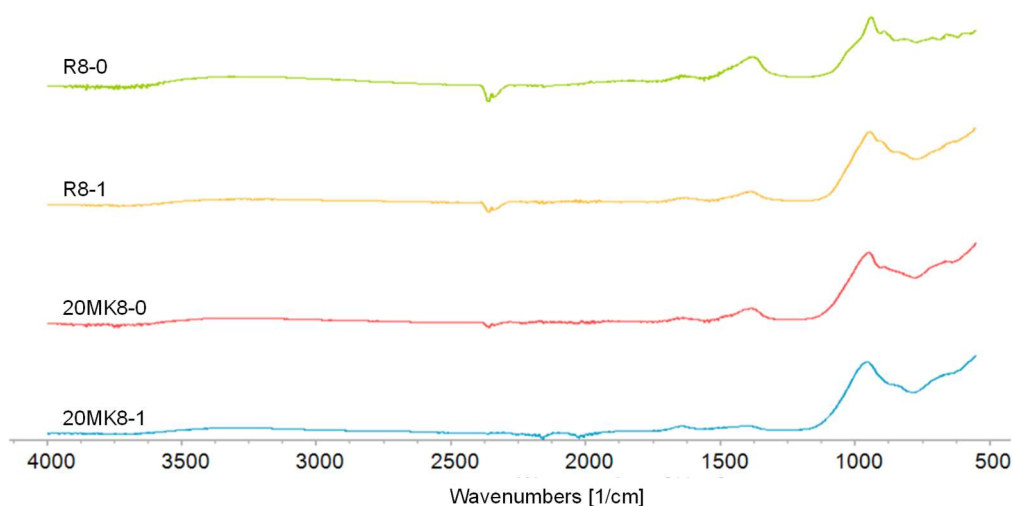


Figure 5.9. FTIR of starting materials

The FTIR spectra of the four alkali-activated pastes (Figure 5.10) show similar bands for the studied pastes (R8-0, R8-1, 20MK8-0 and 20MK8-1), indicating that they present similar reaction products. The bands located at approximately  $1640\text{ cm}^{-1}$  and  $3500\text{ cm}^{-1}$  are related to the vibrations of O-H and H-O-H groups from water molecules (Bernal et al., 2012; Gao et al., 2020). The carbonation of the reacted samples can be observed with the presence of the vibration bands (C-O) at about  $1390\text{ cm}^{-1}$  (Cao et al., 2020; Soleimani et al., 2012); the intensity of this band is higher for sample R8-0, indicating that the number of free alkalis in this paste is higher and it probably forming more sodium carbonate ( $\text{Na}_2\text{CO}_3$ ).



(a)

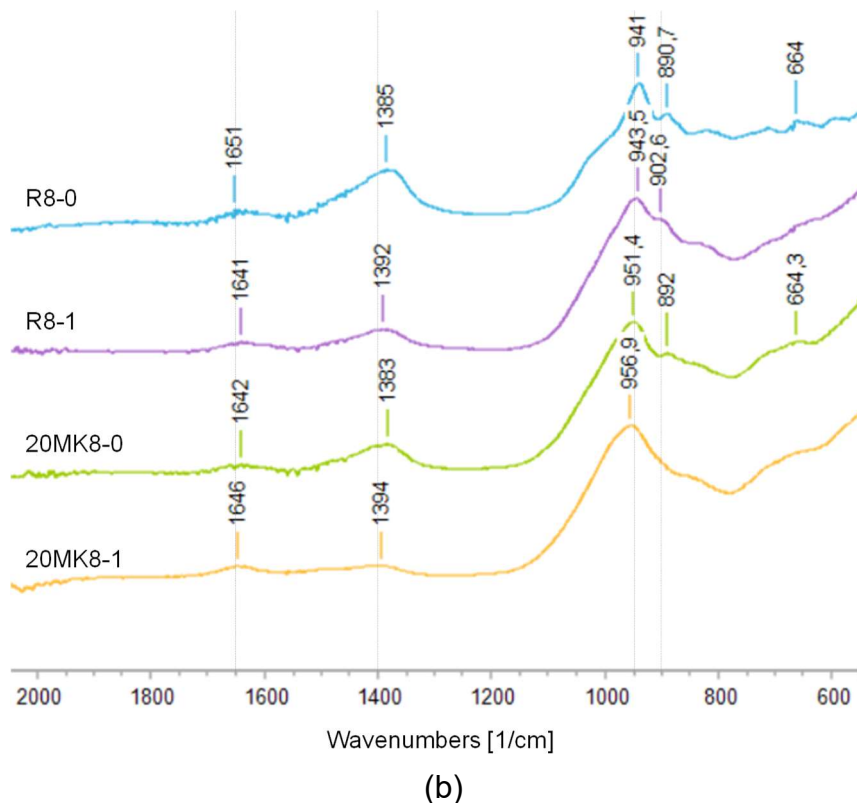


Figure 5.10. FTIR of AAM pastes R8-0, R8-1, 20MK8-0 and 20 MK8-1(a) full spectra; (b) partial spectra with peaks assigned

The main reaction band, centred at approximately  $950\text{cm}^{-1}$ ,  $890\text{ cm}^{-1}$  and  $660\text{cm}^{-1}$ , refers to the formation of aluminosilicate type gel related to the asymmetric stretching vibration and deformation of Si-O-T (Bernal et al., 2012; Li et al., 2019). These results suggest that the samples' main reaction product is C-A-S-H type gel, typical of the AAS (Fu et al., 2021; Li et al., 2019).

It is possible to observe a shift in the main band numbers to higher values as MK is added to the mix. This indicates the incorporation of  $\text{Al}^{3+}$  ions into the hydration products (Peng et al., 2019).

### 5.3.4 SEM and Confocal Microscopy

Figure 5.11 to Figure 5.13 show the Confocal and SEM images of RAP-AAM with different binder compositions, respectively R8-0, 10MK8-0 and

20MK-0. It is possible to identify two main phases in all pictures: the RAP particles and the alkali-activated gel. The RAP particles can be further divided into the fine aggregate and the asphalt mortar. The asphalt mortar is made from filler and bitumen. The combination of the confocal and SEM images is of great assistance to observe all the distinctive features in the microstructure. Sometimes it is difficult to observe the limit between the mastic and the AAM matrix via SEM images, and the confocal microscope offers an easier identification of the boundaries. The confocal image of samples R8-0 (Figure 5.11a) shows each phase and its limits, while on the SEM image (Figure 5.11b), only the aggregates and filler borders are easily identifiable.

Figure 5.12 and Figure 5.13 show a sharper contrast between bitumen and the alkali-activated matrix when confocal microscopy is employed. On the other hand, fine cracks within the gel and between the gel and the mastic can be better observed in the SEM images.

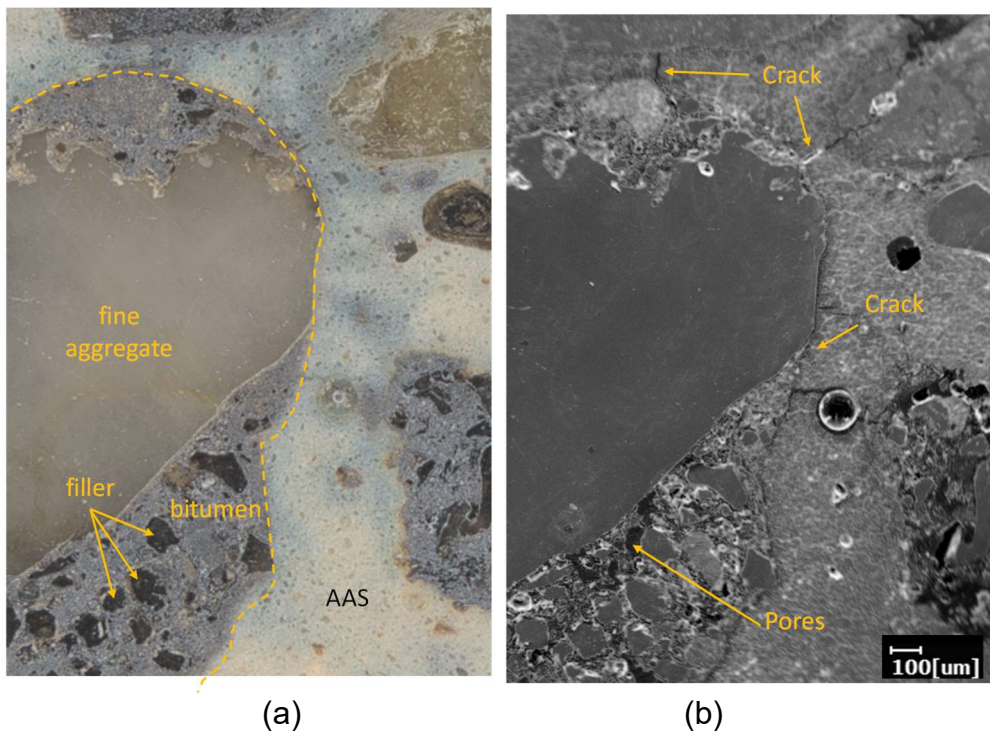


Figure 5.11. (a) Confocal and (b) SEM images of sample R8-0 (magnification 50x)



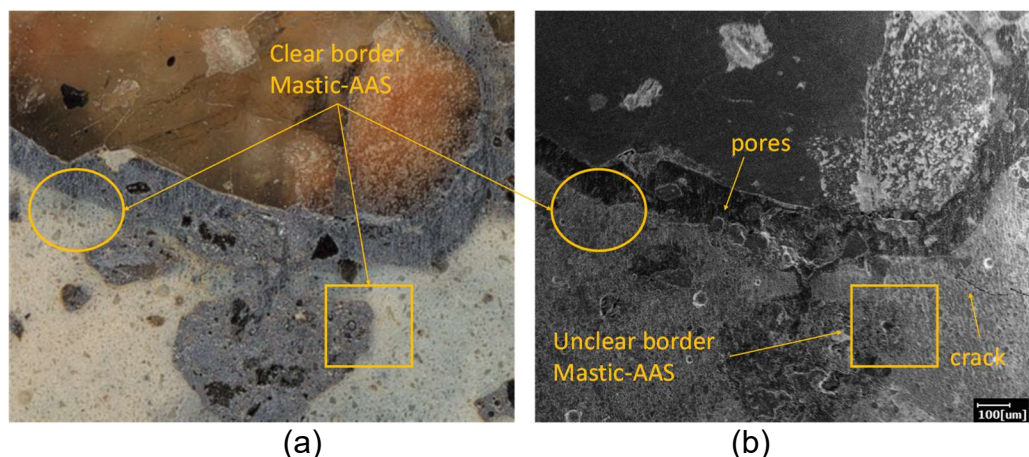


Figure 5.12. (a) Confocal and (b) SEM images of sample 10MK8-0 (magnification 100x)

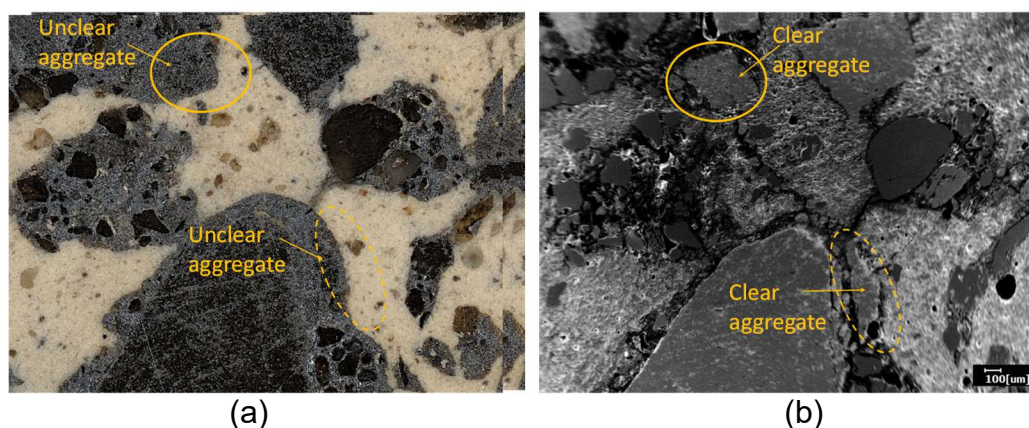


Figure 5.13. (a) Confocal and (b) SEM images of sample 20MK8-0 (magnification 50x)

The darker colour of the mastic region indicates much more porous materials. The crack observed at the mastic, and alkali-activated gel interface suggests a bonding issue between these two materials. The increased porosity and weaker interface were also observed by other authors (Brand and Roesler, 2016). From the SEM images, it is not possible to conclude whether the addition of up to 20% MK increases the density of the gel or reduces the tendency of the material to develop microcracks. In addition, it is also possible that the formation of cracks was induced during the preparation of samples for SEM, given the poor adhesion between gel and RAP particles.

### 5.3.5 Compressive and flexural strength and apparent porosity

The hardened RAP-AAM mortars were tested for flexural strength and compression strength at 3, 7 and 28 days. The apparent porosity was determined at the same ages.

Figure 5.14 shows that the replacement of BFS with MK decreased the flexural strength of all mortars at 3 days; this effect was more significant for those activated with NaOH (10MK8-0 and 20MK8-0). The flexural strength gain is considerably high from 3 to 7 days for 10MK8-0 and 20MK8-0. The former mortars had similar flexural strength to their reference (R8-0) at 28 days (5.05 MPa), which indicates that the strength reduction from the combination of MK + NaOH in the activator is compensated at later ages.

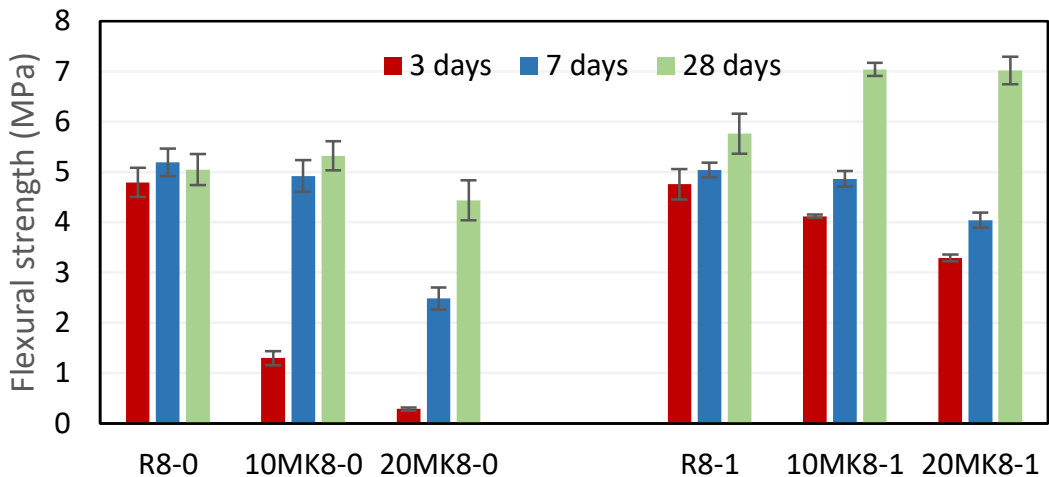


Figure 5.14. Flexural strength of RAP-AAM at 3, 7 and 28 days

The mortars activated with sodium silicate (R8-1, 10MK8-1, and 20MK8-1) suffer much less effect of the MK addition to the matrices at 3 days, and marginal strength gain is observed from 3 to 7 days. The highest flexural strength is found for 10MK8-1 and 20MK8-1 at 28 days (7.04 MPa and 7.02 MPa respectively) with less than 0.5% difference between the mean strength, but 22% higher than the reference R8-1 at 28 days (5.76 MPa).

In general, the effect of MK replacement on the compressive strength of the mortars was similar to the flexural strength. Figure 5.15 also shows that there was a reduction in compressive strength at early ages (3 and 7 days) when  $M_s = 0$ . As an example, 20MK8-0 presented a 94% strength reduction compared to the reference R8-0 at 3 days (from 15.68 MPa to 0.95 MPa). The strength reductions at earlier ages are less prominent as the samples matured and all formulations presented approximately the same strength results at 28 days.

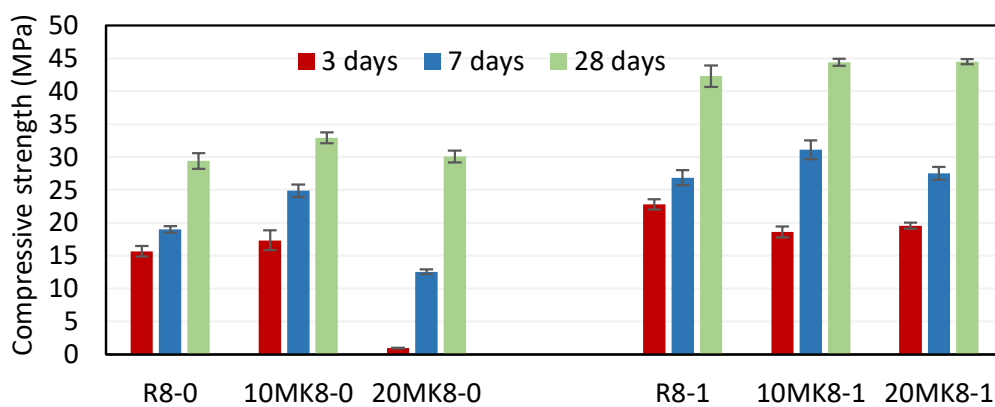


Figure 5.15. Compressive strength of RAP-AAM at 3, 7 and 28 days

The strength results suggest that the early strength of blended RAP-AAM (MK+BFS) is dependent on the presence of sodium silicate. According to literature, the dissolution and reaction of the CaO in the BFS is facilitated in systems with lower alkalinity (i.e., systems with higher  $M_s$  ratios), which promotes early strength (Peng et al., 2019).

The porosity of the RAP-AAM mortars at 3, 7 and 28 days is shown in Figure 5.16. The porosity of the samples reduced from 1 day to 28 days, as expected from the strength evolution (Figure 5.14 and Figure 5.15). This result indicates that more reaction products formed as the samples aged, and the gel got denser.

The increase in MK content represented an increase in porosity, which was not observed in the microscopy analysis (section 5.3.4). This effect is



more significant for mortars activated with NaOH ( $M_s = 0$ ) and practically negligible for those prepared with sodium silicate ( $M_s = 1$ ).

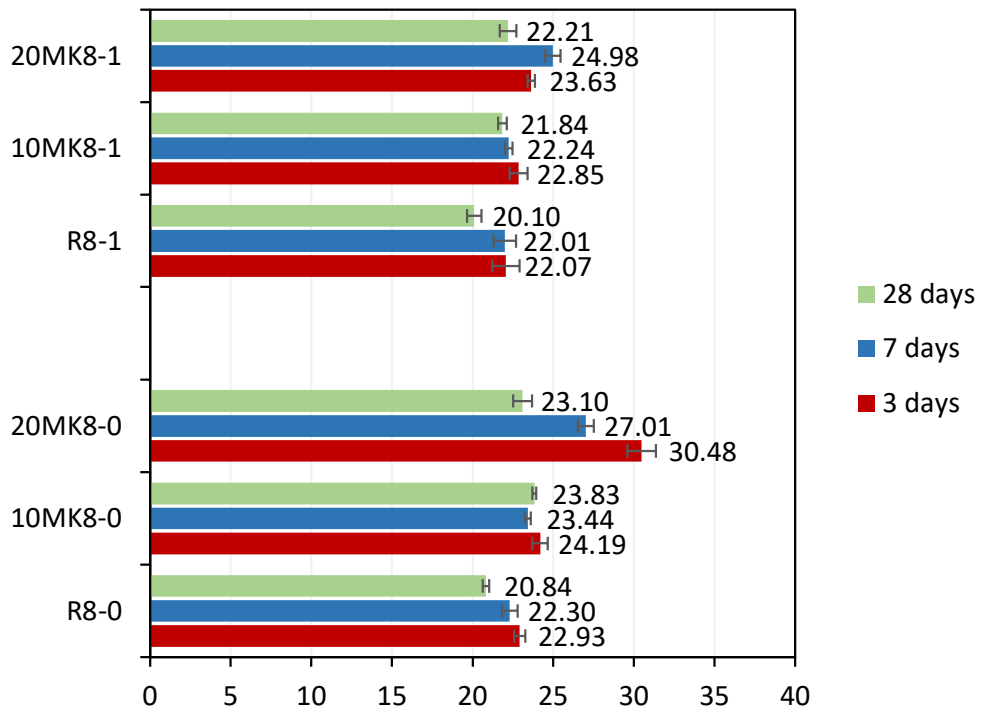


Figure 5.16. Apparent porosity of RAP-AAM mortar samples at 3, 7 and 28 days

### 5.3.6 Discussion overview

There are several studies based on MK-BFS-activated systems. Different authors reported different optimum MK replacements for strength improvement. Jithendra et al. (2021) investigated the effect of MK on alkali-activated BFS-PFA matrices in the presence of sodium silicate and found that the compressive strength increased with MK content reaching an optimum level of 15%; Huseien et al. (2016) suggested 5%MK as ideal. Li et al (2019) and Fu et al. (2021) reported a loss in compressive strength for up to 30% MK replacement. Based on flexural strength, Li et al. (2019) found ideal gains at 10%MK. Different reports on optimum MK replacement are likely related to differences in the raw material used or to differences in the activator (type and quantity).

This research found that the MK replacement could compromised the early age compressive and flexural strength (at 3 days). The calorimetry results have shown that the formation of reaction products (main peak) is delayed when MK is incorporated into the system. However, at later ages, the incorporation of up to 20 vol. % MK (in 8% Na<sub>2</sub>O activated samples) had a minimal negative effect on the compressive strength. Li et al. (2019) suggested that the presence of MK improves mechanical performance by mitigating the micro cracks in the matrix. Indeed, depending on the activators used for AAM, the inclusion of MK could assist in strength development due to the formation of more reaction products and filler effect. However, this will happen at later ages (> 7 days).

There is a benefit in terms of mechanical performance of blended systems (BFS/MK) when sodium silicate is used in the activator ( $M_s = 1$ ). First, the employment of sodium silicate reduces the alkalinity and promotes the reaction of calcium from the BFS at an early age (Peng et al., 2019). The compressive strength MK/BFS RAP-AAM strongly correlates with the activator's silica module, as already found in the literature (Fu et al., 2021; Peng et al., 2019). At the low activator module, the 28 days strength decreases while it increases at high modules (up to an optimum point). According to Peng et al. (2019), the N-A-S-H gel and C-A-S-H coexist in an alkali-activated MK-BFS system, filling each other's pores and improving the mechanical properties.

Although the shifting in the bands observed in the FTIR results suggests the formation of more reaction products, they are likely to be C-A-S-H gel with little to no N-A-S-H gel. The formation of more reaction products is consistent with the higher flexural strength observed at later ages when MK and silicates are used.

The durability and performance of RAP-AAM systems need to be considered when defining the optimum percentage of MK and the composition of the activator. The results of this present study show that it is the absence of silicates ( $M_s = 0$ ) in the activator that plays a significant role in the shrinkage reduction, although the presence of MK may contribute to the shrinkage mitigation. In other words, if the lower early mechanical performance is acceptable, it is better not to use silicates in

the activator and employ tiny amounts of MK to reduce the susceptibility to shrinkage and cracking in RAP-AAM pavements.

The durability-related property studied in this paper (apparent porosity) correlates well with the compressive strength results i.e., an increase in strength is usually associated with denser (less porous) matrices. Shi et al. (2011) pointed out that the porosity in AAM systems is dependent on the activators used; the mortars with lowest porosity tend to be those activated with silicates (Puertas et al., 2018; Shi et al., 2018). Puertas et al. (2018) observed that AAS slag had 16-20% porosity when activated with NaOH and 7-8% in the presence of sodium silicate. The present results are much higher (between 20.10% and 30.48%), likely due to recycled RAP aggregates employed.

Fu et al. (2021) found that the addition of MK in AAS reduces the total pore volume. From the microstructure analysis (confocal and SEM) and apparent porosity results, the RAP-AAM studied herein did not show any reduction in pores due to the use of MK. The use of recycled aggregates is one explanation for the discrepancy with findings in the literature. In fact, the SEM images indicate a large concentration of pores around the aggregates (the region with asphalt mortar). MK may help improve the density of the AAM gel, but it has a negligible impact on the pores surrounding the RAP particles. This very porous zone could also be the reason behind the poor improvement in strength caused when MK is employed. The stress accumulates around the pores and accentuates crack development and failure. The choice of MK content in RAP-AMM is not so relevant in terms of porosity, assuming that the latter is governed by the transition zone between the matrices and the RAP particles.

The shrinkage assessment through image analysis proved to be a simple and readily available comparison method, however, each experiment generates an overwhelming amount of data. Since the colours of AAM change during the hydration period, the automated thresholding methods commits constant mistakes and must be frequently checked and fixed. This activity can be very time-consuming due to the large amount of data each experiment creates. The use of a coloured camera (this experiment used a black and white camera) and a coloured background, such as green, can possibly assist the software to better interpret the data.

## 5.4 Conclusions

This study investigated the replacement of BFS with up to 20% MK in the development of RAP-AAM mortars. MK was chosen as a replacement because has a micro-filler and could induce the production of more reaction products which could refine the pore structure and improve mechanical and durability properties.

The initial assessment concluded that, for the studied system, MK replacement with 4%  $\text{Na}_2\text{O}$  activation will not yield a material with sufficient early strength.

When mortars were activated with 8% $\text{Na}_2\text{O}$  (wt.% of binder) and silica modulus of either 1 or 0 (i.e., no sodium silicate) the following conclusions can be drawn:

- The use of MK slowed down the reaction. This significantly impacted the early strength results of RAP-AAM but samples showed little detrimental effects at later ages. The mechanical performance of RAP-AAM at early stages may be significantly improved by employing silicates in the activator.
- Although the employment of silicates in the activator ( $M_s=1$ ), may contribute to strength gain, it also increases shrinkage tendency in RAP-AAM. The replacement of BFS with MK may help reduce RAP-AAM shrinkage (depending on the choice of activator and up to an optimum level). In this study, mortars without sodium silicate shrank 75% less than their counterparts that contain silicates. Shrinkage is undesirable distress to pavements and should be controlled.
- The combination of SEM and Confocal microscopy is helpful to visualise the interfaces between the several zones present in RAP-AAM: aggregates, mastic, and alkali-activated gel. The microstructure observation indicated that the mastic layer onto the RAP aggregates presents variable thicknesses and remarkably high concentrations of pores.

Moreover, it appears logical to choose NaOH as the sole activator ( $M_s = 0$ ) and MK as a partial replacement of BFS in RAP-AAM to reduce the shrinkage. Despite the expected delay early strength development, system with 10%MK replacement (activated with 8%  $Na_2O$  and  $M_s=0$ ) gained flexural and compressive strength at later ages. This choice will not likely affect the porosity of the composites. The employment of MK did not mitigate the pores at the mastic region nor the cracking connecting these regions. As in PC-RAP composites, it is the RAP-matrix's poor interface that governs the low mechanical properties and high porosity compared to other composites made with natural aggregates.

**Highlights:**

1. The use of MK compromises the early strength of the studied mixes by delaying the formation of main reaction products. The filler effect may have helped anchor RAP particles to the matrix and caused improvements in later compressive strength.
2. There is an optimum MK replacement level that depends on the properties of raw material (such as fineness) and the amount/type of activator. Based on the 28 days compressive strength, the ideal MK replacement is 5% and 10% for systems activated with 4% $Na_2O$  and 8% $Na_2O$  respectively.
3. Shrinkage in RAP-AAM systems can be best mitigated by avoiding the use of silicates ( $M_s=0$ ) or with the use of small amounts of MK (less effective).

*The preliminary study of this Chapter is a modified version of the paper "Reclaimed asphalt and alkali-activated slag systems: the effect of metakaolin" published in Engineering Proceedings in May 2022. It has been published in this thesis with the authorisation of the copyright holders.*

# BIBLIOGRAPHY

---

Bakharev, T., Sanjayan, J.G., Cheng, Y.B., 2001. Resistance of alkali-activated slag concrete to carbonation. *Cem. Concr. Res.* 31, 1277–1283. [https://doi.org/10.1016/S0008-8846\(01\)00574-9](https://doi.org/10.1016/S0008-8846(01)00574-9)

Ballekere Kumarappa, D., Peethamparan, S., Ngami, M., 2018. Autogenous shrinkage of alkali activated slag mortars: Basic mechanisms and mitigation methods. *Cem. Concr. Res.* 109, 1–9. <https://doi.org/10.1016/j.cemconres.2018.04.004>

Barbosa, V.F.F., MacKenzie, K.J.D., Thaumaturgo, C., 2000. Synthesis and characterisation of materials based on inorganic polymers of alumina and silica: Sodium polysialate polymers. *Int. J. Inorg. Mater.* 2, 309–317. [https://doi.org/10.1016/S1466-6049\(00\)00041-6](https://doi.org/10.1016/S1466-6049(00)00041-6)

Behfarnia, K., Rostami, M., 2017. An assessment on parameters affecting the carbonation of alkali-activated slag concrete. *J. Clean. Prod.* 157, 1–9. <https://doi.org/10.1016/j.jclepro.2017.04.097>

Bernal, S.A., Rodríguez, E.D., Mejia De Gutiérrez, R., Provis, J.L., Delvasto, S., 2012. Activation of metakaolin/slag blends using alkaline solutions based on chemically modified silica fume and rice husk ash. *Waste and Biomass Valorization* 3, 99–108. <https://doi.org/10.1007/s12649-011-9093-3>

Brand, A.S., Roesler, J.R., 2016. Expansive and concrete properties of SFS-FRAP aggregates. *J. Mater. Civ. Eng.* 28, 1–10. [https://doi.org/10.1061/\(ASCE\)MT.1943-5533.0001403](https://doi.org/10.1061/(ASCE)MT.1943-5533.0001403)

Cao, R., Zhang, S., Banthia, N., Zhang, Y., Zhang, Z., 2020. Interpreting the early-age reaction process of alkali-activated slag by using combined embedded ultrasonic measurement, thermal analysis, XRD, FTIR and SEM. *Compos. Part B Eng.* 186, 107840. <https://doi.org/10.1016/j.compositesb.2020.107840>

Costa, J.O., Borges, P.H.R., dos Santos, F.A., Bezerra, A.C.S., Blom, J., Van den bergh, W., 2021. The Effect of Reclaimed Asphalt Pavement (RAP) Aggregates on the Reaction, Mechanical Properties and Microstructure of Alkali-Activated Slag. *CivilEng* 2, 794–810. <https://doi.org/10.3390/civileng2030043>

Duran Atış, C., Bilim, C., Çelik, Ö., Karahan, O., 2009. Influence of activator on the strength and drying shrinkage of alkali-activated slag mortar. *Constr. Build. Mater.* 23, 548–555. <https://doi.org/10.1016/J.CONBUILDMAT.2007.10.011>

Fedrigo, W., Núñez, W.P., Kleinert, T.R., Matuella, M.F., Ceratti, J.A.P., 2017. Strength, shrinkage, erodibility and capillary flow characteristics of cement-treated recycled pavement materials. *Int. J. Pavement Res. Technol.* 10, 393–402. <https://doi.org/10.1016/j.ijprt.2017.06.001>

Fernandez-Jimenez, A., Puertas, F., Arteaga, A., 1998. Determination of kinetic equations of alkaline activation of blast furnace slag by means of calorimetric data. *J. Therm. Anal. Calorim.* <https://doi.org/10.1023/A:1010172204297>

Fu, B., Cheng, Z., Han, J., Li, N., 2021. Understanding the role of metakaolin towards mitigating the shrinkage behavior of alkali-activated slag. *Materials (Basel)*. 14, 1–19. <https://doi.org/10.3390/ma14226962>

Gao, L., Zheng, Y., Tang, Y., Yu, J., Yu, X., Liu, B., 2020. Effect of phosphoric acid content on the microstructure and compressive strength of phosphoric acid-based metakaolin geopolymers. *Heliyon* 6, e03853. <https://doi.org/10.1016/j.heliyon.2020.e03853>

Gebregziabiher, B.S., Thomas, R.J., Peethamparan, S., 2016. Temperature and activator effect on early-age reaction kinetics of alkali-activated slag binders. *Constr. Build. Mater.* 113, 783–793. <https://doi.org/10.1016/j.conbuildmat.2016.03.098>

Huanhai, Z., Xuequan, W., Zhongzi, X., Mingshu, T., 1993. Kinetic study on hydration of alkali-activated slag. *Cem. Concr. Res.* 23, 1253–1258. [https://doi.org/10.1016/0008-8846\(93\)90062-E](https://doi.org/10.1016/0008-8846(93)90062-E)

Huseien, G.F., Mirza, J., Ismail, M., Ghoshal, S.K., Ariffin, M.A.M., 2016. Effect of metakaolin replaced granulated blast furnace slag on fresh and early strength properties of geopolymer mortar. *Ain Shams Eng. J.* <https://doi.org/10.1016/j.asej.2016.11.011>

Ismail, I., Bernal, S.A., Provis, J.L., San Nicolas, R., Hamdan, S., Van Deventer, J.S.J., 2014. Modification of phase evolution in alkali-activated blast furnace slag by the incorporation of fly ash. *Cem. Concr. Compos.* 45, 125–135. <https://doi.org/10.1016/j.cemconcomp.2013.09.006>

Jithendra, C., Dalawai, V.N., Elavenil, S., 2021. Effects of metakaolin and sodium silicate solution on workability and compressive strength of sustainable Geopolymer mortar. *Mater. Today Proc.* <https://doi.org/10.1016/j.matpr.2021.10.399>

Kashani, A., Provis, J.L., Qiao, G.G., Van Deventer, J.S.J., 2014. The interrelationship between surface chemistry and rheology in alkali activated slag paste. *Constr. Build. Mater.* 65, 583–591. <https://doi.org/10.1016/j.conbuildmat.2014.04.127>

Lee, N.K., Jang, J.G., Lee, H.K., 2014. Shrinkage characteristics of alkali-activated fly ash/slag paste and mortar at early ages. *Cem. Concr. Compos.* 53, 239–248. <https://doi.org/10.1016/j.cemconcomp.2014.07.007>

Li, Z., Liang, X., Chen, Y., Ye, G., 2020. Effect of metakaolin on the autogenous shrinkage of alkali-activated slag-fly ash paste. *Constr. Build. Mater.* 278, (under review). <https://doi.org/10.1016/j.conbuildmat.2021.122397>

Li, Z., Nedeljković, M., Chen, B., Ye, G., 2019. Mitigating the autogenous shrinkage of alkali-activated slag by metakaolin. *Cem. Concr. Res.* 122, 30–41. <https://doi.org/10.1016/j.cemconres.2019.04.016>

Liu, S., Li, Q., Han, W., 2018. Effect of various alkalis on hydration properties of alkali-activated slag cements. *J. Therm. Anal. Calorim.* 131, 3093–3104. <https://doi.org/10.1007/s10973-017-6789-z>

Mastali, M., Kinnunen, P., Dalvand, A., Mohammadi Firouz, R., Illikainen, M., 2018. Drying shrinkage in alkali-activated binders – A critical review. *Constr. Build. Mater.* 190, 533–550. <https://doi.org/10.1016/j.conbuildmat.2018.09.125>

Melo Neto, A.A., Cincotto, M.A., Repette, W., 2008. Drying and autogenous shrinkage of pastes and mortars with activated slag cement. *Cem. Concr. Res.* 38, 565–574. <https://doi.org/10.1016/j.cemconres.2007.11.002>

Palacios, M., Puertas, F., 2005. Effect of superplasticizer and shrinkage-reducing admixtures on alkali-activated slag pastes and mortars. *Cem. Concr. Res.* 35, 1358–1367. <https://doi.org/10.1016/j.cemconres.2004.10.014>



Peng, H., Cui, C., Liu, Z., Cai, C.S., Liu, Y., 2019. Synthesis and Reaction Mechanism of an Alkali-Activated Metakaolin-Slag Composite System at Room Temperature. *J. Mater. Civ. Eng.* 31, 04018345. [https://doi.org/10.1061/\(asce\)mt.1943-5533.0002558](https://doi.org/10.1061/(asce)mt.1943-5533.0002558)

Puertas, F., González-Fonteboa, B., González-Taboada, I., Alonso, M.M., Torres-Carrasco, M., Rojo, G., Martínez-Abella, F., 2018. Alkali-activated slag concrete: Fresh and hardened behaviour. *Cem. Concr. Compos.* 85, 22–31. <https://doi.org/10.1016/j.cemconcomp.2017.10.003>

Shi, C., Ana, F.-J., Palomo, A., 2011. New cements for the 21st century: The pursuit of an alternative to Portland cement. *Cem. Concr. Res.* 41, 750–763. <https://doi.org/10.1016/j.cemconres.2011.03.016>

Shi, Z., Shi, C., Wan, S., Zhang, Z., 2018. Effects of alkali dosage and silicate modulus on alkali-silica reaction in alkali-activated slag mortars. *Cem. Concr. Res.* 111, 104–115. <https://doi.org/10.1016/J.CEMCONRES.2018.06.005>

Soleimani, M.A., Naghizadeh, R., Mirhabibi, A.R., Golestanifard, F., 2012. Effect of calcination temperature of the kaolin and molar Na<sub>2</sub>O/SiO<sub>2</sub> activator ratio on physical and microstructural properties of metakaolin based geopolymers. *Iran. J. Mater. Sci. Eng.* 9, 43–51.

Wang, J., Li, X., Wen, H., Muhunthan, B., 2020. Shrinkage cracking model for cementitiously stabilized layers for use in the mechanistic-empirical pavement design guide. *Transp. Geotech.* 24, 100386. <https://doi.org/10.1016/j.trgeo.2020.100386>

Zhang, B., Zhu, H., Cheng, Y., Huseien, G.F., Shah, K.W., 2022. Shrinkage mechanisms and shrinkage-mitigating strategies of alkali-activated slag composites: A critical review. *Constr. Build. Mater.* 318, 125993. <https://doi.org/10.1016/j.conbuildmat.2021.125993>





# RAP-AAM LEAN CONCRETE FOR PAVEMENTS BASE LAYER

---

The work so far in this thesis assessed the effect of RAP as aggregates for alkali-activated mortars. The objective of this **experimental chapter** is to compare RAP-PC and RAP-AAM concretes. It explores and evaluates the impact of RAP's bitumen content on lean concrete produced with alkali-activated slag (AAS) and coarse RAP granules targeting the employment of this composite material as an alternative pavement base layer.

A reference lean concrete (RC) was compared with three RAP-AAM lean concrete mixes that contained different RAP as coarse aggregates: (i) locally sourced RAP (4.8% bitumen); (ii) lab-made RAP with low (4.5%) bitumen content (RAPL) and (iii) lab-made RAP with high (5.7%) bitumen content (RAPH). The chapter presents the results of the mechanical performance (i.e., compressive strength, indirect tensile strength, and modulus of elasticity) and resistance to freeze and thaw cycles.

The results show that the studied RAP-AAM lean concrete has higher compressive strength, indirect tensile strength, and static modulus of elasticity than the reference RAP-PC lean concrete. Further improvements in the mechanical performance may be also achieved if sodium silicate is employed as an activator, although not recommended to keep costs and environmental impact at a lower level.

In general, the bitumen content on the RAP particles did not play an important role to determine the mechanical properties. The Freeze &

Thaw tests were not severe enough to show damage and significant mechanical loss in both RAP-PC and RAP-AMM concretes. Overall, one can say that the performance under frost tends to be equivalent for both types of lean concrete, RAP-PC and RAP-AAM.

### 6.1 Introduction

RAP can be incorporated in either base layers or surface layers. The possibility of recycling larger amounts of RAP is more feasible in base layers, since the latter is thicker, with lower performance requirements, and less regulated (Plati, 2019). RAP is often fractionated into two or more sizes (such as fine and coarse) for better control, although it is also possible to use it “all-in”. The fine fraction (<4mm or 4.75mm) is often recycled in new asphalt mixtures since it has higher bitumen content and, therefore, is easily heated (Han et al., 2019; Howard et al., 2009). The coarse RAP fraction, on the other hand, needs more prospects of reuse (Brand et al., 2012).

Most of the results presented in the literature are restricted to the employment of RAP aggregates in alkali-activated pulverized fly ash (PFA) (Avirneni et al., 2016; Hoy et al., 2016a; Rahman and Khattak, 2021). The use of up to 80% RAP aggregates in AAM reaches minimum strength requirements (superior to 4.5MPa) at low levels of NaOH activation (2-4 wt.%); low leaching of hazardous materials and adequate resistance to wet-dry cycles (less than 14% weight loss) are also observed (Mohammadinia et al., 2017) (Avirneni et al., 2016; Hoy et al., 2016b). Roller-compacted concrete mixes were also studied either with PC or alkali-activated PFA; the latter presented higher values for compressive strength, flexural strength, and modulus of elasticity, with values ranging from 8-21MPa, 2.9-4.1MPa and 18-35GPa, respectively (Rahman and Khattak, 2021). Overall, there is little literature on the use of RAP-AAM, and more research is needed to address other types of precursors (such as alkali-activated slag) and whether the bitumen content that covers the RAP aggregates may impact the performance of RAP-AAM.

This chapter aims to compare the performance of a reference lean concrete (RC) with RAP-AAM lean concretes. Three coarse RAP aggregate with different bitumen content was used.

Proctor compaction was used in the RAP aggregates to assess the effect of compaction on the gradation, and the effect of the bitumen content on optimum moisture. The compressive strength and indirect tensile strength of the lean concrete were determined at both 7 and 28 days; the ultrasonic pulse velocity (UPV) of the samples, was recorded before crushing and used to determine the dynamic modulus of elasticity. The static modulus of elasticity was performed at 28 days.

The Freeze and Thaw (F&T) procedure adopted in this research is a modified version of ASTM C666 when three samples from each composition were subjected to two complete freeze and thaw cycles ( $-20^{\circ}\text{C}$  to  $+20^{\circ}\text{C}$ ) every 24 hours, starting after 14 days of curing. The samples had their weight and pulse velocity measured after 18 and 36 cycles. At the end of the experiment, the F&T and reference samples were tested for compressive strength.

## 6.2 Experimental summary

This chapter aims to compare the performance of a reference lean concrete (RC) with RAP-AAM lean concretes. To produce the lean concrete three types of coarse RAP aggregate were used (Table 6.1). RC was produced with cement CEM III/A 42.5 N LA (PC) and locally sourced RAP (RAP1). Three RAP-AAM lean concrete mixes were studied (NR, LB and HB); they differed in the type of RAP used as coarse (Table 6.2). The matrix of the alkali-activated concretes comprised of a 9/1 BFS/MK (vol.%) precursor activated with 8%  $\text{Na}_2\text{O}$  solution (binder wt.%). This composition was chosen based on the results of Chapter 5 for RAP alkali-activated mortars.

*Table 6.1. Coarse RAP aggregates*

<b>Aggregate</b>	<b>Origin</b>	<b>Bitumen content (%)</b>
RAP1	Supplied	4.8
RAPL	Lab Manufactured	4.5
RAPH	Lab manufactured	5.7

*Table 6.2. Lean concrete compositions (kg/m<sup>3</sup>)*

Notation	Binder			Solution		Aggregates			
	PC	BFS	MK	NaOH	Water	Fine (NA)	RAP1	RAPL	RAPH
<b>RC</b>	122	-	-	-	132	730	1217	-	-
<b>NR</b>	-	110	11	12.7	130	730	1217	-	-
<b>LB</b>	-	110	11	12.7	130	730	-	1217	-
<b>HB</b>	-	110	11	12.7	130	730	-	-	1217

Two types of proctor test were performed in this chapter. The first one was performed only on the coarse RAP aggregates and the second one used the concrete mix (without the activator). Each test consumed approximately 6kg of materials, totalizing 36kg of raw material for proctor testing.

The mechanical and durability assessment was performed on cylinders and cubes and a total of 72 samples were produced (Table 6.3). All samples were also subjected to a non-destructive test.

*Table 6.3. Samples produced*

Type of sample (mm)	Number of samples
Cylinder 100x200	24
Cylinder 150x300	16
Cubes 100x100	16

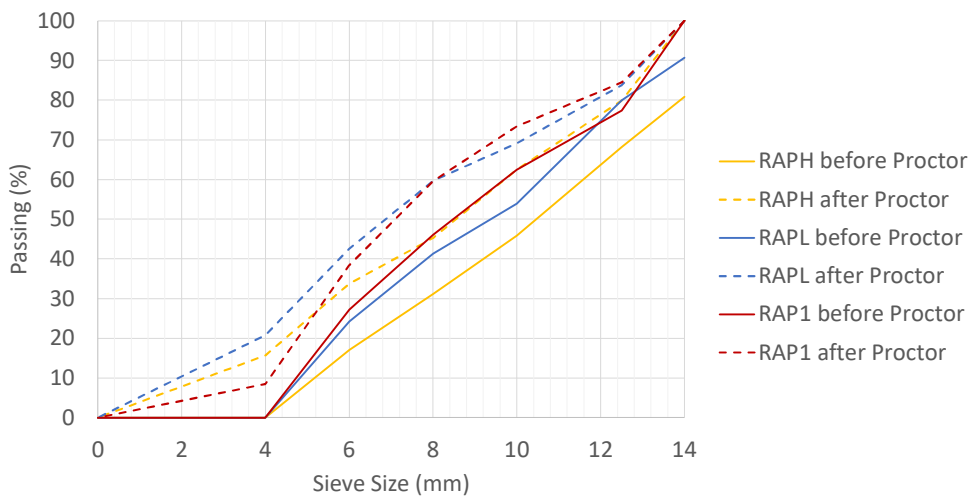
## 6.3 Results & Discussion

### 6.3.1 Proctor compaction on RAP aggregates and AAM lean concrete

The RAP samples produced in the laboratory presented a coarser particle size distribution than the locally sourced RAP, even though they were produced to be similar. One of the reasons for the difference in the initial gradation is due to the absence of a milling procedure for the lab-produced RAP. The effect of the proctor compaction on the gradation of the lab-made RAP aggregates is presented in Figure 6.1. The curves in Figure 6.1 indicate that the samples produced in the lab (RAPL and RAPH) had more clusters than the locally sourced (RAP1), especially for

the aggregates produced with higher bitumen content (RAPH, yellow curve).

The gradation of all RAP aggregates changed after the modified proctor compaction (dashed curves). This breakage of RAP aggregates after proctor compaction has been observed in previous research, especially for bigger particles of RAP (Pradhan and Biswal, 2022). Herein, the action of the rammer broke down some of the clusters and increased the fine content in the aggregates. It is possible to observe that the compaction has a greater effect on the samples produced in the lab due to the absence of a milling procedure.



*Figure 6.1. Impact of compaction on RAP gradation*

Figure 6.2 shows the proctor compaction results for the RAP-AMM lean concretes. The optimum moisture content (OMC) was 5.6%, 5.7% and 5.9% for samples LB, HB, and NR respectively, and the maximum dry density (MDD) was 2.20, 2.11, and 2.16 Mg/cm<sup>3</sup>. All studied samples presented very similar results for OMC and MDD, suggesting that the bitumen content and the different gradations had little impact on the results. The steeper curve (yellow, for HB) indicated that the higher bitumen content increased the water sensitivity of the composition.

The OMC and MDD are closely related to the quantity of fines in the mix. While the incorporation of fines will act as a filler and improve compactability, an excess of fines will absorb more water and thus reduce compactability. Studies of RAP-AAM (FA-based) reported that reductions in compaction results start at about 15-20% FA replacement (Hoy et al.,

2016a; Rahman and Khattak, 2021). Hoy et al. (2018, 2016a) studied RAP-AAM mixes and observed that increasing the FA content from 10% to 30% the OMC values increased from 7% to 9% and the MDD went from 2.18 to 2.28 Mg/m<sup>3</sup>. Similar results were observed for 10% and 20% BFS – 7.40% and 8.20% for OMC and 1.84 and 1.95 for MDD. Avirneni et al. (2016) investigated systems with 80-60% RAP and 20-30%FA and observed OMC results ranging from 7-7.50% and MDD ranging from 3.12-2.16 Mg/m<sup>3</sup>. The results observed in this study follow what has been presented by other authors, and the slight difference in results can be justified by the different nature of the fines used (this research used BFS instead of FA) and the replacement levels adopted (this research has approximately 6% BFS in the mix).

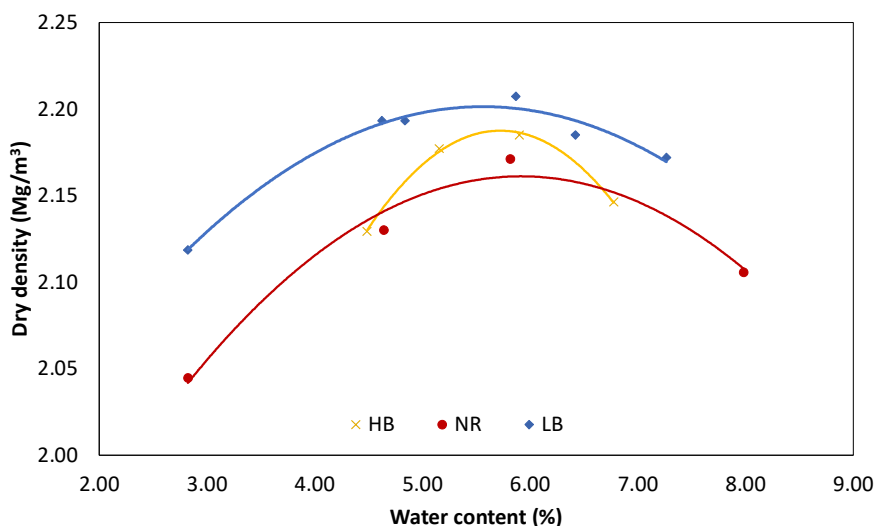


Figure 6.2. Moisture x density curves for concrete compositions

### 6.3.2 Compressive and splitting tensile strength

Figure 6.3 and Figure 6.4 show, respectively, the mean compressive strength ( $f_{ccub100m}$ ) and mean splitting tensile strength ( $f_{ct,spl}$ ) for the RAP-AAM and reference lean concrete. The first presented higher mean strength (both compressive and tensile) than samples prepared with PC. It is possible to see that improved performance is more significant at an early age. At 7 days, the change from PC matrix to AAM improved the compressive strength by at least 39% and tensile strength by 53%. The improvement in strength caused by replacing PC with AAM was also observed by Rahman and Khattak (2021). In their work the replacement



of PC with NaOH-activated FA (8.4%  $\text{Na}_2\text{O}$ ) increased compressive strength by approximately 33%; the rise was much higher (83%) by increasing the activator concentration to 11%  $\text{Na}_2\text{O}$ . However, the authors found the opposite performance in splitting strength, where activated samples had a 6% strength reduction.

Increasing the bitumen content had a negative impact on both compressive and flexural strength, as 28 days results for HB samples were 12% to 14% lower than LB (respectively). The higher bitumen content is associated with the formation of more clusters of asphalt mortar and natural aggregates, this can be confirmed with the coarser gradation observed in Figure 6.1. Although RAP aggregates are often described as natural aggregates covered with a thin asphalt mortar layer, the RAP clusters can concentrate large quantities of old asphalt (Costa et al., 2021) which can significantly reduce the strength of the composite. Remarkably, at 7 days the strength of HB samples was higher than LB.

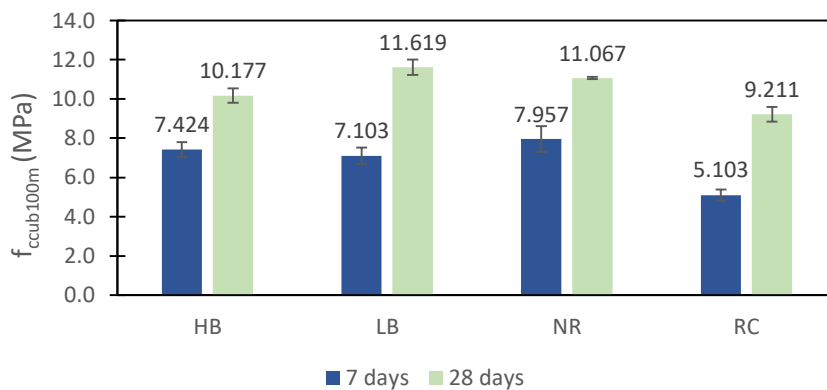


Figure 6.3. Mean compressive strength of 100mm lean concrete cubes

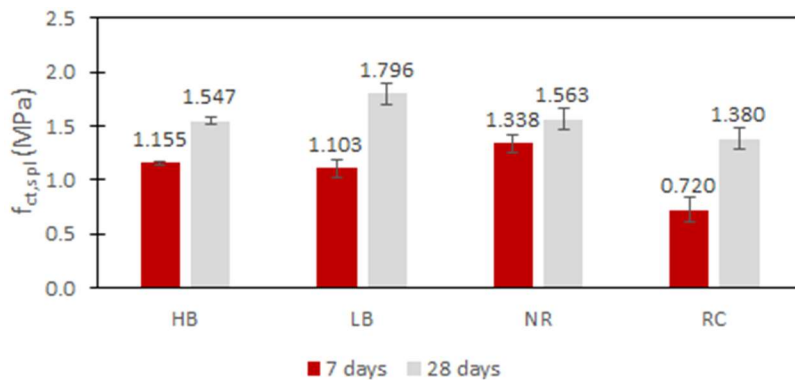


Figure 6.4. Mean splitting tensile strength of lean concrete cylinders

The results indicate that the studied compositions of alkali-activated slag binders can achieve higher strength values than PC, and this stronger matrix will create more resistance to the formation, expansion, and interconnection of micro cracks and therefore increase the overall strength of RAP-AAM. Improvements in both compressive and splitting strength are both positive for pavement design, however, better splitting performance is more desirable than compressive. Pavement design is often controlled by tensile stresses.

### 6.3.3 Modulus of elasticity (ME)

The values for the secant modulus of elasticity ( $E_s$ ) and the dynamic modulus of elasticity ( $E_d$ ) are summarized in Table 6.4, as well as the average compressive strength of the cylinder ( $f_{cyl}$ ). The 28 days compressive strength of the cylinders ( $f_{cyl}$ ) was estimated from a relationship to the 28 days compressive strength of the cubes ( $f_{cub}$ ) as per Equation 6.1.

$$f_{cyl} = \frac{0.79f_{cub}}{1.05} \quad \text{Equation 6.1}$$

Table 6.4. Average modulus of elasticity of lean concrete mixtures with RAP

	Density (kg/m <sup>3</sup> )	Wave velocity (m/s)	$f_{cyl}$ (MPa)	$E_d$ (GPa)	$E_s$ (GPa)
<b>RC</b>	2258.18	3451.18	6.93	22.42	16.96
<b>NR</b>	2245.75	3844.47	8.33	27.66	23.86
<b>LB</b>	2255.85	3734.35	8.74	26.22	24.58
<b>HB</b>	2217.7	3734.99	7.66	25.78	22.00

In general, Table 6.4 shows lower results of both moduli of elasticity ( $E_d$  and  $E_s$ ) and compressive strength ( $f_{cyl}$ ) for the reference concrete (RC), when compared with RAP-AAM (NR, LB, and HB). Those results are in line with the strength results found in the previous section 6.3.2. However, this behaviour is different from what is found in the literature for concretes with normal strength and made with NA. BFS-based AAM made with NA tends to have lower ME than their PC concretes

counterparts (Cartwright et al., 2015; Ding et al., 2018; Farhan et al., 2019). This will be discussed in the following paragraphs.

Figure 6.5 presents a comparison between the secant ME for RAP-AAM (Table 6.4) and the results from the literature found for RAP-PC concretes containing at least 75% RAP as aggregates (Ashteyat et al., 2021; Boussetta et al., 2018; Brand and Roesler, 2017; El Euch Ben Said et al., 2018; Euch Khay et al., 2015; Ghazy et al., 2022; Nguyen et al., 2020; Panditharadhya et al., 2019; Settari et al., 2015; Su et al., 2014). The figure also includes two reference curves, red and yellow, for concrete defined respectively by EN 1992-1 (EC2) and ACI 318. The curves were built based on the relationship between compressive strength and secant ME at 28 days from Eurocode 2 (Equation 6.2) and ACI 318-11 (Equation 6.3):

$$E_c = 22(f_{cm}/10)^{0.3} \quad \text{Equation 6.2}$$

$$E_c = 4.7\sqrt{f_{cm}} \quad \text{Equation 6.3}$$

It is possible to see that in the range of lean concretes (compressive strength between 5-15 MPa at 28 days), the studied RAP-AAM (marked as black x points) has higher ME than would be expected from ACI-318 (yellow dashed curve) and close results to Eurocode (red dashed-dot curve) (Figure 6.5). The reference lean concrete from this present study (RAP-PC, green triangle points) stands close to the literature data (blue points and trendline) and between the two reference standards. RAP-AAM also presented a higher secant modulus of elasticity than RAP-PC concretes reported in the literature, which suggests a different interaction of RAP with either PC or AAM matrix.

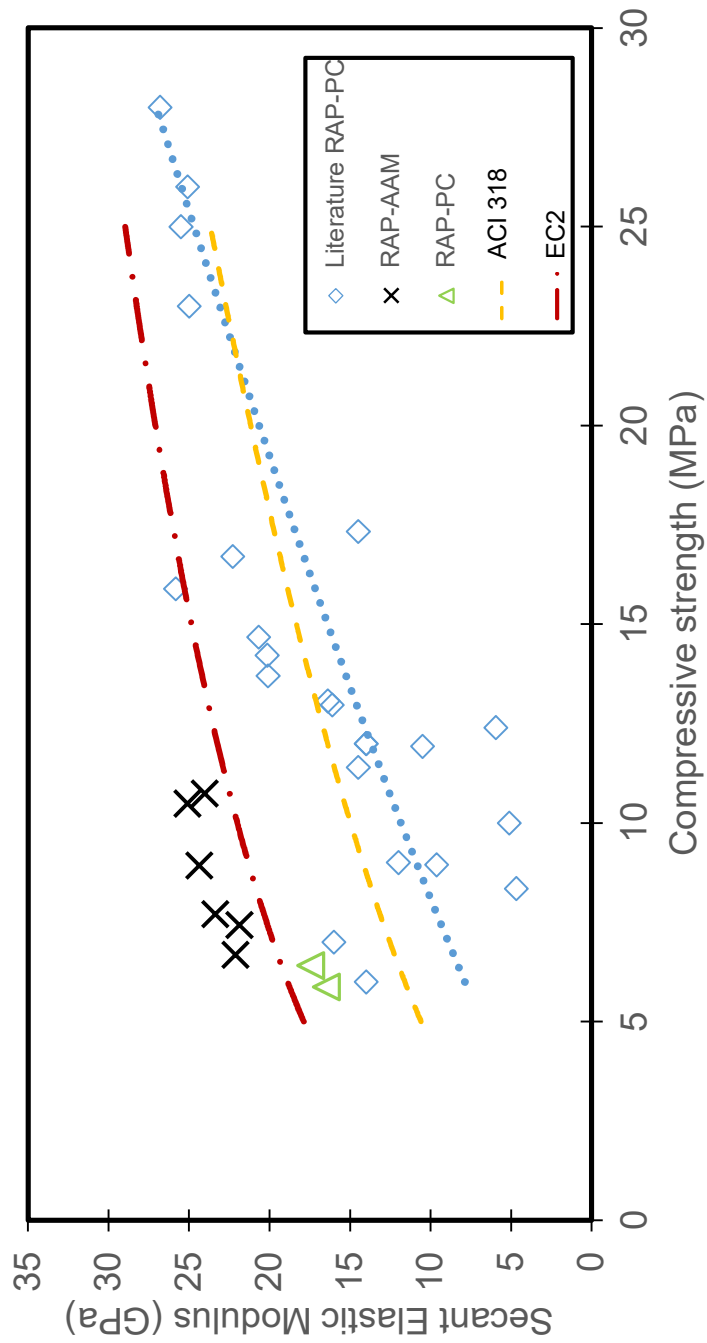


Figure 6.5. Elastic Modulus and compressive strength at 28 days: studied RAP-AAM and RAP-PC, data from literature and ACI 318 and EC2 reference curves

The mix design of RAP-PC concretes found in the literature varies considerably. Therefore, it appears reasonable to compare concretes with similar binder content to help the analysis. That is the purpose of Figure 6.6. It contains the same data from Figure 6.5. However, the RAP-PC concretes are gathered according to their binder content. The blue, red and yellow curves are trendlines for RAP-PC concretes with cement consumption ranges of 125-296 kg/m<sup>3</sup>, 300-380 kg/m<sup>3</sup> and 400-425 kg/m<sup>3</sup>, respectively. The lean concrete studied in this chapter are also plotted. They contained 122 kg/m<sup>3</sup> of either cement (RAP-PC, green triangles) or 9/1 GBFS/MK (black x points).

The first observation in Figure 6.6 is the inclination of the trendlines. RAP-PC concretes with a lower binder content (blue and red trendlines) present a steeper trendline compared to RAP-PC concretes with higher binder content (yellow trendline). A steeper curve indicates that the former tends to be more sensitive to variations i.e., small changes in the strength significantly affect the ME. The black trendline for the studied RAP-AAM has a similar inclination to RAP-PC concretes with the highest binder content, i.e., 400-425 kg/m<sup>3</sup> (yellow curve), which may be interpreted as concrete less susceptible to ME variations.

Naturally, it is not possible to generalize and make a clear conclusion based on the present data, given that the RAP-PC concretes reported in the literature also differ in terms of the RAP composition, particle size distribution, bitumen content, etc. However, this preliminary analysis herein shows that RAP-AAM mixes not only are more brittle than RAP-PC concretes but also are less prone to changes in the ME at different strength levels. In other words, in the range of lean concretes (5-15 MPa strength and binder content < 200 kg/m<sup>3</sup>), RAP-PC tends to present higher deformation upon stresses, which may happen with little changes in the mix design. RAP-AAM is characterised by a narrow ME range (20-25 GPa) which positively helps predict the deformation for different mix designs. However, they are more brittle and, therefore, more prone to cracking under service if employed as pavement base layers.

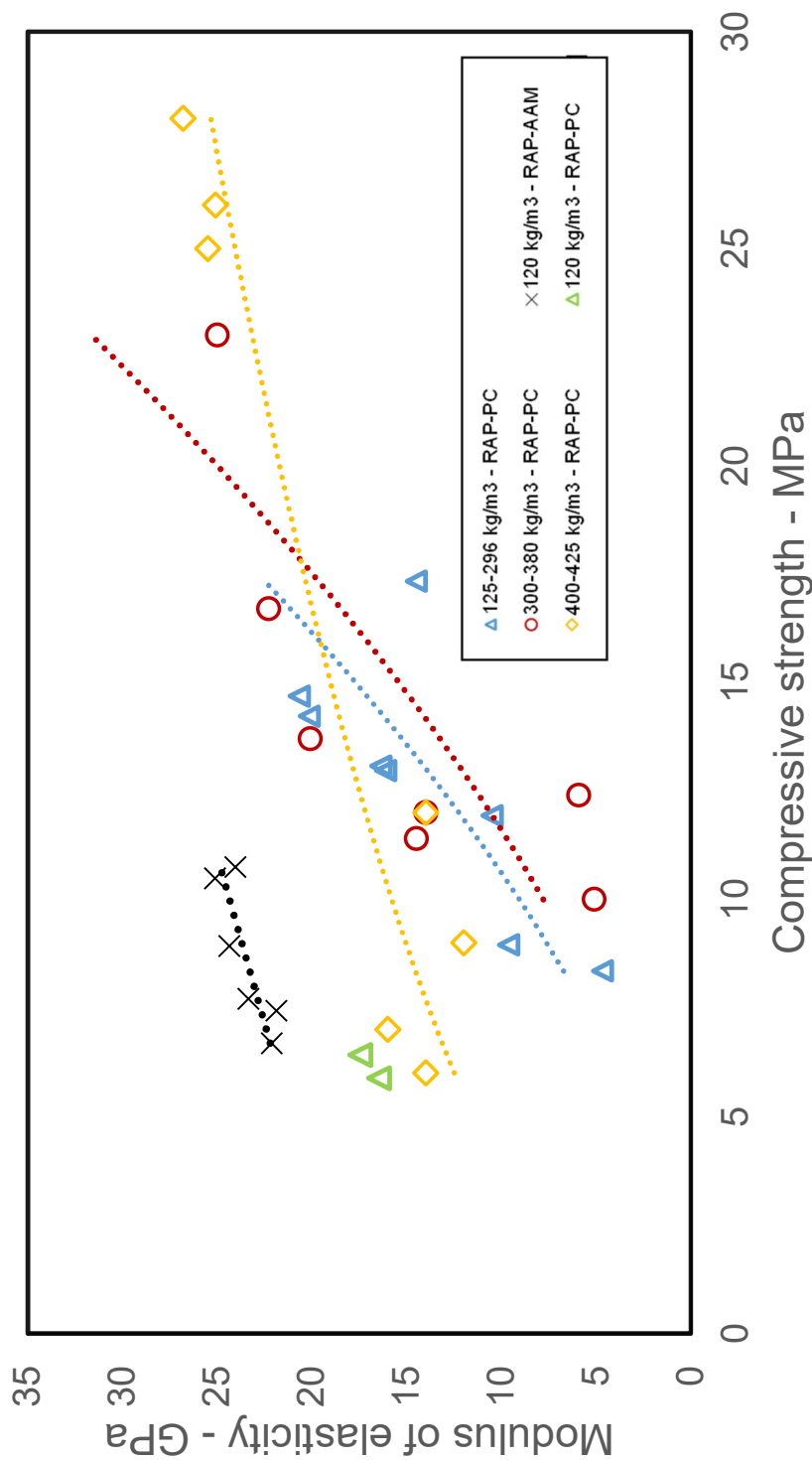


Figure 6.6. Modulus of elasticity and compressive strength at 28 days for concretes with different binder consumption: studied RAP-AA and literature data for RAP-PC

It is also important to establish a comparison between AAM concretes, made either NA or RAP. Figure 6.7 presents results from the lean concretes produced with RAP in this study (RAP-AAM) and data from other BFS-based AAM made with NA collected from the literature (Diaz-Loya et al., 2011; Thomas and Peethamparan, 2015; Yang et al., 2012). The authors cited in Figure 6.7 studied the mechanical properties of either alkali-activated FA or BFS and performed regression analysis to propose a correlation to determine a static modulus equation similar to the ones proposed on standards. It is possible to see that the RAP-AAM presented higher ME than NA-AAM, especially when the lean concrete strength range is considered (within 5-15 MPa). The results presented in Figure 6.7 suggest that the RAP-matrix interface is somehow impacted by the alkali-activation, so RAP-AAM has higher ME than both NA-AAM and RAP-PC. Brand and Roesler (2017) studied the impact of NaOH treatment in RAP granules and observed an increase in ME for concretes with NaOH-treated RAP. The authors observed that the alkali treatment oxidized the bitumen layer, which became more brittle and helped increase the ME. The RAP aggregates employed in this present study were not pre-treated, but the alkaline solution may have somehow contributed to the embrittlement of the bitumen layer and rose the ME. However, it is important to note that the highest  $E_s$  in Table 6.4 (24.58 GPa) was found for LB, which is a lean concrete made with an aggregate with the lowest bitumen content (RAPL, 4.5%) (Table 2). So, the variations in the bitumen content in the RAP aggregates used herein (4.5 – 5.7%) are not sensitive to establishing a correlation between any possible embrittlement from the NaOH activator and ME.

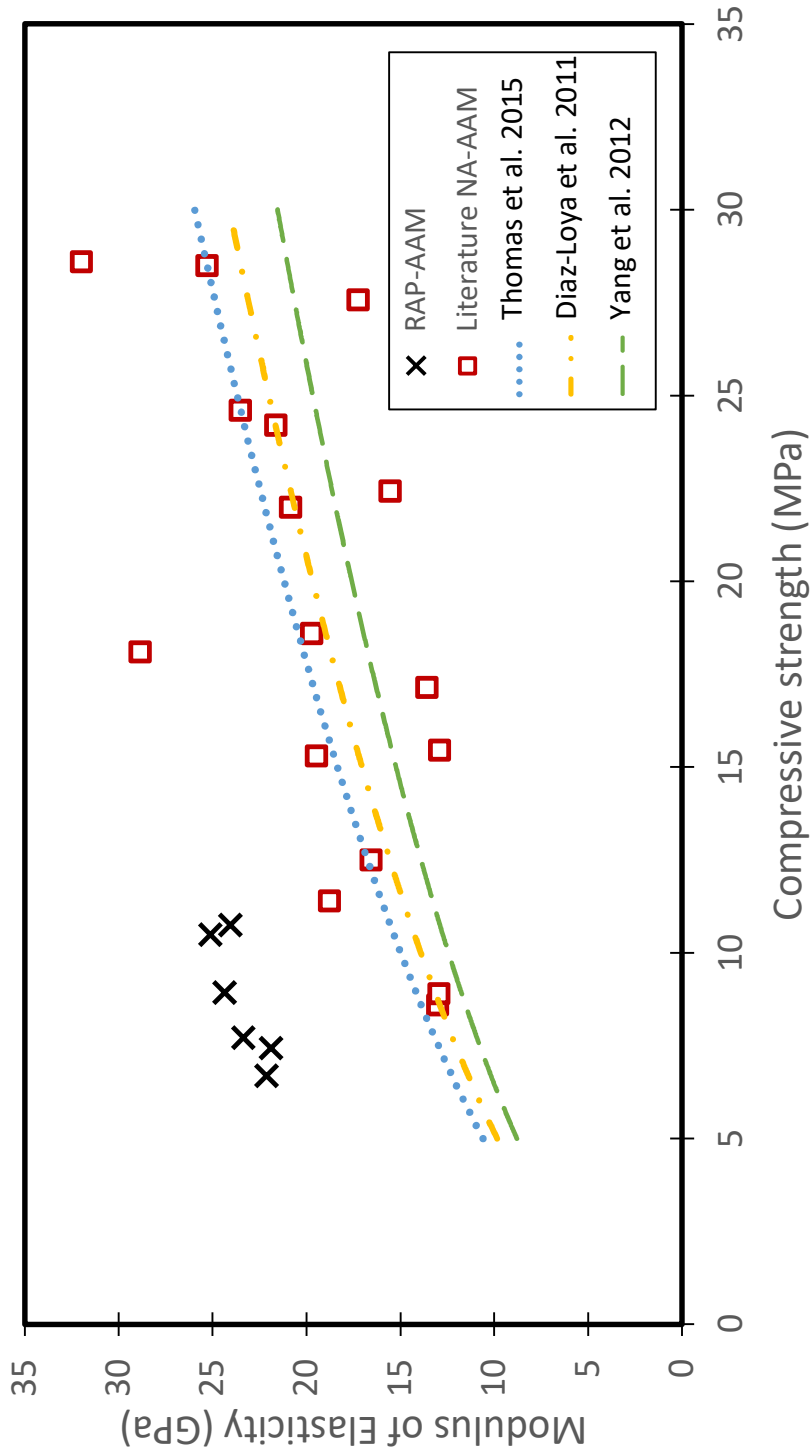


Figure 6.7. Elastic Modulus and Compressive strength: RAP-AAM and NA-AAM from the literature



### 6.3.4 Dynamic modulus of elasticity ( $E_d$ )

The UPV results were used to calculate the dynamic modulus of the concrete cubes, as described in Section 3.4.3.2. The UPV of the mixes ranged from 3.583 to 4.097 km/s (Figure 6.8) and the  $E_d$  was calculated by assuming a poison ratio of 0.25. The results ranged from 22.1 to 33.3 GPa. Concretes produced with alkali-activated binders provided higher values for UPV and  $E_d$  (at the same age). The different bitumen content in the RAP-AAM samples (HB, LB, and NR) showed no impact on the results. A linear and positive correlation between compressive strength and  $E_d$  can be seen in Figure 6.9. The RAP-AAM concretes presented a similar correlation to the reference concrete (RC).

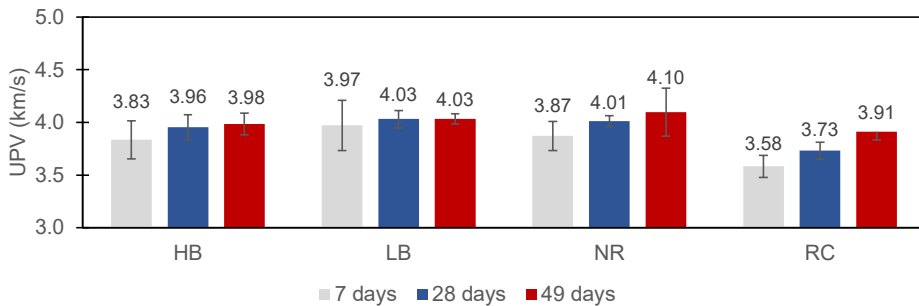


Figure 6.8. Pulse velocity of lean RAP concrete samples

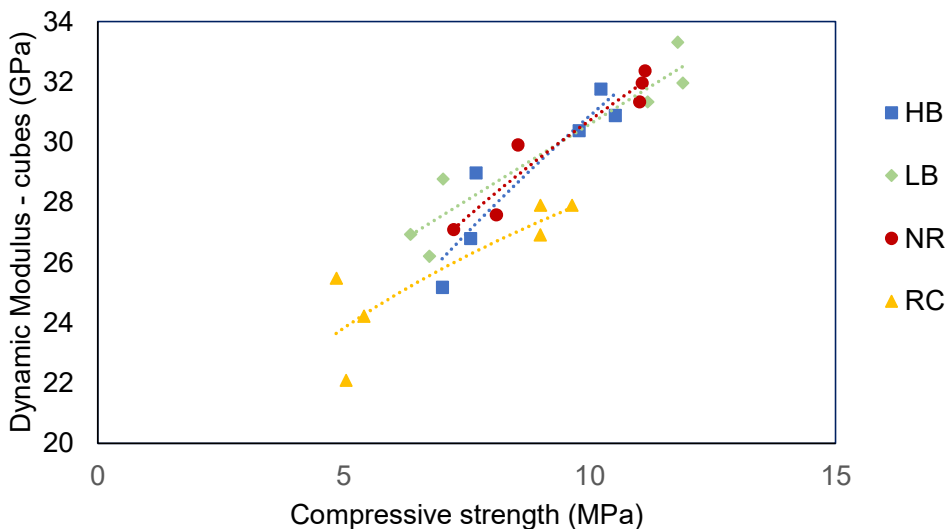


Figure 6.9.  $E_d$  of lean RAP concrete samples at 28 days

The relationship between  $E_d$  and  $E_s$  is presented in Figure 6.10 for each specimen. The results of the study showed a dynamic modulus is always greater than the static modulus. Although there is insufficient data to establish a relationship for each composition, the dynamic modulus was on average 32% and 13% higher for RAP-PC and RAP-AAM respectively. Yildirm and Sengul (2011) studied the modulus of low strength concretes (PC-based) and observed that the dynamic modulus is on average 30% higher than the static modulus. The authors suggested that this may be related to the fact that the UPV test is performed at low-stress levels and therefore the results resemble an initial tangent modulus.

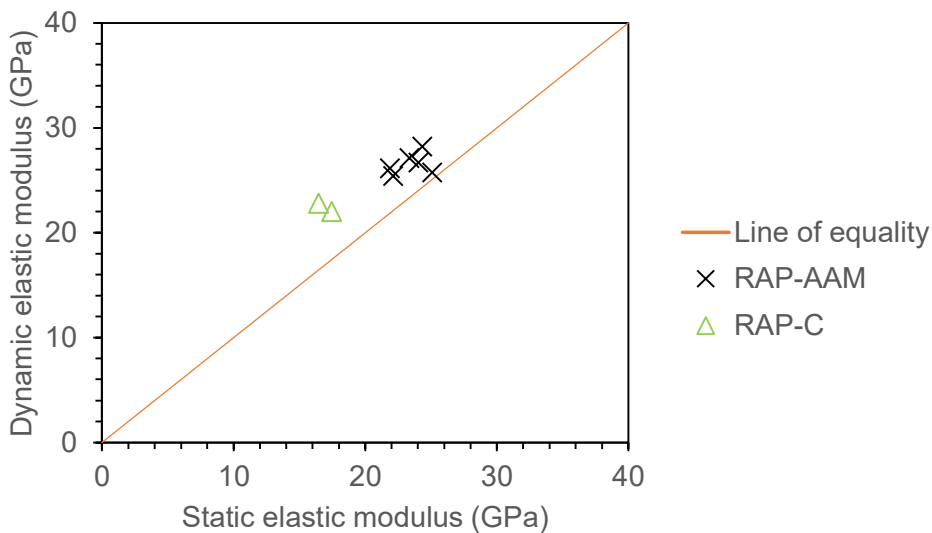
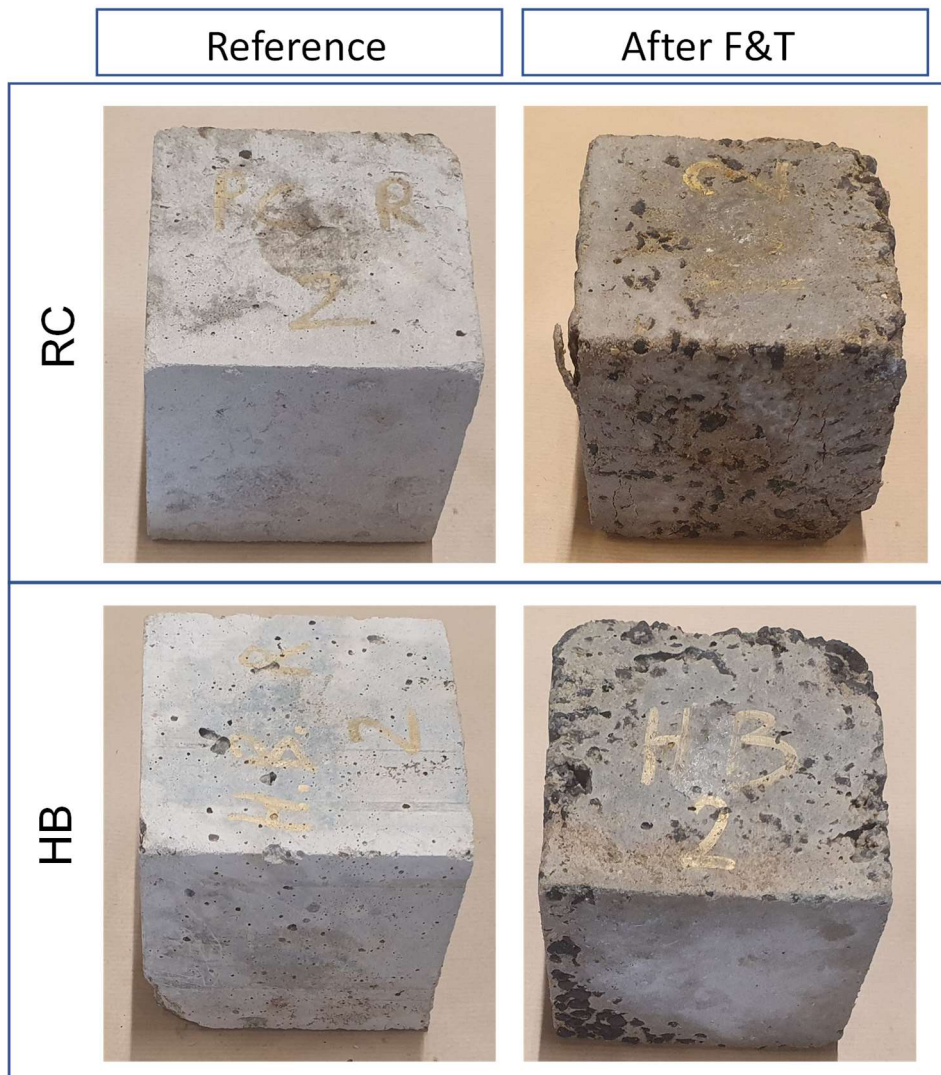


Figure 6.10. Relationship between static and dynamic modulus of elasticity

### 6.3.5 Freeze and thaw (F&T)

Durability to freezing and thawing cycles refers to the ability of cementitious matrixes to accommodate the water expansion during thermal changes. This property is closely related to the matrices' pore structure, i.e., if the pores have sufficient size and connectivity to allow water expansion without applying pressure (Thomas 2018). Pavements with improved F&T resistance are more sustainable as they will likely demand less maintenance. This test compares the concrete samples subjected to F&T cycles to a reference sample that hasn't been through the test as shown in Figure 6.11.



*Figure 6.11. Concrete samples RC and HB - reference and after F&T cycles*

Figure 6.12 and Figure 6.13 show, respectively, the weight changes and strength losses for RAP-AAM (NR, LB and HB) and RAP-PC (RC) after 18 and 36 F&T cycles. It is possible to see a low variation in weight (0.12-0.30%) and strength loss (28-34%) after 36 cycles for all concretes. In both cases, the variation is lower than 6%, which suggests similar performance under testing. HB and RC presented both the lowest weight variation and strength loss after the accelerated testing (99.35% and 100.08% mass retention and 29% and 28% strength loss). The mass gain of cement-based samples was also observed by others (Mataalkah and

Soroushian, 2018) at up to 60 cycles, and attributed to the increase in the water absorption caused by the induced microcracking and cracking of the specimens. The lean concrete with highest strength prior to accelerated testing (LB and NR) were those that presented the highest strength losses, 34% and 32% respectively for LB and NR.

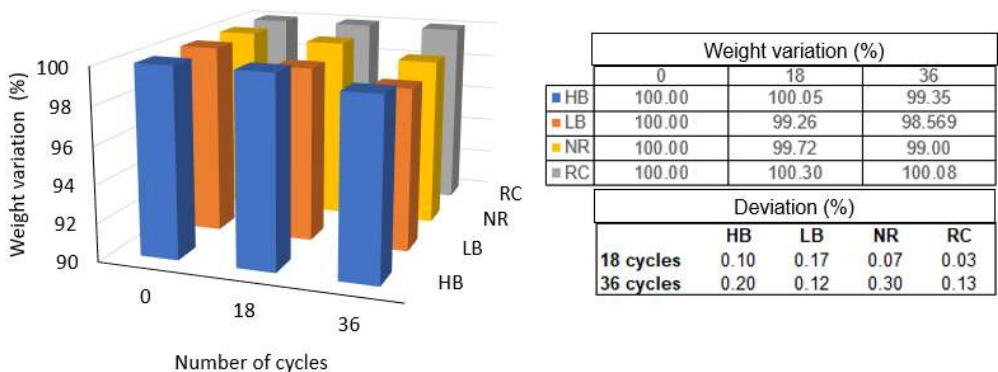


Figure 6.12. Weight changes in samples subjected to 36 F&T cycles

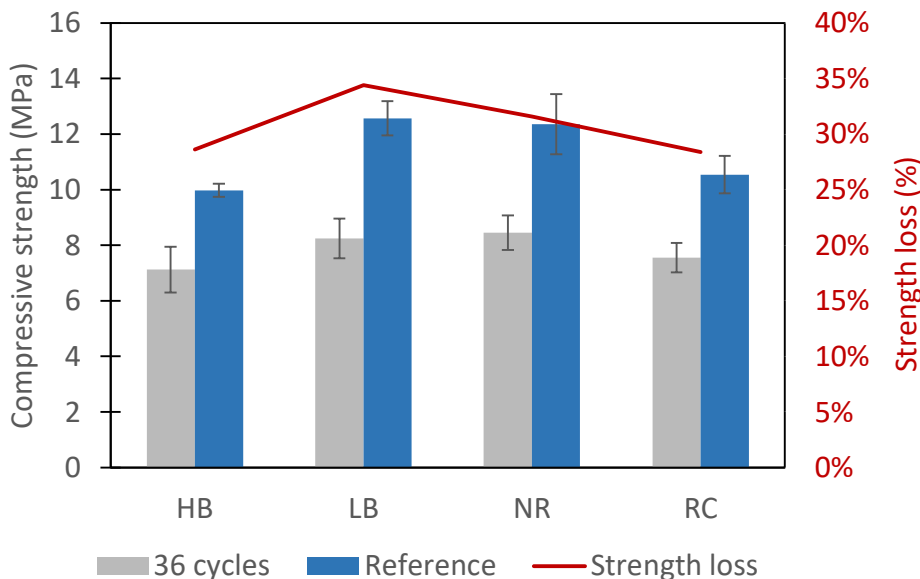


Figure 6.13. Compressive strength results after F&T cycles

Figure 6.14 and Figure 6.15 present the variation in the UPV and  $E_d$  for the same concretes. The results show a similar behaviour for all samples

(considering the error bars) from 18 to 36 F&T cycles, and point out that the experiment should have extended further than 36 cycles.

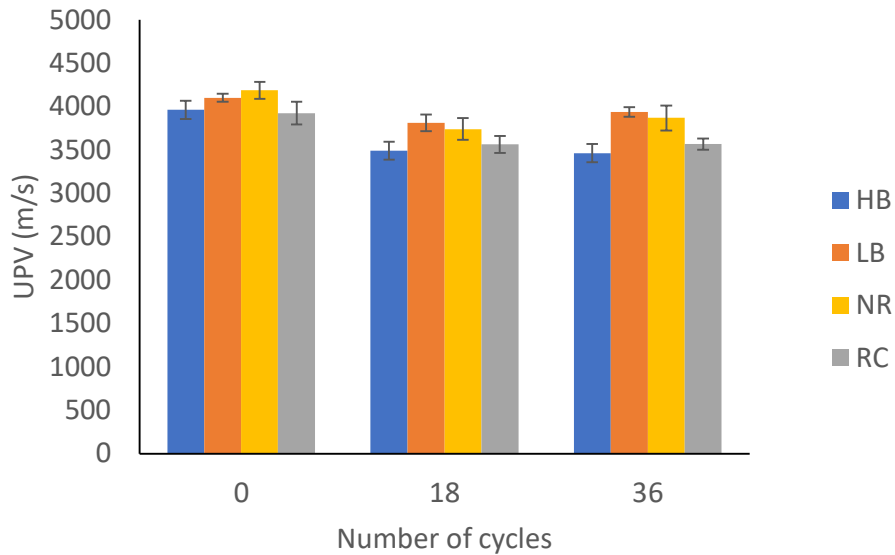


Figure 6.14. UPV variation after F&T cycles

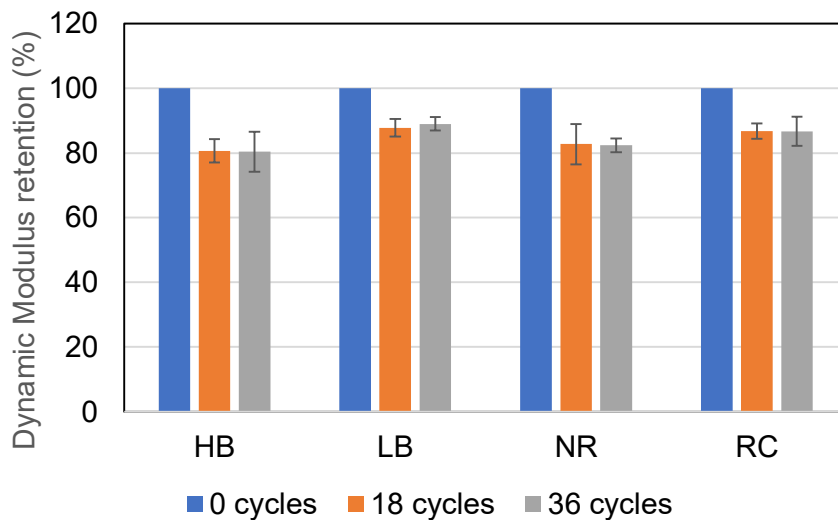


Figure 6.15.  $E_d$  variation after F&T cycles

The results in the literature on F&T performance for RAP-PC concrete state insignificant changes and even improvements at low RAP content, and slightly but acceptable reductions in performance at high

replacement levels of NA (Brand et al., 2012; Guo et al., 2018; Thomas et al., 2018). Thomas et al. (2018) reported improved F&T performance and no reduction in ME at up to 50% replacement. Abraham and Ransinchung (2019) presented evidence that the presence of entrained air in RAP mortars protected the PC matrix from frost damage and salt decay.

AAM materials, on the other hand, have reportedly better F&T performance than PC (Pacheco-Torgal et al., 2012), although Matalkah and Soroushian (2018) only noticed better performance of AAM after 60 cycles. The improved F&T performance of AAM is increased with binder content (Uğurlu et al., 2021) and reduced water/binder ratio.

The results indicate that the use of AAM for the production of RAP-lean concrete has little impact on short-term (up to 36 cycles) F&T resistivity, and all samples showed little mass losses for the period studied and similar compressive strength and Ed losses. The same can be said about the bitumen content of the RAP sources.

Longer testing F&T testing periods (more cycles) could give an even better indication of long-term durability performance and is an important recommendation if this material is used in regions with frost. Although all samples had very similar F&T resistance, the higher mass retention from HB suggests that there is more entrained air in RAP samples with higher bitumen content. This formulation was the one with lower compressive strength at 28 days among the RAP-AAM lean concretes (Figure 6.3).

## 6.4 Conclusion

The strength of cementitious concretes in the presence of RAP aggregates is compromised due to the weaker interface between aggregates and their adjacent mortars. Recycled aggregates have higher porosity, which translates into more voids. In the case of RAP aggregates, bitumen layers and clusters attached to the aggregates, not only hinder the aggregates from binding to the matrix but also act as voids due to the lower stiffness of the bitumen compared to the aggregates and matrix (Sachet et al.2013). These “acting voids” are imperfections in the internal structure and the starting point of microcracks around the interface (Yildirim and Sengul, 2011). Depending on the load, a network

of microcracks will spread across the matrix, connecting the once isolated imperfections, and bringing the composite to an earlier failure.

Alkali-activated binder may improve the mechanical properties of lean concretes containing RAP aggregates when compared to RAP-PC concretes. However, the weaker interface limits improvements in durability properties such as freeze-thaw resistance.

The main conclusions from this chapter are:

- The replacement of PC with AAM increases the mechanical strength by up to 38% and indirect tensile strength by 30%. Further improvements in strength could be achieved if sodium silicate is also used as an activator. In general, the bitumen content had a very little detrimental impact on strength properties.
- Static and dynamic modulus of elasticity of RAP-AAM were higher than RAP-PC. This was an unpredicted result since BFS-based AAM usually has lower modulus of elasticity compared to Portland cement concretes. It is suggested that the high alkalinity of the cementitious binder accelerated the oxidation of the bitumen layer thus increasing the ME of the system.
- For lean concretes (5-15 MPa), RAP-PC may present higher deformation upon stresses, but more sensitivity to changes in the mix design. RAP-AAM is marked by a narrow ME range (20-25 GPa) that positively helps predict the deformation for different mix designs. However, they are more brittle and, therefore, more prone to cracking under service if employed as pavement base layers.
- UPV performed after F&T cycles had a sharp decrease after the first 18 cycles and no apparent difference from 18 to 36 cycles. All samples presented similar responses despite the type of binder (PC or AAM) or aggregate used. This is a positive result as the UPV is directly related to dynamic ME and the durability factor to F&T.

Further research is needed to generate and accumulate more experimental data, as well as to understand the impact of high alkalinity on bitumen properties. Although design codes are often based on 28 days mechanical properties, more research on the strength development at later ages is needed – especially because of the late hydraulic development of BFS-based cements. Future research should also consider longer exposure to F&T cycles to assess whether there is a further variation in UPS and Ed.

### Highlights:

1. The higher mechanical performance of AAM compares to PC and similar performance under F&T is a good indication that RAP-AAM is suitable for base layer applications.
2. ME values for RAP-AAM were superior to what was expected by the design standards. This result was contradictory to common sense that the presence of asphalt would reduce ME. More investigation is needed to understand if the high alkalinity of the matrix is impacting the stiffness of the asphalt.
3. The results showed that the bitumen content did not play a significant role in most of the properties assessed. This finding suggests that the following studies should focus more on developing the AAM matrix than into RAP beneficiation methods.



# BIBLIOGRAPHY

---

- Abraham, S.M., Ransinchung, G.D.R.N., 2019. Pore Structure Characteristics of RAP-Inclusive Cement Mortar and Cement Concrete Using Mercury Intrusion Porosimetry Technique. *Adv. Civ. Eng. Mater.* 8, 20180161. <https://doi.org/10.1520/acem20180161>
- Ashteyat, A., Obaidat, A., Kirgiz, M., AlTawallbeh, B., 2021. Production of Roller Compacted Concrete Made of Recycled Asphalt Pavement Aggregate and Recycled Concrete Aggregate and Silica Fume. *Int. J. Pavement Res. Technol.* <https://doi.org/10.1007/s42947-021-00068-4>
- Avirneni, D., Peddinti, P.R.T.T., Saride, S., 2016. Durability and long-term performance of geopolymer stabilized reclaimed asphalt pavement base courses. *Constr. Build. Mater.* 121, 198–209. <https://doi.org/10.1016/j.conbuildmat.2016.05.162>
- Boussetta, I., El Euch Khay, S., Neji, J., 2018. Experimental testing and modelling of roller compacted concrete incorporating RAP waste as aggregates. *Eur. J. Environ. Civ. Eng.* 8189, 1–15. <https://doi.org/10.1080/19648189.2018.1482792>
- Brand, A.S., Roesler, J.R., 2017. Bonding in cementitious materials with asphalt-coated particles: Part II – Cement-asphalt chemical interactions. *Constr. Build. Mater.* 130, 182–192. <https://doi.org/10.1016/j.conbuildmat.2016.10.013>
- Brand, A.S., Roesler, J.R., Al-Qadi, I.L., Shangguan, P., 2012. Fractionated Reclaimed Asphalt Pavement (FRAP) as a Coarse Aggregate Replacement in a Ternary Blended Concrete Pavement, University of Illinois.
- Cartwright, C., Rajabipour, F., Radlińska, A., 2015. Shrinkage Characteristics of Alkali-Activated Slag Cements. *J. Mater. Civ. Eng.* 27, 1–9. [https://doi.org/10.1061/\(asce\)mt.1943-5533.0001058](https://doi.org/10.1061/(asce)mt.1943-5533.0001058)
- Costa, J.O., Borges, P.H.R., dos Santos, F.A., Bezerra, A.C.S., Blom, J., Van den bergh, W., 2021. The Effect of Reclaimed Asphalt Pavement (RAP) Aggregates on the Reaction, Mechanical

Properties and Microstructure of Alkali-Activated Slag. *CivilEng* 2, 794–810. <https://doi.org/10.3390/civileng2030043>

Diaz-Loya, E.I., Allouche, E.N., Vaidya, S., 2011. Mechanical Properties of Fly-Ash-Based Geopolymer Concrete. *ACI Mater. J.* 108, 300–306. <https://doi.org/10.14359/51682495>

Ding, Y., Dai, J.G., Shi, C., 2018. Fracture properties of alkali-activated slag and ordinary Portland cement concrete and mortar. *Constr. Build. Mater.* 165, 310–320. <https://doi.org/10.1016/j.conbuildmat.2017.12.202>

El Euch Ben Said, S., El Euch Khay, S., Loulizi, A., 2018. Experimental Investigation of PCC Incorporating RAP. *Int. J. Concr. Struct. Mater.* 12, 8. <https://doi.org/10.1186/s40069-018-0227-x>

Euch Khay, S. El, Euch Ben Said, S. El, Loulizi, A., Neji, J., 2015. Laboratory Investigation of Cement-Treated Reclaimed Asphalt Pavement Material. *J. Mater. Civ. Eng.* 27, 04014192. [https://doi.org/10.1061/\(asce\)mt.1943-5533.0001158](https://doi.org/10.1061/(asce)mt.1943-5533.0001158)

Farhan, N.A., Sheikh, M.N., Hadi, M.N.S., 2019. Investigation of engineering properties of normal and high strength fly ash based geopolymer and alkali-activated slag concrete compared to ordinary Portland cement concrete. *Constr. Build. Mater.* 196, 26–42. <https://doi.org/10.1016/J.CONBUILDMAT.2018.11.083>

Ghazy, M.F., Abd Elaty, M.A.A., Abo-Elenain, M.T., 2022. Characteristics and optimization of cement concrete mixes with recycled asphalt pavement aggregates. *Innov. Infrastruct. Solut.* 7, 1–15. <https://doi.org/10.1007/s41062-021-00651-5>

Guo, S., Hu, J., Dai, Q., 2018. A critical review on the performance of portland cement concrete with recycled organic components. *J. Clean. Prod.* 188, 92–112. <https://doi.org/10.1016/j.jclepro.2018.03.244>

Han, S., Cheng, X., Liu, Y., Zhang, Y., 2019. Laboratory performance of hot mix asphalt with high reclaimed asphalt pavement (RAP) and fine reclaimed asphalt pavement (FRAP) content. *Materials (Basel)*.

12. <https://doi.org/10.3390/ma12162536>

Howard, I.L., Cooley, L.A., Doyle, J., 2009. Laboratory Testing and Economic Analysis of High RAP Warm Mixed Asphalt. Ridgeland.

Hoy, M., Horpibulsuk, S., Arulrajah, A., 2016a. Strength development of Recycled Asphalt Pavement - Fly ash geopolymer as a road construction material. *Constr. Build. Mater.* 117, 209–219. <https://doi.org/10.1016/j.conbuildmat.2016.04.136>

Hoy, M., Horpibulsuk, S., Arulrajah, A., Mohajerani, A., 2018. Strength and microstructural study of recycled asphalt pavement: Slag geopolymer as a pavement base material. *J. Mater. Civ. Eng.* 30. [https://doi.org/10.1061/\(ASCE\)MT.1943-5533.0002393](https://doi.org/10.1061/(ASCE)MT.1943-5533.0002393)

Hoy, M., Horpibulsuk, S., Rachan, R., Chinkulkijniwat, A., Arulrajah, A., 2016b. Recycled asphalt pavement – fly ash geopolymers as a sustainable pavement base material: Strength and toxic leaching investigations. *Sci. Total Environ.* 573, 19–26. <https://doi.org/10.1016/j.scitotenv.2016.08.078>

Mataalkah, F., Soroushian, P., 2018. Freeze thaw and deicer salt scaling resistance of concrete prepared with alkali aluminosilicate cement. *Constr. Build. Mater.* 163, 200–213. <https://doi.org/10.1016/j.conbuildmat.2017.12.119>

Mohammadinia, A., Arulrajah, A., Horpibulsuk, S., Chinkulkijniwat, A., 2017. Effect of fly ash on properties of crushed brick and reclaimed asphalt in pavement base/subbase applications. *J. Hazard. Mater.* 321, 547–556. <https://doi.org/10.1016/j.jhazmat.2016.09.039>

Nguyen, T.H.G., Nguyen, T.D., Tran, T.H., Dao, V.D., Bui, X.C., Nguyen, M.L., 2020. Investigation of the use of reclaimed asphalt pavement as aggregates in roller compacted concrete for road base pavement in Vietnam. pp. 513–518. [https://doi.org/10.1007/978-981-15-0802-8\\_80](https://doi.org/10.1007/978-981-15-0802-8_80)

Pacheco-Torgal, F., Abdollahnejad, Z., Camões, A.F., Jamshidi, M., Ding, Y., 2012. Durability of alkali-activated binders: A clear advantage over Portland cement or an unproven issue? *Constr.*

Build. Mater. <https://doi.org/10.1016/j.conbuildmat.2011.12.017>

Panditharadhya, B.J., Mulangi, R.H., Ravi Shankar, A.U., Kumar, S., 2019. Mechanical properties of pavement quality concrete produced with reclaimed asphalt pavement aggregates, *Lecture Notes in Civil Engineering*. Springer Singapore. [https://doi.org/10.1007/978-981-13-3317-0\\_47](https://doi.org/10.1007/978-981-13-3317-0_47)

Plati, C., 2019. Sustainability factors in pavement materials, design, and preservation strategies: A literature review. *Constr. Build. Mater.* 211, 539–555. <https://doi.org/10.1016/j.conbuildmat.2019.03.242>

Pradhan, S.K., Biswal, G., 2022. Utilization of reclaimed asphalt pavement (RAP) as granular sub-base material in road construction. *Mater. Today Proc.* <https://doi.org/10.1016/j.matpr.2021.12.564>

Rahman, S.S., Khattak, M.J., 2021. Mechanistic and microstructural characteristics of roller compacted geopolymer concrete using reclaimed asphalt pavement. *Int. J. Pavement Eng.* 0, 1–19. <https://doi.org/10.1080/10298436.2021.1945057>

Settari, C., Debieb, F., Kadri, E.H., Boukendakdji, O., 2015. Assessing the effects of recycled asphalt pavement materials on the performance of roller compacted concrete. *Constr. Build. Mater.* 101, 617–621. <https://doi.org/10.1016/j.conbuildmat.2015.10.039>

Su, Y.-M., Hossiney, N., Tia, M., Bergin, M., 2014. Mechanical Properties Assessment of Concrete Containing Reclaimed Asphalt Pavement Using the Superpave Indirect Tensile Strength Test. *J. Test. Eval.* 42, 20130093. <https://doi.org/10.1520/jte20130093>

Thomas, R.J., Fellows, A.J., Sorensen, A.D., 2018. Durability analysis of recycled asphalt pavement as partial coarse aggregate replacement in a high-strength concrete mixture. *J. Mater. Civ. Eng.* 30, 1–7. [https://doi.org/10.1061/\(ASCE\)MT.1943-5533.0002262](https://doi.org/10.1061/(ASCE)MT.1943-5533.0002262)

Thomas, R.J., Peethamparan, S., 2015. Alkali-activated concrete: Engineering properties and stress-strain behavior. *Constr. Build. Mater.* 93, 49–56. <https://doi.org/10.1016/j.conbuildmat.2015.04.039>

- Uğurlu, A.İ., Karakoç, M.B., Özcan, A., 2021. Effect of binder content and recycled concrete aggregate on freeze-thaw and sulfate resistance of GGBFS based geopolymer concretes. *Constr. Build. Mater.* 301. <https://doi.org/10.1016/j.conbuildmat.2021.124246>
- Venkiteela, G., Sun, Z., Najm, H., 2013. Prediction of Early Age Normal Concrete Compressive Strength Based on Dynamic Shear Modulus Measurements. *J. Mater. Civ. Eng.* 25, 30–38. [https://doi.org/10.1061/\(asce\)mt.1943-5533.0000528](https://doi.org/10.1061/(asce)mt.1943-5533.0000528)
- Yang, K., Cho, A., Song, J., 2012. Effect of water – binder ratio on the mechanical properties of calcium hydroxide-based alkali-activated slag concrete. *Constr. Build. Mater.* 29, 504–511. <https://doi.org/10.1016/j.conbuildmat.2011.10.062>
- Yildirim, H., Sengul, O., 2011. Modulus of elasticity of substandard and normal concretes. *Constr. Build. Mater.* 25, 1645–1652. <https://doi.org/10.1016/J.CONBUILDMAT.2010.10.009>
- Zhou, Y., Gao, J., Sun, Z., Qu, W., 2015. A fundamental study on compressive strength, static and dynamic elastic moduli of young concrete. *Constr. Build. Mater.* 98, 137–145. <https://doi.org/10.1016/j.conbuildmat.2015.08.110>



# CONCLUSIONS & RECOMMENDATIONS

---

## 7.1. Research Summary

The present thesis provides a better understanding of the main factors involved in the use of reclaimed asphalt particles (RAP) as aggregates for alkali-activated materials (AAM), as an alternative solution for base courses for new pavement sections. This research presents another possibility of recycling RAP since the adopted practices - i.e., as unbound base material or in new asphalt mixes – are unable to consume all the disposed old asphalt pavement. At the same time, it also combines the recycled aggregate (RAP) with the alkaline activation of ground granulated blast furnace slag, an industrial by-product readily available both in Brazil and Belgium.

While the focus was on the mechanical performance of the proposed material (RAP-AAM), some relevant durability properties for base layers were also investigated. The main research question of this thesis was:

**Could AAM incorporate high amounts of RAP, and be used as pavement base layers without compromising mechanical and durability performance?**

The main concern regarding the use of RAP in any cementitious system relates to the old and aged asphalt mortar/ bitumen layer coating and,

sometimes, the clustering of the natural aggregates. Recent interest from the research community can give some indication of how RAP impacts the properties of PC matrices; however, there are very few reports on alkali-activated matrices.

AAM is an alternative cementitious binder that can often achieve remarkable strength and durability while using industrial by-products, wastes, or clays combined with a strong alkali source. Although it is regularly regarded as a greener alternative to PC, the fact that a wide variety of materials is suitable for alkali-activation means that not every recipe may be regarded as such. The recurrent advice when designing an AAM with lower environmental impact is to mind the use of alkalis (amount and type) and use local materials. Alkalis are regarded as the main environmental burden in the recipe and locally sourced precursors (binders) will reduce the impacts involved in transportation. After careful consideration, ground granulated blast furnace slag (BFS) was selected as the main raw material due to its availability in both Brazil and Belgium, and its lower alkali demand when activated.

The experimental procedure was divided into three main assessments, each of which provided information for the development of the next one.

- (i) The first part (Chapter 4) focused on comparing alkali-activated mortars prepared with 100% natural aggregates (NA) and with 100% RAP aggregates. The matrix was produced using only BFS as a precursor and different amounts of sodium hydroxide and sodium silicate as activators. To eliminate the effect of the aggregate gradation, both aggregates (NA and RAP) had the same particle size distribution. The hydration kinetics was accessed using calorimetry, and the properties of the hardened materials were investigated through compressive strength, flexural strength, MIP, and microscopy.
- (ii) The following part of the research (Chapter 5) investigated whether it was possible to improve the properties of (some of) the studied formulations by replacing part of the BFS with metakaolin (MK). The different MK replacement levels were investigated through calorimetry, shrinkage, FTIR, microscopy, compressive strength, flexural strength, and apparent porosity.



The experiments assessed if the employment of MK could be an effective option to reduce the high shrinkage that is inherent to alkali-activated slag systems.

- (iii) The last experimental part of the research (Chapter 6) was based on the production of lean concrete using RAP with different bitumen content. The composition of the alkali-activated binder was selected based on the previous findings. The mechanical and durability properties of the concrete were assessed. The tests performed at this stage of the research were Proctor, compressive strength, splitting tensile strength, static modulus of elasticity, UPV, and freeze & thaw.

During this research, two innovative characterization methods were used as an alternative to those often employed for Portland concrete. Firstly, the observation of the interfacial transition zone (ITZ) was improved by combining a laser scanning confocal microscope (LSCM) and a scanning electron microscope (SEM). The combination of both techniques permitted a better observation of the heterogeneous coating of the RAP particles, the presence of clusters, and cracks at the border and within the activated matrix. Secondly, the thesis proposes an alternative methodology to observe and quantify the shrinkage of RAP-AAM or any other cementitious materials by employing simplified optical imaging. Although this method only allows for the observation of total shrinkage, it is an almost inexpensive method that could give a clear indication of volume changes over time.

## **7.2. Conclusions**

An overview of the state-of-the-art of RAP and cementitious systems showed that the literature on RAP-AAM systems is limited; however, it is possible to identify challenges based on previous studies on PC. The main challenge regards the presence of asphalt mortar/ bitumen coating on the RAP granules. The coating weakens the ITZ, making it larger and more porous, which compromises mechanical performance and durability. Another challenge concerns the environmental impact of the proposed material. The environmental gain of AAM depends on the choice of precursors and especially the amount of alkali solution. A carefully designed RAP-AAM could take advantage of (i) the high-early

strength and durability of AAM; (ii) the low strength requirement of base layers, and (iii) a possible environmental gain due to the low alkali demand to activate BFS.

The replacement of NA with RAP on alkali-activated BFS was assessed using different types of activators; a significant reduction in both compressive and flexural strength of the mortars was confirmed (on average 44% and 38% respectively). A sharp increase in compressive strength for most ages was observed when sodium silicate was present in the solution. The maximum improvement was 234% for samples with NA and only 88% for RAP. These results indicated a reduced efficiency of sodium silicate on RAP-AAM compared to RAP-PC.

The initial concern was that somehow the activator used could be leaching chemicals from the asphalt that interfered with the binder's reaction. However, calorimetric studies indicated that the presence of RAP did not compromise the reaction of the matrices. Mercury intrusion porosimetry, confocal laser scanning microscopy, and scanning electron microscopy suggested that the reason might lie in the ITZ. In general, RAP-AAM presented higher porosity, a thicker ITZ, and heterogeneous distribution of bitumen around the surfaces of the aggregate.

The use of a blended source of precursors could help in the performance improvement (mechanical and durability) of RAP-AAM. A blended precursor made of BFS and MK was tested at up to 20 vol% MK for selected formulations activated with sodium hydroxide or sodium hydroxide + sodium silicate. The activators contained either 4% or 8% of  $\text{Na}_2\text{O}$  and Ms ratios of 0 or 1. Calorimetry assessment indicated that the presence of MK slowed down the reaction, with a consequent reduction in the early-age strength. Some formulations did not even harden after 3 days. There was no detrimental effect on the incorporation of MK at later ages.

The shrinkage of the mortars was assessed using optical measurement. This method is not a standard procedure and, therefore, difficult to correlate with previous studies. However, it works for comparison purposes. The experiment indicated that the use of sodium silicate significantly increases the shrinkage (75% higher than samples activated only with sodium hydroxide). The replacement of BFS with MK could help

mitigate shrinkage at different replacement levels depending on the choice of activator. The optimum replacement levels were 10% vol. MK and 20% vol. MK, respectively for formulations activated with 8% Na<sub>2</sub>O and Ms=0 and 8% Na<sub>2</sub>O and Ms = 1.

The experimental data suggested that an ideal alkali-activated binder composition to produce RAP-AAM lean concrete should have 10% MK replacement (BFS vol%) and the activator would have 8% Na<sub>2</sub>O and Ms= 0 (i.e., activated with NaOH and no sodium silicate). This selection was based on the minimum activator amount required to reach the target compressive strength for a weak to medium lean concrete (5 to 10 MPa), while also minimizing the shrinkage effect. This AAM composition was mixed with natural fine aggregates and three types of RAP as coarse aggregates: (i) locally supplied RAP (RAP1) with bitumen content equal to 4.8%; lab-produced RAP with low (4.5%) bitumen content (RAPL) and (iii) lab-produced RAP with high (5.7%) bitumen content (RAPH). The formulations were compared to a reference sample produced with the same aggregates, but with type CEMIII Portland cement as a binder.

The RAP-AAM presented increased compressive, indirect tensile strength, and modulus of elasticity compared to the PC reference (38%, 30%, and 38% higher on average, respectively). Among the RAP-AAM formulations, the lab-produced RAP initially appeared disadvantageous due to worsened mechanical performance when compared to the locally supplied RAP1. However, when the standard deviation of the results is taken into account, the variation is not significant, suggesting that the performance of the RAP-AAM is not governed by the bitumen content of the RAP, at least for the levels of bitumen employed between 4.5% and 5.7%.

Contrary to the expectation, the modulus of elasticity of the RAP-AAM was higher than the literature prediction for AAM. Although this could be due to either the composition, type, and shape of RAP particles used in the study, it is worth considering that the alkalis available in the mix could be further oxidating the asphalt and consequently making the overall material more brittle.

The durability assessment to freeze and thaw indicated similar performance for RAP-AAM and reference (RAP-PC). The performance

to freeze and thaw was likely governed by the increased porosity caused by the use of RAP aggregates which equally impacted both samples (RAP-Pc and RAP-AAM).

Asphalt is a much softer material than NA and AAM, and its presence in a cementitious binder act as pores inside the matrix initiating, connecting, and distributing micro-cracks. Although this network of cracks weakens the concrete, the material can still achieve the strength requirements for a lean concrete base layer. The mechanical performance can be tailored by changing the amount and type of alkalis, but care must be taken to avoid increasing the shrinkage of the material and the environmental impact due to the activating solution. The initial durability assessment suggests similar performance to a reference concrete produced with RAP and CEM III. The findings of this research suggest that RAP-AAM is a promising material for pavement base layers. The suggested composition would have a 9/1 BFS/MK (vol) activated with NaOH (8% Na<sub>2</sub>O).

### 7.3. Recommendations for future research

This study offers an initial validation for the use of RAP and AAM for pavement base layers and may also be used as a reference for other applications. Some considerations and ideas for further research may improve the understanding of RAP-AAM and accelerate the implementation of this alternative solution for base pavement layers:

- Study of other binders: AAM may be produced with a very wide variety of precursors and activators. Any attempt to produce and use AAM should always investigate local available materials or wastes in an attempt to improve the sustainability of the binder. Uncalcined clays, glass waste, biomass ash, Bayer liquor, and agricultural waste are all examples of alternative raw materials for AAM with potential lower environmental impact. The low strength demand of pavement base layers is also an encouragement to use alternative low-reactive raw materials, otherwise ignored in the formulations of traditionally studied AAM.
- The use of waste materials, such as RAP, always merits strong consideration. RAP is subjected to strong variations due to the

asphalt production methods, different removal, and milling procedure. Every batch of material could have very different gradation, shape, constitution, and contaminants. Better control and legislation could help mitigate these problems but is very likely that RAP batches will always need to be tested and the composition of the final mix will need to be adjusted before it is used.

- Alternative shrinkage assessment: the optical measurement is a good, simple, and inexpensive comparison method for shrinkage; however, it does not allow a direct comparison with other shrinkage methods often used by the research community. More investigation on how to correlate the methods would be helpful for the future development of the technique.
- Effect of oxidized RAP particles: The oxidation of asphalt is an aging phenomenon that occurs during most of its service life and continues after reclamation. While RAP granulates are generated from old pavement sections assumed oxidized, the oxidation levels vary from the more exposed asphalt and the “inner” asphalt. This research found an indication that a highly alkaline environment may contribute to the further oxidation of the asphalt in the RAP granules. An oxidized asphalt would become more brittle, and this could interfere with the mechanical performance of the RAP-AAM composite over time. The possibility of the alkali-oxidation of the asphalt present in the RAP granules and the effects on the properties of RAP-AAM should be investigated.
- LCA studies: The choice of raw materials was based on the literature indication of environmentally friendlier materials; however, the environmental impact of the proposed composition was not assessed. Life cycle analysis is needed to validate the solution as a suitable alternative for pavement base layers.

In general, more data is needed to validate and expand the indicated trends. This is achieved with a sequence of different designs of experiments. We believe that more variables and combinations of RAP-AAM should be studied also at longer ages. Concrete structures are designed based on their 28 days strength, but it is the long-term

properties that will dictate the lifespan, maintenance needs/costs, and consequently durability and sustainability of the civil engineering works.